THE DISTRIBUTION OF VENTILATION AND PERFUSION IN THE NORMAL LUNG, STUDIED WITH XENON^{133}

by

A. C. Bryan, M. B., B. S.

A thesis submitted in partial fulfillment of the requirements

for the degree of Doctor of Philosophy (Experimental Medicine).

FACULTY OF GRADUATE STUDIES
McGILL UNIVERSITY
MONTREAL, P. Q.
1964

TABLE OF CONTENTS

TABLE OF CONTENTS

TABLE OF CONTENTS

TABLE OF CONTENTS

LIST OF FIGURES

LIST OF FIGURES

LIST OF TABLES

PART I

INTRODUCTION AND METHOD

INTRODUCTION

Anatomically the lung consists of two conducting systems to bring the inspired air and venous blood into contact. The effectiveness of gas exchange is largely dependent on the efficiency of these distribution systems. If parts of the lung are ventilated but not perfused, or perfused but not ventilated, no gas exchange will occur in these areas. Furthermore, ventilation in excess of perfusion, or perfusion in excess of ventilation are relatively inefficient. The optimum distribution is clearly when the quantities of ventilation and perfusion are matched, that is, the Ventilation/Perfusion ratio is equal in all lung units. To predict gas exchange it is therefore necessary to know not only the total quantities of alveolar ventilation and pulmonary capillary blood flow, but also their distribution.

The problem of the distribution of Ventilation/Perfusion ratios have been recognised for many years, but only recently has it been realized that mal-distribution is the major cause of gas exchange failure in lung disease. It is relatively easy to detect the presence of an abnormal Ventilation/Perfusion distribution. However, these methods can only describe the lung as "spaces" behaving as if they had various Ventilation/Perfusion patterns. These "spaces" are not real volumes and have no topographical significance. Clinically it is of considerable importance to be able to locate the regions with abnormal distribution. Until recently

the only method available for this was regional or lobar broncho-spirometry. This technique gives valuable information, but the measurements are made under un-physiological conditions, which must be interpreted with caution.

Recently great advances have been made in the understanding of these distribution problems using radio-active isotopes, oxygen^{15} and Xenon^{133}. With both isotopes the regional distribution of ventilation and perfusion can be measured. This data is of fundamental importance in understanding the factors which influence distribution and in clarifying the process of gas exchange in health and disease.

This thesis describes the methods and results of measuring ventilation and perfusion distribution using Xenon^{133} in normal subjects. The primary purpose of the study is to describe the various distribution patterns that occur in normal subjects. This data has been used to discuss some of the factors which affect the normal distribution of ventilation and perfusion. It has also been used to construct Ventilation/Perfusion lung models to predict the normal variations in gas exchange.

HISTORICAL BACKGROUND

Early in the development of Pulmonary Physiology the presence of uneven distribution of both ventilation and perfusion were suspected. In 1887 Johannes Orth [1] wrote a treatise on tuberculosis and in discussing its localisation he postulated that the apex of the lung would be anaemic because of the effect of gravity on the fluid column of blood. In 1911 Siebeck [2] had experimental evidence that the distribution of inspired air was not uniform. Furthermore there were some remarkable early attempts to predict the consequences of inequality of distribution. In 1917 Krogh [3], wrote "So far we have tacitly assumed - as all other physiologists have done - that alveoli from different bronchi contain the same gas mixture .....If the different lobes of the lungs are not equally dilated during inspiration the air in them must obtain a different composition". He added a footnote: "Unless indeed the circulation through such lobe should be in proportion to its ventilation".

And in 1922 Haldane [4] wrote: "We have no guarantee that even during quiet normal breathing the distribution of air in the individual lung alveoli corresponds exactly with the distribution of blood to them... It is probable that in some way or other the air supply is proportioned to the blood supply..... The fact that in animals the aerotonometer gives a lower arterial oxygen pressure than the alveolar oxygen pressure is most naturally explained on the theory that the proportioning is only

approximate".

Despite these speculations the importance of the blood/gas relationship was not fully recognised. This lack of progress is partially explained by the inadequacy of early equipment, but is also due to the absence of a clear theoretical development.

The distribution of perfusion which is grossly uneven received very little study. Laurell in 1927 [5] suggested that the upper part of the lung was less vascular than the lower on the basis of the chest x-ray. This technique, supplemented later by tomography [6] and angiography has been of value clinically to estimate the distribution of blood flow, but this information is qualitative and subjective. Some quantitative evidence has been obtained by bronchospirometry. In 1934 Bjorkman [7] showed that in the lateral decubitus position the "down" lung had a greater oxygen uptake than the "up" lung. He suggested that: "it is plausible that this is caused by increased perfusion in the lower lung and decreased perfusion in the upper, resulting from body position". This hesitant, but entirely correct conclusion was not followed up for many years. After cardiac catheterisation had demonstrated that the pulmonary circulation was a low pressure system, Orth's speculations on the effect of gravity were revived. Dock [8] in 1946 arguing from the mean pulmonary artery pressure and the hydrostatic column within the thorax, concluded that blood flow must be very low at the apices of the lung in the upright position. As a consequence of the apical anaemia he suggested that the alveolar oxygen tension would be high and provide the most appropriate

environment for the tubercle bacillus. The odd fact that bats, who spend much of their time upside down, get tuberculosis at the base of the lung[9] provided attractive support for the gravitational theory of localisation. It was largely this problem of the localisation of tuberculosis and the effect of postural treatment which stimulated subsequent studies on the pulmonary circulation. In 1953 Martin [10] sampled the expired gas from various lobes in man and showed that the oxygen content was higher and the carbon dioxide content lower in the upper lobe than in the lower lobe. These differences decreased in the supine position. More conclusive evidence came from the same author [11, 12] and from Mattson [13] using similar techniques of lobar broncho-spirometry. By using cuffed endobronchial catheters the upper lobe could be separated from the middle and lower lobes so that their ventilation and oxygen uptake could be measured separately. In the upright position they showed that the oxygen uptake of the upper lobe was a small fraction (18%) of the total uptake, while in the supine position the upper lobe fraction increased considerably (37%). The difference in tidal ventilation between the lobes was much smaller and did not alter significantly with position. As oxygen uptake is a function of the blood flow this conclusively showed the postural basis for the distribution of perfusion.

Although there is much less unevenness of ventilation distribution in normal subjects, much more work has been done on this subject. Siebeck [1] in 1911 appears to have been the first worker to suggest uneven ventilation, because of the lack of agreement between lung volumes calcu-

lated from a single breath of hydrogen and those calculated by a multiple breath technique. This idea was developed by Krogh and Lindhard [14] who showed that, after a single breath of hydrogen, sequential samples during the expiration contained decreasing quantities of hydrogen. This finding has been confirmed repeatedly. Its most elegant development has been by continuous analysis of expired nitrogen, after a single breath of oxygen recorded with a nitrogen meter [15] or Mass Spectrometer [16]. Three phases can be seen in the expired nitrogen concentration: a rapidly rising phase, representing dead space washout, a phase of transition from dead space gas to alveolar gas, and a final "plateau" representing alveolar gas. A continuous rise in this third phase must be due to uneven distribution of nitrogen in the alveoli. The slope is proportional to the degree of unevenness, but it is difficult to quantitate this.

Multiple breath techniques for measuring uneven distribution have been generally more useful. In measuring lung volumes, the early studies were often a compromise between the time taken to equilibrate the patient with the hydrogen circuit and the progressive error due to tissue uptake. The significance of prolonged equilibration time in abnormal subjects was overlooked for many years. Sonne [17] in 1936 appears to have first clearly associated this with uneven ventilation. It was not until 1944 that quantitative expressions of this unevenness were attempted. At this time Birath [18] using a closed circuit hydrogen wash-in method and Darling [19] using an open circuit nitrogen washout derived equations showing that, in a perfect mixing system, the wash-in or washout curve would have an

exponential form. The time constant of the exponential would be determined by the lung volume and the effective tidal volume (and in the closed circuit, by the spirometer volume). Many subsequent studies [20, 21, 22, 23] have shown that in normal subjects the nitrogen or helium open circuit washout curve deviates from the single exponential and therefore some unevenness of distribution or "poor mixing" is present. Helium closed circuit curves do not show this [24, 25], however this is probably artefact due to slow catharometer response in the critical early part of the curve and the complex concentration changes that occur in closed circuit systems[26]. A variety of methods have been proposed to express the degree of unevenness and the most useful are the simplest: the Helium Mixing Index [24] for closed circuit, and the Nitrogen Clearance Index [22] for open circuit. Attempts have been made [20, 46, 47] to extract more meaningful information from the non-linearities of the semi-log plot of the washout curve. In a simple two chambered model with unequal ventilation per unit volume, the semi-log washout plot is curved but by geometric analysis it is possible to separate two exponential components in the curve. From the intercepts and the slopes of the lines it is possible to deduce the volumes and ventilations of the two chambers. This technique has been applied to lung washouts, separating the lung into two and sometimes three "compartments". These "compartments" have no anatomical significance and only imply that the lung behaves as if it consisted of two or three parallel volumes with separate exponential washout rates. There are a number of objections to this technique. To extract two exponentials it is essential to

positively define the asymptote of the curve and this depends on the number of logarithmic decades through which the analyser can record the washout. Nye [27] has recently shown the limitations of current gas analysers in this situation. Slight degrees of unevenness are undetectable and the volume of the poorly ventilated space is liable to be exaggerated, particularly in the open-circuit techniques. A more fundamental objection is that the lung obviously does not behave like two or three homogeneous spaces, in reality the washout must represent a statistical distribution of multiple exponential washout terms. Gomez [28] has recently shown that a normal washout curve can be analysed as a frequency distribution of washout rates. As one would expect this is a skew "normal" distribution, covering a wide range of washout rates and not the discrete bimodal distribution that one gets by "stripping" exponentials [29].

DEVELOPMENT OF VENTILATION/PERFUSION CONCEPT

The full importance of the interrelationship between the distribution of ventilation and perfusion was not clearly expressed until 1949. Two groups, Rahn and Fenn [30, 31] attempting to define "Equivalent Altitude" and Riley and Cournand [32, 33] seeking "Ideal Alveolar Air" graphically assembled the equations governing gas exchange. Their graphical approach was similar and was of great importance, because it displayed visually the interrelationship of the factors governing gas exchange, which is not readily apparent from the individual equations.

The basic equations are simple and may be developed in the following manner:

The amount of CO_2 leaving the blood is equal to pulmonary capillary blood flow multiplied by the arteriovenous CO_2 difference (i.e. the Fick equation or the Second Law of Thermodynamics).

1. $\dot{V}CO_2 = \dot{Q}c \quad (C\bar{v}CO_2 - C\acute{c}CO_2)$

The amount of CO_2 leaving the lung is equal to the alveolar CO_2 concentration, multiplied by the volume of alveolar ventilation, corrected from BTPS to STPD).

2. $\dot{V}CO_2 = Fa_{CO_2} \times \dot{V}a \times 0.83$

If in the steady state the respiratory quotient of the blood equals the RQ of the alveoli, their CO_2 output is equal, then Equation 1 equals Equation 2.

3. $\dot{Q}c\ (C\bar{v}CO_2 - C\acute{c}CO_2) = \dot{V}a \times Fa_{CO_2} \times 0.83$

Re-arranging this:

$$4. \quad \frac{\dot{V}a}{\dot{Q}c} = \frac{C\bar{v}C0_2 - C\acute{c}C0_2}{F_{AC0_2}\ 0.83}$$

It is more convenient to express F_{AC0_2} as P_{AC02} and equation 4 becomes:

$$5. \quad \frac{\dot{V}A}{\dot{Q}c} = \frac{863\ (C\bar{v}C0_2 - C\acute{c}C0_2)}{P_{AC0_2}}$$

A similar equation can be derived for arterio-venous oxygen difference, but in this case correction must be made for the differences in inspired and expired volume:

$$6. \quad \frac{\dot{V}A}{\dot{Q}c} = 0.863 \times R \times \frac{(C\bar{v}0_2 - C\acute{c}0_2)}{P_{AC0_2}}$$

These equations 5 and 6, can be applied to the lung as a whole or to single alveoli, when $\dot{V}_A$ and $\dot{Q}c$ become the gas and blood flow to the unit. It is clear that for any given composition of mixed venous blood and inspired air the alveolar and arterial gas tensions will be determined by the ratio of alveolar ventilation to perfusion and are independent of metabolic rate. If the Ventilation/Perfusion ratio is equal in all alveoli, then from Equation 6 the P_{AC0_2} and R must be the same and if these are constant, P_{A0_2} must be the same in all alveoli. Predictions of the effects of differences in the $\dot{V}_A/\dot{Q}$ ratio cannot be made easily from Equations 5 and 6, there are too many unknowns. However, a graphical solution is possible on the "0_2 - $C0_2$ Diagram" (Figure 1) which has $p0_2$ as the abscissa and $pC0_2$ as the ordinate. The solution assumes that the Blood R equals the Gas R and locates the point of equality on the graph. Gas R lines are plotted by solving the alveolar air equation [34] and

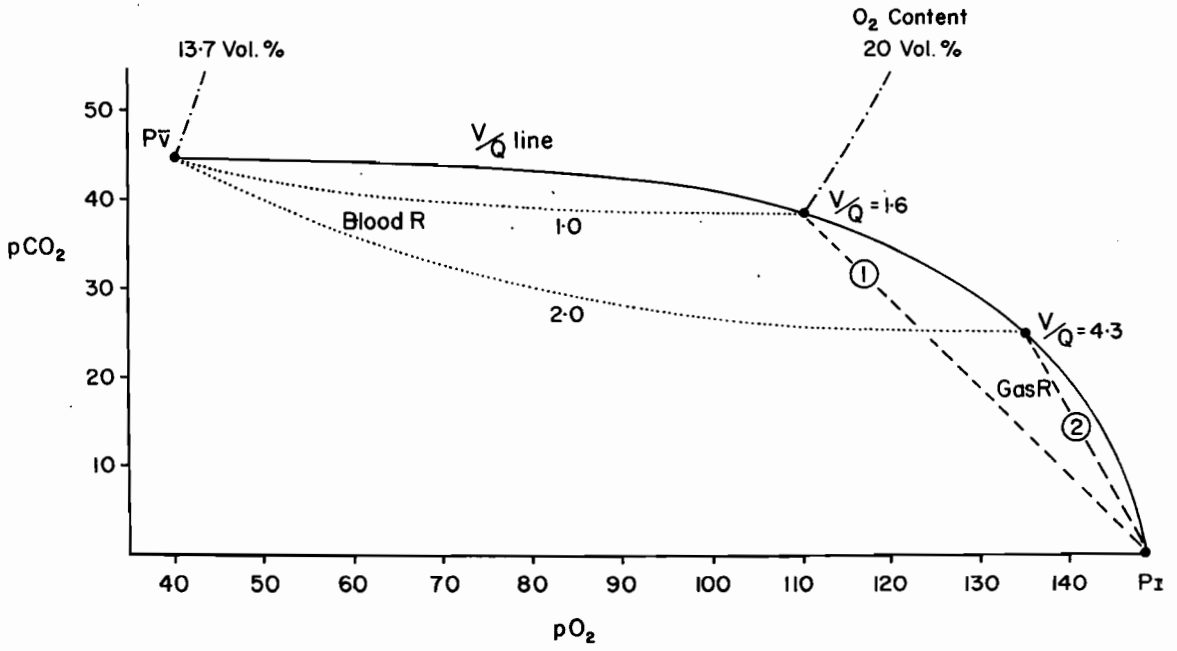

Figure I - Construction of $\dot{V}_A/\dot{Q}$ line on the 0_2:$C0_2$ Diagram. $\dot{V}_A/\dot{Q}$ points are solved at the intersects of equal blood and gas R lines. From Rahn [34].

produce a series of lines radiating from the inspired gas tensions. Blood R lines are obtained from Dill's nomogram [35] producing a series of curves originating from the mixed venous gas tension. It can be seen from Figure I that if the blood is exchanging at R = 1.6, then the only point where the blood and gas R could be equal is where the blood R = 1.6 line intersects the gas R = 1.6 line. This intersect also defines the only pO_2 and pCO_2 that could exist when R = 1.6, in both the gas and the blood (assuming no diffusion defect). By joining up all the equal R intercepts a curve is described between the mixed venous and inspired gas tensions, on which all the gas tensions that might exist between R = 0 and R = ∞ must lie. From the oxygen dissociation curve, oxygen content isopleths can be superimposed on this graph so that the arterio-venous oxygen difference can be calculated from any point on the line to the mixed venous point. Thus from any point on the curve R, $(C\acute{c}O_2 - C\bar{v}O_2)$ and P_{ACO_2} are known and all the information is available for Equation 6 to calculate the $\dot{V}_A/\dot{Q}$ ratio of the point. Hence this curve between a fixed mixed venous and inspired gas tensions describes all possible gas tensions that could exist between a $\dot{V}_A/\dot{Q}$ = 0 (i.e. the mixed venous point) and a $\dot{V}_A/\dot{Q}$ = ∞ (the inspired gas tension). Although this graph is only drawn for pO_2 and pCO_2 the nitrogen tension can be calculated by subtracting the sum of the pO_2 and pCO_2 from the barometric pressure minus the water vapour pressure. Alternatively this graph may be redrawn with pN_2 as the abscissa and pCO_2 as the ordinate, which is particularly useful for some purposes. (Figure IV).

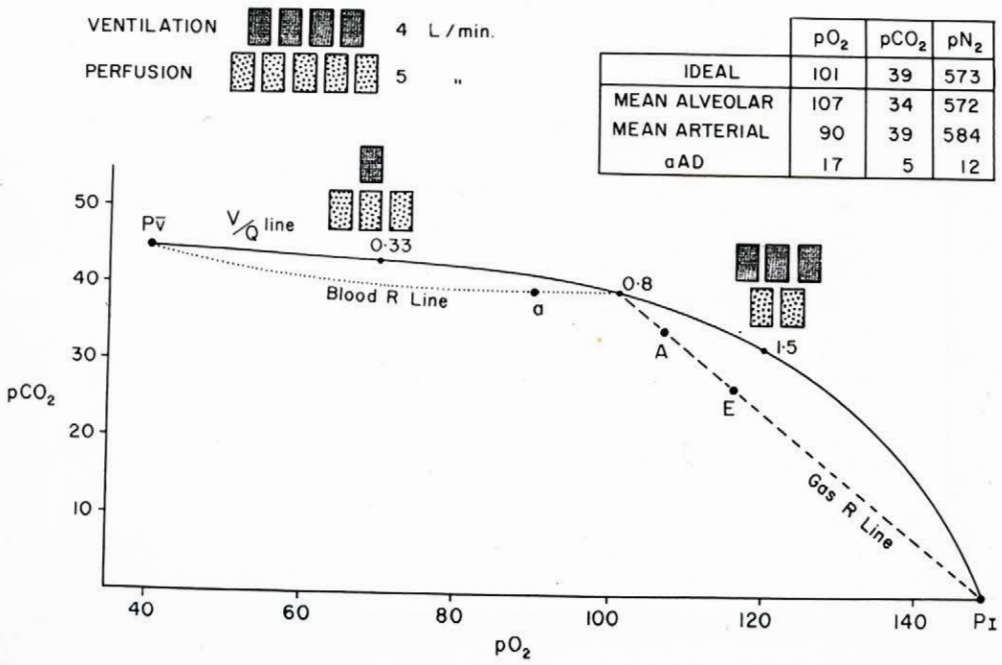

Figure II - Effect of unequal distribution on alveolar and arterial gas tensions. With an ideal $\dot{V}_A/\dot{Q}$ ratio = 0.8 ideal gas tensions would exist in the alveolar air and arterial blood. When there is unequal distribution between two units, their gas tensions will not be the same and there will be alveolar-arterial gas tension differences.

If the Ventilation/Perfusion ratio is the same throughout the lung, the alveolar gas tensions will be identical in all alveoli (Riley's Ideal Alveolar Air). Assuming that there is no diffusion defect or venous admixture the gas tensions in the capillaries will equal the alveolar gas tensions. However, if the Ventilation/Perfusion ratio is not equal throughout the lungs the arterial gas tensions cannot equal the alveolar gas tensions [36, 37]. Arterial alveolar differences (aAD) will occur for pO_2, pCO_2 and pN_2, which are characteristic of the type of underlying $\dot{V}/\dot{Q}$ abnormality. The way in which these arise is illustrated in Figure II. Given an Alveolar Ventilation = 4 l/min and Cardiac Output = 5 l/min and uniform distribution, the $\dot{V}/\dot{Q}$ ratio = 0.8 in all alveoli and the gas tensions will be pO_2 = 101, pCO_2 = 39 and pN_2 = 573. If there is no venous admixture or diffusion defect the tensions will be exactly the same in the arterial blood. If the ventilation and perfusion are unevenly distributed as illustrated in Figure II, the $\dot{V}_A/\dot{Q}$ of one lung would be 0.33 and 1.5 in the other. Three times as much of the alveolar gas is contributed by the high $\dot{V}_A/\dot{Q}$ lung so that the mean alveolar gas tensions will be closer to the gas tensions of the high $\dot{V}_A/\dot{Q}$ lung. The reverse is true for the mixed arterial gas tensions as more blood is contributed from the low $\dot{V}_A/\dot{Q}$ lung. As a result there is an aAD_{O_2} = 17, aAD_{CO_2} = 5 and an $aADN_2$ = 12. In the case of pure distribution defects these differences should be approximately equal:

$$aAD_{O_2} = aADC_{O_2} + aADN_2$$

The effect of this distribution is to move the alveolar (A) point

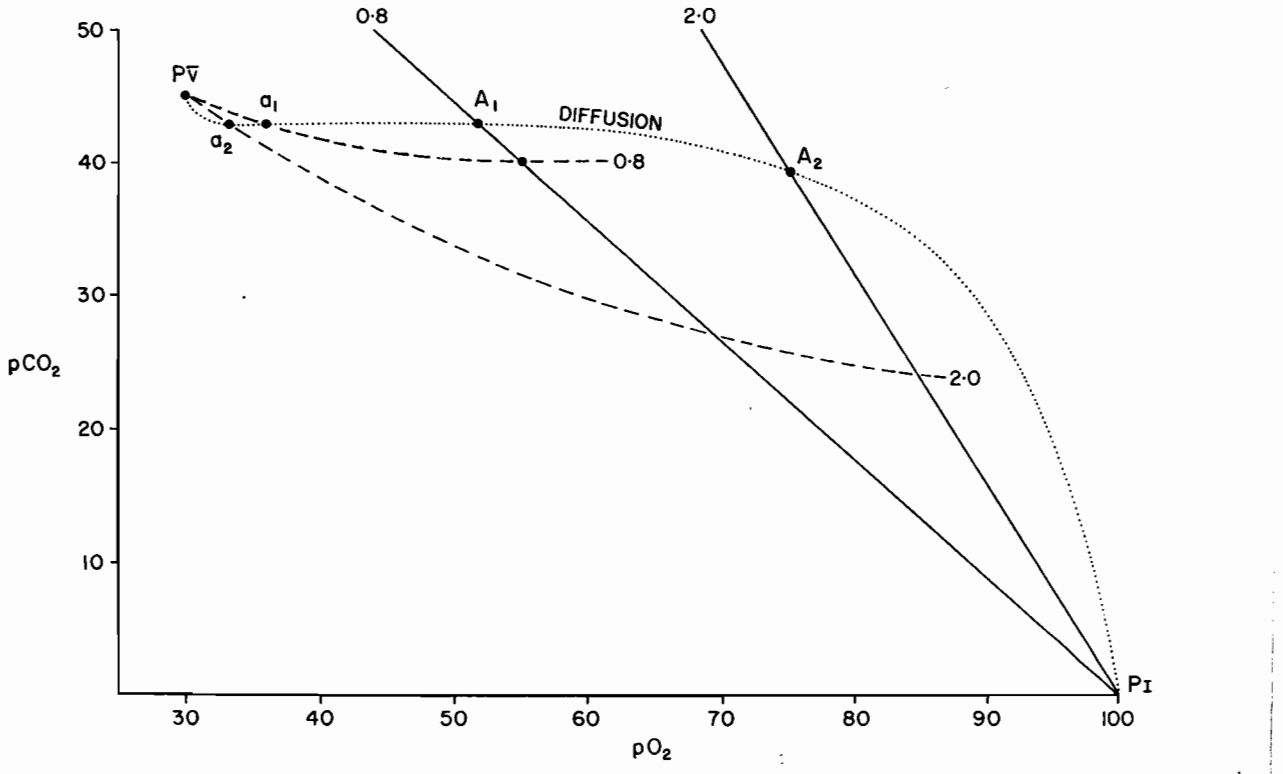

Figure III - Effect of diffusion defects on gas tensions. From the ideal point (blood and gas R = 0.8) a moderate diffusion defect will shift the alveolar tension to A_1 and the arterial tension to a_1. A severe diffusion defect will shift them to A_2 and a_2 on a higher R line. A large AD_{O_2} is produced but the $aADC_{O_2}$ is small. From Riley (32).

and the arterial (a) point away from the ideal alveolar air point and displace them respectively along the equal gas and blood R lines. The more severe the inequality of distribution the further they separate. The distance the alveolar point is displaced is proportional to the amount of "wasted" ventilation or "Air Shunt" [38]. Similarly the displacement of the arterial point is proportional to the "Blood shunt".

So far this discussion has pre-supposed no venous admixture or diffusion defect. Venous admixture (from bronchial veins or arterio-venous shunts) will lower the arterial pO_2 because of the large arterio-venous oxygen difference. However, because normally there is a small a - v CO_2 difference, unless the shunt is very large the change in arterial pCO_2 will be insignificant. Similarly there will be little effect on the pN_2 as there is no net nitrogen exchange in the lung.

Diffusion defects have much the same effect on arterial/alveolar differences. Riley [33] has drawn a theoretical diffusion defect curve on the O_2/CO_2 Diagram (Figure III) which shows the effect of increasing the diffusion defect on a lung with a uniform $\dot{V}/\dot{Q}$ ratio. With no diffusion defect the arterial and alveolar points would be superimposed at the Ideal Alveolar Air point (intersect of blood and gas R = 0.8). With a diffusion defect the arterial and alveolar points move along their respective R lines to points a_1 and A_1, producing a large $aADO_2$ but no significant $aADCO_2$ because of the much greater diffusivity of CO_2. With a very severe diffusion defect the RQ of the system must rise and the points move to the R = 2 line to a_2 and A_2. Only under these extreme conditions

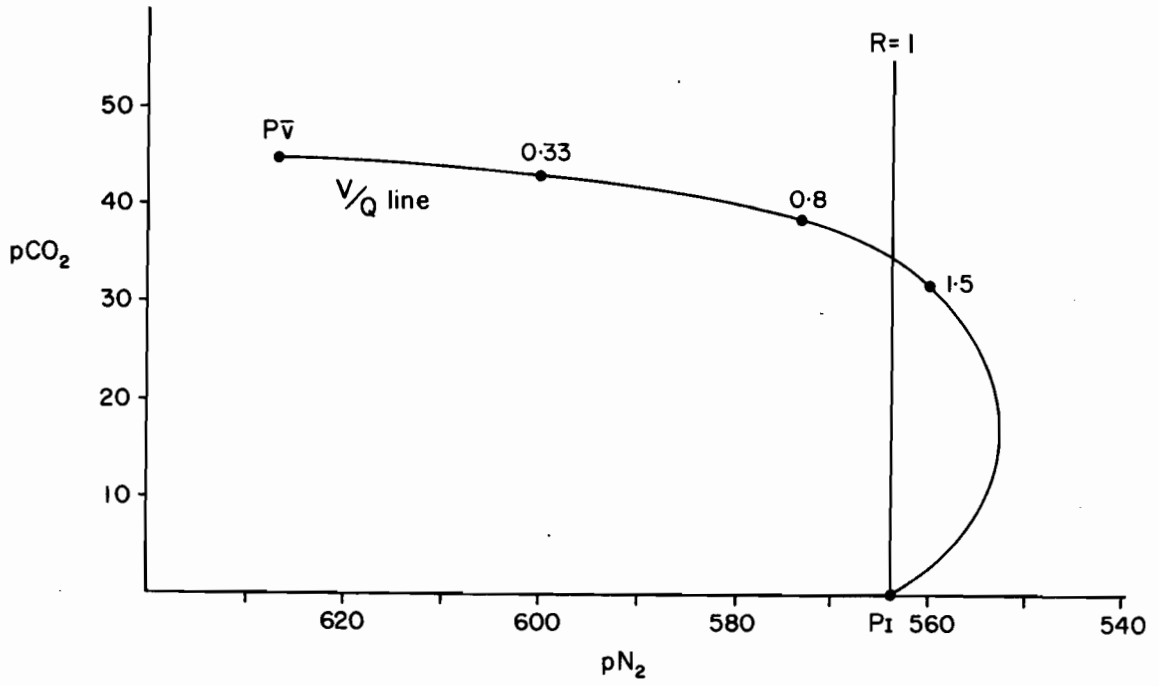

Figure IV - $\dot{V}_A/\dot{Q}$ curve on the N_2:$C0_2$ Diagram. Over the low $\dot{V}_A/\dot{Q}$ range there is a large change in pN_2 and little change in $pC0_2$. Over the high $\dot{V}_A/\dot{Q}$ range there is a large change in $pC0_2$ and little change in pN_2. From Rahn (34).

is there any $aADCO_2$. As the net nitrogen exchange in the lung is zero, the $aADN_2$ is also relatively uninfluenced by diffusion defects.

It should be noted that this discussion refers to pure diffusion defects, that is, the impedance between the alveolus and the red-cell. It does not apply to the measured diffusing capacity, which measures not only impedance across the membrane but is highly sensitive to abnormalities of the Ventilation/Perfusion ratio. This point will be elaborated later, because in some respects the diffusing capacity is a simple method of showing the presence of Ventilation/Perfusion abnormalities.

These considerations make arterial alveolar oxygen differences difficult to interpret and distribution problems are best studied by differences in CO_2 and N_2. For this purpose the N_2/CO_2 Diagram is particularly useful [39] (Figure IV). This diagram is constructed in basically the same way as the O_2/CO_2 diagram, and contains the same information. The value of this diagram is that it focuses attention on nitrogen, which has been the "Cinderella" of the respired gases [40] and shows how valuable it can be in differentiating patterns of $\dot{V}/\dot{Q}$ abnormality. Over the low $\dot{V}/\dot{Q}$ range the curve is practically horizontal; consequently regions with a low $\dot{V}/\dot{Q}$ ratio (0 to 0.8) will produce large arterial alveolar differences for pN_2, with little difference in the $aADCO_2$. Over the high $\dot{V}/\dot{Q}$ range (0.8 to 00) the curve is steep and therefore regions with a high V/Q ratio will produce a large $aADCO_2$ with little $aADN_2$. Therefore by measuring the arterial alveolar differences for CO_2 and N_2, the pattern of $\dot{V}/\dot{Q}$ distribution can be recognised.

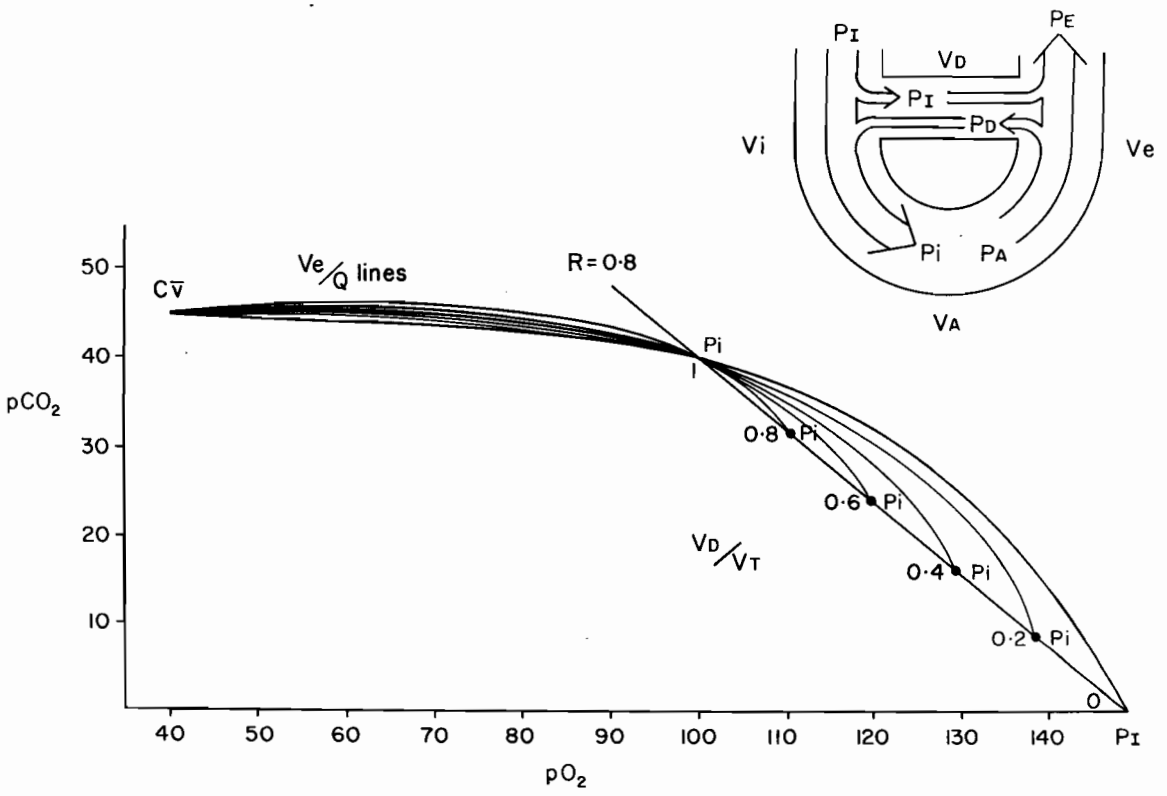

Figure V - The effect of dead space reflux on gas tensions. Inspired gas P_I mixes with dead space gas P_D and the gas reaching the alveolus has a tension Pi. The difference between P_I and Pi depends on the $V_D/\dot{V}_T$ ratio. The true origin of the $\dot{V}_A/\dot{Q}$ line is Pi and a family of curves can be constructed depending on the $V_D/\dot{V}_T$ ratio. From Ross (41).

The original approach to the relationship between the Ventilation/Perfusion ratio and the gas tensions has over-simplified the composition of the alveolar inspired air. The gas entering an alveolus from the dead space may differ from the gas composition in the alveolus for a number of reasons. If the inspired gas tensions are P_I (see inset of Figure V) this will be modified by contributions from the dead space P_D, so that the actual tensions entering the alveolus will be Pi. The magnitude of this effect will depend on the alveolar ratio of Dead Space Ventilation to Tidal Ventilation ($V_D/\dot{V}_T$). Ross and Fahri [41] have calculated the effect that variations of the $V_D/\dot{V}_T$ ratio will have on the alveolar gas tensions. This is illustrated in Figure V where the effects of $V_D/\dot{V}_T$ ratios from 0 to 1 have been calculated producing a family of $\dot{V}e/\dot{Q}$ lines. Essentially the reflux of dead space gas changes the inspired gas tension P_I to various Pi points, so that the $\dot{V}/\dot{Q}$ line changes its origin. The conclusion from such an analysis is depressing. As the $V_D/\dot{V}_T$ ratio of the alveolus is unknown it is impossible to know which $\dot{V}_e/\dot{Q}$ line to work on. The possible gas tensions are enclosed in an envelope and no longer precisely located on a single line. Presumably in normal subjects the alveolar $V_D/\dot{V}_T$ ratio is small and the error introduced by working off a standard $\dot{V}/\dot{Q}$ line drawn from P_I will be small. However, in patients with lung disease the presence of a large physiological dead space could introduce major problems in predictions between $\dot{V}/\dot{Q}$ and gas tension.

EXPERIMENTAL APPROACHES TO $\dot{V}/\dot{Q}$ VARIANCE OVER-ALL DISTRIBUTION

The experimental work on variations in the Ventilation/Perfusion ratio is, in general, less satisfying than the theoretical studies. This is inevitable, becuase it has been necessary to measure the remote effects of $\dot{V}/\dot{Q}$ variation on the arterial and alveolar gas tensions, and the argument back to the underlying cause is often tortuous. However, the following techniques have proved to be of considerable practical or theoretical value:

1. EQUIVALENT SHUNTS

This approach was introduced by Riley and Cournand [32, 33], and quantitates the discrepancy between the "Ideal Alveolar Air" and the measured arterial gas tension. Basically it divides the lung into three hypothetical groups of alveoli:

(a) Those with the "Ideal" $\dot{V}/\dot{Q}$ ratio.

(b) Those with ventilation in excess of perfusion, with a higher than the "Ideal" $\dot{V}/\dot{Q}$ (Equivalent Air Shunt).

(c) Those with perfusion in excess of ventilation with a lower than "Ideal" $\dot{V}/\dot{Q}$ (Equivalent Blood Shunt).

The "Air Shunt" component is calculated from manipulation of the Bohr Dead Space equation.

$$(1)\quad V_D(ANAT) = \frac{(P_{AC0_2} - P_{EC0_2})}{P_{AC0_2}} \dot{V}T$$

If the distribution of $\dot{V}/\dot{Q}$ ratios is uniform the alveolar and

arterial gas tensions are equal and (assuming alveolar gas can be adequately measured) the same value for dead space will be obtained using $P_{A}C0_2$ or $P_{a}C0_2$ in equation (1). However, if there is variation in $\dot{V}/\dot{Q}$ ratios within the lung some alveoli will be ventilated in excess of the perfusion and behave as if they were relatively dead space. As a consequence of the $\dot{V}/\dot{Q}$ variance an $aADC0_2$ will exist, proportional to the magnitude of the variance. If the arterial value is now used in the Bohr equation:

$$(2)\quad V_D\,(phys) = \frac{(Pa C0_2 - PE C0_2)\ \dot{V}T}{PaC0_2}$$

a higher value for the dead space will be obtained which is known as the Physiological Dead Space. The difference between the Anatomic Dead Space calculated from Equation (1) and the Physiologic Dead Space from Equation (2) is the Alveolar Dead Space which is a function of the ventilation of the non-perfused or under-perfused alveoli. This alveolar dead space volume is purely hypothetical, any alveolus with a higher than ideal $\dot{V}/\dot{Q}$ contributes to it; if an alveolus is at a slightly higher $\dot{V}/\dot{Q}$, it only contributes a fraction of its ventilation; only alveoli that are not perfused ($\dot{V}/\dot{Q}$ - ∞) contribute their whole ventilation.

Variations in the physiological dead space have been used extensively [42,-44] to infer changes in the distribution of perfusion, without always appreciating how insensitive a measurement this is. The calculation depends on the arterial $pC0_2$, which is primarily determined by the low $\dot{V}/\dot{Q}$ regions (where most of the blood is coming from). As the $\dot{V}/\dot{Q}$

line on the O_2/CO_2 Diagram is practically flat over the low $\dot{V}/\dot{Q}$ range, little change will occur in the arterial pCO_2 despite large changes in the distribution of blood flow. This has recently been confirmed by Sheppard [44] by an analog computer analysis of a two alveolus model.

The measurement of the "Equivalent Blood Shunt" was also originally described by Riley and Cournand [33]. Since the amount of oxygen in the arterial blood equals the amount of oxygen from the pulmonary capillaries plus the amount of oxygen in the shunted blood, then:

(1) $Ca_{O_2} \cdot \dot{Q} = C\acute{c}_{O_2} \cdot \dot{Q}c + C\bar{v}_{O_2} \cdot \dot{Q}s$

where $\dot{Q}$ is the total flow, $\dot{Q}c$ the capillary flow and $\dot{Q}s$ the shunt flow.

As $\dot{Q}c = \dot{Q} - \dot{Q}s$ equation (1) becomes:

(2) $Ca_{O_2}\, \dot{Q} = C\acute{c}_{O_2}\, (\dot{Q} - Qs) + C\bar{v}_{O_2}\, \dot{Q}s$

or re-arranging (2),

(3) $$\dot{Q}s = \frac{Ca_{O_2} - C\acute{c}_{O_2}}{C\bar{v}_{O_2} - C\acute{c}_{O_2}}$$

Ca_{O_2}, $C\bar{v}_{O_2}$ and Q can be measured but $C\acute{c}_{O_2}$, the end capillary oxygen tension cannot be obtained directly. It has to be calculated by Bohr integration or by the trial and error method of Lillienthal [45].

The value for shunt flow obtained includes both the true anatomical shunt and the contributions from alveoli with low $\dot{V}/\dot{Q}$ that are functionally shunting blood. The latter is included because the end-capillary oxygen is calculated in a way which deliberately excludes any effect due to non-uniform $\dot{V}/\dot{Q}$ ratios. One technique to separate the anatomical shunt is to repeat these measurements after breathing 100% oxygen. At high oxygen

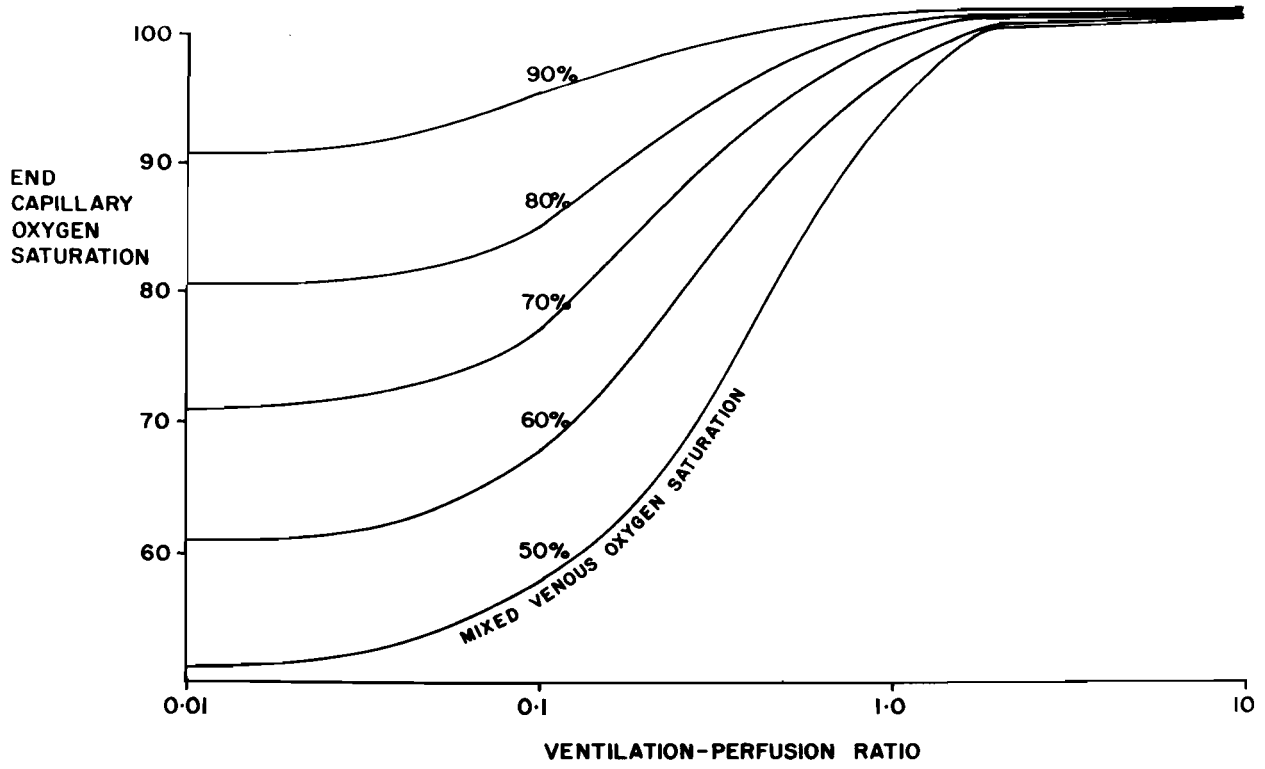

Figure VI - Relationship between the $\dot{V}_A/\dot{Q}$ ratio and the end capillary oxygen tension at various levels of mixed venous oxygen saturation. At low $\dot{V}_A/\dot{Q}$ ratios, $S\bar{v}O_2$ has a great effect on the end capillary oxygen tension.

tensions the $aAD0_2$ due to $\dot{V}/\dot{Q}$ variance becomes negligible in the calculation of shunt flow. Unfortunately at high oxygen tensions accurate measurements of oxygen content differences is difficult. An alternative and more elegant way of partitioning the blood shunt is to utilise the $aADN_2$ [39]. Blood from pure anatomical shunts does not alter its nitrogen content. However, blood returning from alveoli with a low $\dot{V}/\dot{Q}$ ratio will have a higher than "ideal" nitrogen tension. Therefore, the $aADN_2$ is only produced by the $\dot{V}/\dot{Q}$ abnormality. A mixing equation similar to that for oxygen can be applied which gives the volume of equivalent blood shunt due to $\dot{V}/\dot{Q}$ distribution effects.

2. NITROGEN WASHOUT AND 0_2 SATURATION METHOD

This method has been described in a series of papers by Briscoe [46, 47]. On the basis of nitrogen washout curves they have concluded that in Emphysema there is a large homogeneous, poorly ventilated space. In contrast the well ventilated alveoli are a smaller volume and do not have a homogeneous ventilation, however, the ventilation is quite adequate to fully saturate the blood passing by them. The oxygen saturation of blood leaving an alveolus cannot exceed a limit determined by its Ventilation/Perfusion ratio and the mixed venous saturation; these limits were calculated by Briscoe (Figure VI). From this he has argued that the amount of perfusion going to the homogeneous poorly ventilated space must impose an upper limit on the arterial oxygen saturation. Therefore, if the arterial and mixed venous oxygen saturations, and the cardiac output are known an upper limit can be placed on

the amount of perfusion going to the slow space to give the observed oxygen saturation.

The objection to this procedure is the assumption of a large homogeneously ventilated slow space existing as a general rule in emphysema. It is probable that this extraordinary distribution is an artefact, due to limitations of the resolution of the nitrogen meter and incomplete mathematical analysis of the washout curve. Despite this criticism the data reported with this technique compares well with other methods of analysis (aAD). Because the normal washout curve does not show such a ventilation distribution this technique cannot be applied to normal subjects.

3. KRYPTON METHODS

When radio-active Krypton^{85} is injected intravenously about 98% passes into the alveolar spaces during the first circulation because its blood/air partition coefficient is 1:17 (48, 49). This Kr^{85} is washed out of the lungs during subsequent respirations and its washout can be followed by analysis of the expired air. In emphysema, the fast spaces wash out Krypton rapidly, but the washout from the slow spaces is very prolonged. The amount of Kr^{85} in the "slow spaces" is proportional to the blood flow to the slow spaces. Hence the fraction of Krypton that is slowly eliminated is the same as the fraction of the cardiac output perfusing the slow spaces. As the ventilation of the slow space is "known" from the nitrogen washout curve (see above), the $\dot{V}/\dot{Q}$ ratio of the slow space can be determined. This technique has the same inherent dangers as the analysis of the nitrogen washout curve, magnified by the poor resolution of radio-

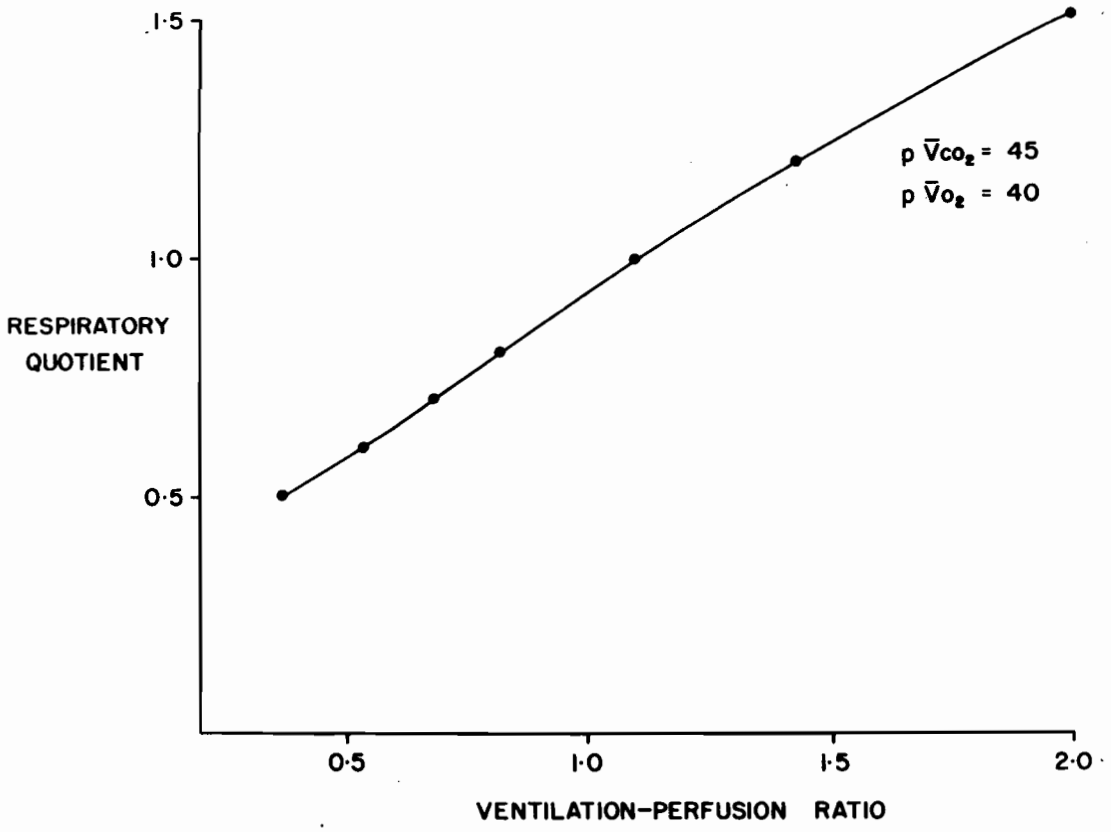

Figure VII - Relationship between RQ and $\dot{V}_A/\dot{Q}$ ratio for a given set of mixed venous gas tensions.

active counting techniques. Our experience with the analysis of washout of radio-active Xenon^{133} has been that exact mathematical analysis of the curve into compartments is not feasible.

Using the same basic technique a further method of partitioning flow has been described by the same group (50). After the Krypton^{85} has been deposited in the alveoli some will re-enter the capillary blood. After the fast spaces have washed out, the only Krypton^{85} entering the blood will be from the slow spaces. Then "knowing" the ventilation of the slow space, the expired Krypton^{85} concentration and the arterial Krypton^{85} concentration, the fractional perfusion of the slow space can be determined. This method again depends on confidence in the reality of homogeneous slow spaces.

4. VARIATIONS IN EXPIRED R.Q.

Sequential sampling of a single expirate shows changes in the relative concentrations of the gases. Roelsen (51) showed that the respiratory quotient decreased throughout expiration, particularly in patients with lung disease. The respiratory quotient and the Ventilation/Perfusion ratio are closely related to each other. If the mixed venous and inspired gas tensions are known, the $\dot{V}/\dot{Q}$ can be obtained from the R.Q. and vice versa, with the aid of the $0_2/C0_2$ Diagram. A graph of the R.Q. and $\dot{V}/\dot{Q}$ is shown in Figure VII. West (52, 53, 54) has utilised this relationship to study $\dot{V}/\dot{Q}$ variation by continuous analysis with a Mass Spectrometer of the gas tensions in a single expirate. In this technique oxygen, carbon dioxide, nitrogen and argon tensions were continuously monitored at the

mouth. From this the variation of the R.Q. during expiration was calculated and equated with variation in the $\dot{V}_A/\dot{Q}$ ratio. Ventilation inequality could be calculated from the argon variation, and by dividing one into the other an expression of perfusion inequality could be obtained. They showed a $\dot{V}_A/\dot{Q}$ variation in normal subjects and a much bigger variation in emphysema. There are theoretical objections to this technique. While R. and $\dot{V}_A/\dot{Q}$ are related, the variation of R. at the mouth is a very indirect and rather misleading indication of $\dot{V}_A/\dot{Q}$ variation. The theory of variations in expired gas composition is dealt with in the Discussion on Alveolar Air. A more important objection is that the variation in gas composition depends on the emptying pattern of the lung. There will be a much greater variation if there is sequential emptying of lung units than when the emptying time constants are equal. Thus the greater variation in emphysema might be caused more by altered mechanics than by an abnormal $\dot{V}_A/\dot{Q}$ distribution.

REGIONAL DISTRIBUTION

1. LOBAR SAMPLING

Martin [10] in 1953 reported studies on the lobar gas concentrations in man. Radio-opaque catheters were passed into the upper and lower lobe bronchi from which samples were taken during the last third of expiration and analysed for oxygen and carbon dioxide. Studies were carried out in the upright and supine positions. The results showed a significantly higher oxygen and lower carbon dioxide concentration in the upper lobe in the upright position. In the supine position these differences disappear. In the upright position the upper lobe R.Q. was 0.74 and the lower lobe R.Q. was 0.6. In the supine position there was no significant difference between the lobar R.Q.'s. The authors concluded that these changes must be due to a gravitational redistribution of perfusion. Assuming normal mixed venous tensions, it is possible to estimate the lobar $\dot{V}/\dot{Q}$ ratios from this data using Figure VII. The upper lobe $\dot{V}/\dot{Q}$ ratio is approximately 0.65 and the lower lobe 0.46. As the R.Q. falls during expiration and sampling occurred during the last third of expiration, both lobes reflect their lowest R.Q. and $\dot{V}/\dot{Q}$, which explains the apparent low over-all $\dot{V}/\dot{Q}$. Furthermore, this does not demonstrate the whole range of $\dot{V}/\dot{Q}$ variation, only the lower limit.

Similar results were obtained by Rahn [55] in upright and supine dogs and in this paper the relationship between R.Q. and $\dot{V}/\dot{Q}$ was clearly defined.

The most elegant development of this technique has been by continuous recording of lobar gas tensions with a Mass Spectrometer, reported by West [56] and Hugh Jones [57]. The method is a regional application of their technique of assessing $\dot{V}/\dot{Q}$ abnormality at the mouth and depends on the recognition of patterns of gas concentration within the bronchial tree. Although the method has not been reported quantitatively in man, its underlying principles are interesting. The lobar oxygen, carbon dioxide and argon concentrations are sampled by a catheter, whose tip is protected by a "basket". Once the catheter is in the desired location, the bronchoscope is withdrawn into the trachea to minimize interference with gas flow. From the expiratory plateaux of 0_2 and $C0_2$ the R.Q. and hence the $\dot{V}/\dot{Q}$ ratio can be derived. Following a single breath of argon the peak inspired concentration is recorded and the plateau during the subsequent expiration is proportional to the distribution of argon within the lobe and is, therefore, a measure of ventilation per unit volume. Obstruction to blood flow can be recognized by a reduction in the $C0_2$ and rise in the 0_2 plateau, with no change in the argon plateau. Partial obstruction to ventilation gives opposite changes in $p0_2$ and $pC0_2$ and the argon plateau is reduced. Furthermore, reflux of dead space gas and "Pendeluft" respiration can be recognized by characteristic "pips" on the tension records. Postural differences have been noted, particularly in the right middle lobe, which shows a pattern characteristic of "obstructed" blood flow and normal ventilation. This is presumably because, with the patient on his back the right middle

	RIGHT UPPER LOBE AS PERCENTAGE OF RIGHT LUNG			
	SUPINE		ERECT	
	$\dot{V}A$	$\dot{V}O_2$	$\dot{V}A$	$\dot{V}O_2$
MATTSON & CARLENS	39 %	37 %	38 %	18 %
MARTIN & YOUNG	40 %	37 %	40 %	21 %

Table I - Comparison of lobar spirometry data from Mattson[13] and Martin[11].

lobe is uppermost and is relatively under-perfused. This method appears to be an extremely useful clinical method for lobar localization of Ventilation/Perfusion abnormalities. Its greatest disadvantage is that it requires intra-bronchial instrumentation which may distort the normal behaviour of the lung.

2. LOBAR SPIROMETRY

The introduction of cuffed double lumen bronchial catheters made it possible to isolate the two lungs for separate study. A number of studies [58, 59] have been performed comparing the ventilation and oxygen uptake of the two lungs in the lateral decubitus position. These have all shown striking increases in the oxygen consumption of the "down lung" without accompanying changes in ventilation, suggesting that perfusion had increased in the "down lung".

These studies were advanced by Mattson and Carlens [13] using a triple lumen catheter with which it was possible to isolate and measure the oxygen uptake and ventilation of separate lobes. They studied seven patients with minimal tuberculosis and compared the right upper lobe to the middle and lower lobes of the right lung. Martin and Young [11, 12] carried out a larger series of experiments in normal subjects and patients. The values for the right upper lobe as a percentage of the right lung total have been extracted from their normal data and presented in Table 1. There is excellent agreement between the two sets of data. They show that, in the erect position, the oxygen consumption of the upper lobe is small but that there is a dramatic increase when the subject

is tilted into the supine position. There is little or no change in the fraction of ventilation going to the upper lobe with change in position.

It is not possible to derive absolute $\dot{V}/\dot{Q}$ ratios from these studies, but the relative $\dot{V}/\dot{Q}$ ratios between lobes can be estimated. It is necessary to assume that the ratio of dead space to tidal ventilation is the same for both lobes. It is also necessary to assume that oxygen uptake is directly related to relative flow, i.e. that there is no distribution or diffusion defect within the lobe. This will be true for Mattson's study where the patients were breathing 100% oxygen, and nearly true for Martin's where the subjects breathed air. Calculations from Mattson's data indicate that in the erect position the $\dot{V}/\dot{Q}$ ratio of the upper lobe is 2.7 times higher than the lower lobe ratio. Similar calculations from Martin's data make the upper lobe 2.5 times higher. These must be regarded as the minimum differences, because further $\dot{V}/\dot{Q}$ variance is to be expected within the lobes.

These studies conclusively proved the existance of a postural dependent $\dot{V}/\dot{Q}$ variance due to the effect of gravity on the distribution of perfusion. However, the method has some serious disadvantages. In both studies the mean ventilation and oxygen uptake were very high for "Resting" studies. Also the cardiac output may have been high due to apprehension, or low due to impending syncope (in one case reported by Mattson). As the size of the tidal volume influences ventilation distribution and small changes in perfusion pressure alter perfusion distribution, these results must be interpreted with caution. Finally the influence of

a triple lumen catheter on regional airway resistance must be considered before interpreting small differences in ventilation distribution.

3. RADIO-ACTIVE OXYGEN - 15

A most important development in this field was the use of radio-active oxygen - 15, to study regional lung function. The technique was first described by the Hammersmith group in 1958 [60]. Oxygen - 15 (15_{O_2}) is prepared by deuteron bombardment of nitrogen in a cyclotron. As the half life of this isotope is only 2 minutes, the laboratory must be adjacent to the cyclotron. It decays by the emission of positrons which are almost immediately annihilated by combination with electrons, producing high energy gamma radiation, which is usually emitted as two photons which travel in almost exactly opposite directions. Because of this property, coincidence counting can be used, that is, in a pair of scintillation detectors only the simultaneous arrival of gamma rays is recorded. This allows a very high spatial resolution of the counting field and in these studies the counting field could be reduced to a 4 cm diameter core of lung. However, high spatial resolution produces low count rates. Where higher count rates were desirable (i.e. clearance slopes) they used parallel counting, without coincidence recording which increased the core of lung to approximately 9 cm diameter [61].

The procedure is basically simple (once the 15_{O_2} has been produced). Two pairs of parallel counters are placed over symmetrical points of the left and right chest. The subject inhales 900 ml of air containing a trace of 15_{O_2} and breath-holds for 10 seconds. As the air

containing the radio-active gas enters the counting field the count-rate rises rapidly to a peak, during the subsequent period of breath-holding the count-rate falls as the $15O_2$ is removed by the local blood flow. Measurement of the initial peak activity (extrapolated back to time zero) is proportional to the ventilation per unit volume. Measurement of the rate of clearance during breath-holding is proportional to the local pulmonary blood flow. The experiment is then repeated with different counter positions. Generally six breaths are taken, giving a maximum radiation dose of approximately 400 millirads [62,63].

The measurement of the $15O_2$ clearance slope was not entirely satisfactory. In 1960 West and Dollery [63] reported a considerable improvement in the method in which the labelled oxygen was converted into carbon dioxide $C^{15}O_2$. Carbon dioxide is so diffusible (alveolar clearance $>$ 100% per second) that a rapid inspiration of the gas can be regarded as an instantaneous injection into the pulmonary circulation[64]. Using the same single breath, breath-holding technique the clearance slopes are much easier to analyse and are more repeatable. The rapid uptake of $C^{15}O_2$ may seem incongruous as there is a net CO_2 excretion in the alveoli. In fact CO_2 is passing both ways, from blood to alveolus and from alveolus to blood, but only the latter is labelled. Furthermore, in the blood the CO_2 rapidly forms bicarbonate and there is a very free exchange of oxygen atoms between bicarbonate ions and the hydroxyl ions of water [65]. In effect this exchange greatly increases the capacity of the blood for $C^{15}O_2$ because the activity leaks away into the large

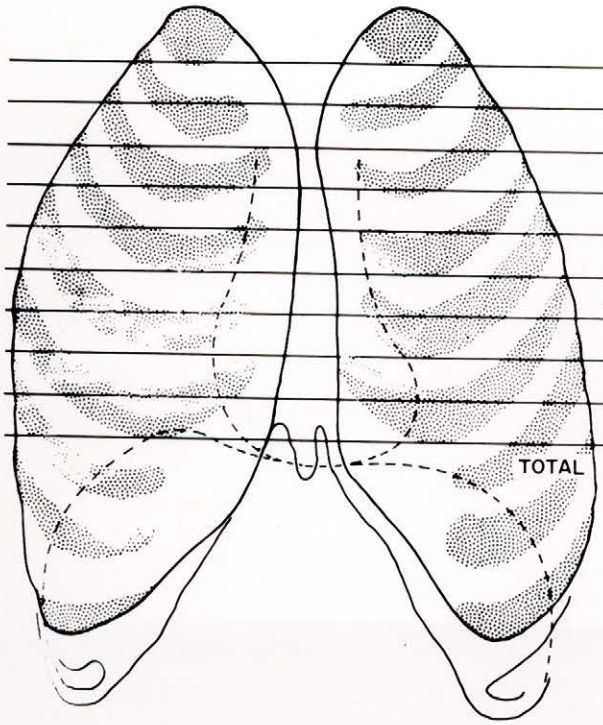

Vol. %	$\dot{V}_A$ litres	$\dot{Q}$ /min.	$\dot{V}_A/\dot{Q}$	P_{O_2} mm Hg	P_{CO_2} mm Hg	P_{N_2} mm Hg	R
7	·24	·07	3·3	132	28	553	2·0
8	·33	·19	1·8	121	34	558	1·3
10	·42	·33	1·3	114	37	562	1·1
11	·52	·50	1·0	108	39	566	·92
12	·59	·66	0·90	102	40	571	·85
13	·67	·83	0·80	98	41	574	·78
13	·72	·98	0·73	95	41	577	·73
13	·78	1·15	0·68	92	42	579	·68
13	·82	1·29	0·63	89	42	582	·65
100	5·09	6·00					

Mixed Alveolar	101	39	572
Mixed arterial	97	40	575
A-a diff.	4	1	3

Figure VIII - Ventilation and perfusion distribution and regional gas tensions calculated from the $C^{15}O_2$ data. From West (63).

oxygen pool of water. The clearance of Carbon-11 labelled carbon-dioxide is only half as fast as Oxygen - 15 labelled CO_2 because the labelled carbon does not disappear into the water pool.

West and Dollery [63] used Oxygen - 15 labelled carbon dioxide to study the regional ventilation and perfusion in a group of sixteen normal subjects seated at rest and made some observations on the perfusion in the supine position and after exercise. By volume weighing the regional measurements they were able to express the local ventilation and perfusion in litres/minute and derive the Ventilation/Perfusion ratio for each region. In subsequent papers West [66, 67] has brilliantly exploited this data to demonstrate the consequences of their observed distribution of $\dot{V}_A/\dot{Q}$ ratios. From an O_2/CO_2 Diagram with assumed mixed venous tensions he has calculated the regional gas tensions. His results are shown in Figure VIII and they demonstrate the great variations that must exist within the lung for all three gas tensions. From this he showed that the oxygen uptake varies greatly down the lung and is nearly proportional to the difference in blood flow. The carbon dioxide uptake varies much less and is more closely related to the ventilation difference. The behaviour of nitrogen is extraordinary, it must leave the blood at the top and enter at the bottom, the net exchange being zero.

These papers are classics, which finally destroy the concept of the normal lung as a box with uniform behaviour. However, it is rather easy to be blinded by the excellent theoretical development to some of the fundamental uncertainty involved in the original measurements. West[66]

has expressed this very clearly: "It should be emphasized that this lung model does not purport to be an accurate representation of the average regional differences in upright man, but rather the aim is to portray the general pattern of gas exchange which will occur if blood flow and ventilation have the distribution indicated by the radio-active gas measurements. These measurements have limitations which must be borne in mind. In particular, the clearance rate of radio-active carbon dioxide measures the rate of loss of labelled blood from the counting field, not the pulmonary capillary flow".

There are indeed good grounds for doubting the absolute accuracy of the perfusion measurements. Experience with attempts to deduce exponentials from radio-active washout curves has convinced us that often considerable imagination has to be used. Generally the lower the initial count rate and the slower the decline, the more difficult it becomes and this must apply to the critical measurements of $C^{15}O_2$ clearance at the top of the lung. It should also be noted that this method only measures the perfusion of ventilated alveoli. West and his colleagues have published a paper [64] on the interpretation of the radio-active gas clearance rates in the lung; however, the interpretation is by no means clear. In the results, the $C^{15}O_2$ clearance is measured as a single exponential, while there is no good reason why it should be an exponential. Furthermore, there appears to be a considerable discrepancy between the $C^{15}O_2$ clearance rate and the $^{15}O_2$ "transfer rate" which they derive, both of which should be proportional to the blood flow. Their conclusion is that the

clearance rate will be determined by the transit time of the label through the counting field. As the label is on the oxygen which rapidly exchanges with the oxygen of water, this may diffuse out of the blood into the lung tissue fluid and delay the clearance rate. "If this occurs the inequality of blood flow between the upper and lower zones may be exaggerated".

West has pointed out (63) that the "inaccuracies of the method used for measuring uneven ventilation hardly need stressing"; however, he also points out, that as the ventilatory inequality is relatively small, these inaccuracies are relatively unimportant in the final calculations. The count rate at end-inspiration is proportional to the local ventilation per unit volume, and the volume of lung in the counting field. It is also dependent on a variety of counting factors: detector sensitivity, distance from the chest, the geometry of the chest wall, its thickness and its consistency. Simply dividing the peak count rate by the AP diameter of chest is therefore only an approximate measure of ventilation per unit volume.

Despite these criticisms the model of distribution obtained by $C^{15}O_2$ is probably generally correct and the use that West has made of it is of great importance to pulmonary physiology. The fact that subsequent studies will revise some of the numbers need not detract from this.

4. $XENON^{133}$

The use of radio-active $Xenon^{133}$ as a tracer gas for assessing regional ventilation was first reported by Knipping in 1955 (68). They used multiple Geiger counters (from 16 to 64) over the chest and monitored the regional wash-in and washout curves. In this way they were able to

detect poorly ventilated or non-ventilated regions of the lung. In subsequent papers [69 - 74] the clinical value of this technique was demonstrated. However, they were not able to effectively quantitate their results. The records had to be analyzed by comparing the outputs from counters over symmetrical lung fields. To make this comparison less subjective the area under the curves was planimetered, which is only satisfactory in fairly severe cases of regional obstruction. For this reason, this work, apart from the original brilliant choice of isotope, proved of limited value.

The full potential of $Xenon^{133}$ was not realized until the work of Ball, Stewart, Newsham and Bates [75] at this laboratory. This work contained two major advances.

(1) A method was devised by which the regional concentration of $Xenon^{133}$ within the lungs could be derived from the external count rate. This method depends on equilibrating the subject with a known concentration of $Xenon^{133}$. The count rate recorded at equilibrium from each counter gives a count rate/concentration calibration factor. If the relationship between the counter and the subject remains constant this calibration factor can be used to solve subsequent unknown concentrations of $Xenon^{133}$ in the lung from the external count rate.

(2) A method was described by which the regional pulmonary blood flow could be measured using $Xenon^{133}$. Xenon has a low solubility (α = 0.0845 ml Xe/ml H_2O at 760 mm. Hg). If Xenon is dissolved in saline and injected intravenously it

will come out of solution as soon as it meets a blood:gas interface in the lung. Approximately 95% of the injected Xenon is cleared into the lung during the first circulation and the amount cleared into any region must be proportional to the regional blood flow.

It therefore became possible to measure the regional distribution of both ventilation and perfusion by calculating the regional concentration of $Xenon^{133}$ after respectively a single breath or an intravenous injection of $Xenon^{133}$. Measurements of regional concentration are proportional to the distribution per unit volume. The original paper [75] described the basic method and the results of ventilation and perfusion distribution in seated normal subjects and in selected patients. Subsequently it has been found that the single breath method of measuring ventilation distribution had serious limitations, particularly in patients with lung disease. Bentivoglio and his colleagues[76] developed a much more informative method of measuring ventilation from the regional wash-in curves. Bryan [77] has described a further method of measuring ventilation from the washout curve of injected $Xenon^{133}$, which has particular value in patients with Ventilation/Perfusion abnormality.

METHOD

PROPERTIES OF XENON

Xenon which means the stranger in Greek, is the rarest of the group of noble gases with a concentration in air of only $1 \times 10^{-5}\%$ It was discovered in 1898 by Ramsay and Travers in the final residue obtained after the evaporation of liquid air. It has excited little interest in the past, although the Handbook of Chemistry and Physics[128], a book not noted for lyricism, does describe the "beautiful blue glow" in vacuum tubes. It has an Atomic number 54 and an Atomic weight of 131.3. Xenon has always been regarded as one of the inert, noble gases belonging to Group VIII-A of the Periodic Table because the orbital election shells were filled and therefore the valence zero. However, recently both the classical theory of valency and the "nobility" of Xenon have been questioned as Xenon will form chemical compounds with Fluorine rather easily [129]. The only physical property of Xenon that is relevant to this study is its solubility characteristics which have an important influence on the method.

XENON SOLUBILITY

Xenon has an almost ideal solubility for respiratory studies. In pulmonary physiology solubility is usually defined by the Bunsen solubility coefficient α which is the amount of gas (in milliliters STPD) which will dissolve in 1 ml of a liquid at a specified temperature and a gas pressure of 760 mm. Hg. The Handbook of Chemistry and Physics[128] only gives Henry's solubility constant K for Xenon and the Bunsen coefficient

has to be derived from this as follows:

1. $K = \frac{P}{X} \quad 10^{-7}$

where P is the partial pressure and X is the mole fraction of the gas, or

2. $X = \frac{\text{Moles of gas}}{\text{Moles in solution}} = \frac{\text{Vol. Gas/22.4 liters}}{\text{Vol. } H_2O\text{/18 ml}}$

Re-arranging 2:

3. $X = \frac{18}{22,400} \times \frac{\text{vol. gas}}{\text{vol. } H_2O}$

As the volume in the gas phase over the volume in the liquid phase is the Bunsen coefficient α, Equation 3 can be re-written:

4. $X = \frac{18}{22,400} \alpha$

Re-arranging 4:

5. $\alpha = 1.245 \times 10^3 X$

Substituting this into Equation 1;

6. $\alpha = 1.245 \times 10^3 \times 10^{-7} \quad \frac{760}{K}$

Clearing 6:

7. $\alpha = \frac{0.0946}{K}$

The following values for Henry's constant $K \times 10^{-7}$ are given for Xenon in the Handbook of Chemistry and Physics:

At 0° C. $K = 0.392$

At 20° C. $K = 0.742$

At 38° C. $K = 1.12$

Utilizing these values to solve the Xenon Bunsen coefficient from Equation 7 gives the following values (with values for oxygen and carbon dioxide for comparison):

	0°C.	20°C.	38°C.
Xenon	0.241	0.128	0.0845
Oxygen	0.0495	0.031	0.0234
Carbon dioxide	1.705	0.876	0.563

Therefore, at 38°C., 19 ml of water will contain 0.845 ml of Xenon at equilibrium when the pXe is 760 mm. Hg. At BTPS (that is pXe 760-47). 10 ml of water will contain 0.79 ml of Xenon. An alternative way of expressing this is by the gas/liquid partition coefficient, which is the amount of Xenon present at equilibrium in equal volumes of gas and liquid. At BTPS the gas/water partition coefficient is 12.7. Xenon is, therefore, a relatively insoluble gas (only one seventh the solubility of CO_2, but three times as soluble as oxygen).

The partition coefficient of Xenon with various physiological tissues has recently been carefully studied by Conn[130]. He gives the following values:

Tissue	Counts/min/g. tissue / Counts/min/g. H_2O	Tissue: Blood / Partition coefficient
Water	1.0	0.4
Plasma	1.45	0.58
Whole blood	2.49	1.00
R.B.C.	3.75	1.51
Fat	19.7	7.94
Skeletal muscle	1.62	0.65
Cardiac muscle	1.79	0.72
Grey matter	1.84	0.74
White matter	3.0	1.14

Its affinity for the red blood cell is surprising, but Conn[130] concludes that this is a solubility or quasi-solubility phenomenon and not an active linkage. An exact partition coefficient with whole blood can only be determined by individual experiment as there are considerable variations in

hemoglobin concentration, serum glyceride level, etc. However, using the above date the gas/blood partition coefficient is approximately 5.12 and the gas/plasma coefficient 8.75.

This solubility data is of fundamental importance to the Xenon^{133} technique as it governs the movement of Xenon^{133} between the gas phase in the lung and solution in the tissues. There is insufficient data to make exact calculations but the following approximations do reveal the order of magnitude of movement between the two phases:

1. UPTAKE OF INHALED XENON

If a single breath of Xenon is taken and diluted in an alveolar volume of 4 liters, with a cardiac output of 5 liters per minute, some Xenon is going to be removed from the lung by the blood. Assuming that the Xenon has to dissolve in plasma before it enters the red cell, then at equilibrium the Xenon in the alveoli will equal 8.75 times the Xenon in the plasma (from the Partition Coefficient). The rate of removal will then be:

$$\frac{1}{8.75} \times \frac{5,000}{4,000} \times 100 = 11\% \text{ per minute.}$$

This figure is probably an over-estimate as experimentally the fall of count rate that occurs during breath-holding after a single breath of Xenon is considerably less than this. Therefore, the distribution of Xenon can be reliably measured from the plateau count rate during breath-holding. However, during long-term rebreathing of Xenon this solubility will become important. For this reason the functional residual capacity determined by Xenon dilution will be an over-estimate of the true volume,

proportional to the Xenon uptake.

2. FATE OF INJECTED XENON

If Xenon is dissolved in saline and injected intravenously, as its solubility in whole blood is 0.195 ml Xenon per ml blood at a Xenon partial pressure of 713 mm. Hg., the amount in 100 ml blood will be:

$$\frac{19.5}{713} = 0.0264 \text{ ml Xenon/mm. Hg. pXe}$$

Assuming that the mean capillary partial pressure of Xenon for diffusion is half the initial value, to clear Xenon completely into the alveoli the diffusion must be 0.0528 ml Xenon/mm. Hg. pXe.

The diffusing capacity for Xenon can be calculated from the diffusing capacity for carbon monoxide by the following formula:

$$(1) \quad \frac{D \text{ Xenon}}{D \text{ Carbon monoxide}} = \frac{\text{Sol. Xe.}}{\text{Sol. C0}} \cdot \frac{\text{Mol. Wt. C0}}{\text{Mol. Wt. Xe.}}$$

Putting in the known solubilities (in water) and molecular weights of Xe and C0, and assuming a normal Dco = 15 ml/mm/min:

$$(2) \quad D \text{ Xenon} = \frac{0.0845}{0.0185} \cdot \frac{28}{131} \cdot 15$$

$$D \text{ Xenon} = 30 \text{ ml/mm/min.}$$

Therefore, the time (t) to completely clear Xenon from the capillary into the alveolus is:

$$t = \frac{0.0528}{30} \times 60 = 0.1056 \text{ seconds.}$$

As the mean transit time through the pulmonary capillaries is approximately 1.5 seconds, Xenon will diffuse out completely in the first 7% of the capillary length, assuming the PAxe = 0. However, at the same

time, the Xenon that has diffused into the alveolus will be re-dissolving in the blood at approximately 11% per minute. It is difficult to balance the effect of these two processes with any precision. Experimentally, Pittinger[131] found that 95% of Xenon in the venous blood was cleared into the alveoli during its passage through the lungs. As injected Xenon^{133} is so completely cleared into the lung, the amount excreted in a region will be proportional to the regional blood flow. This is the basis of the method of measuring regional perfusion with Xenon.

RADIO-ACTIVE XENON^{133}

Isotopes of Xenon have a range of atomic weights from 54 Xe^{121} to 54 Xe^{144}. Nine of these are stable isotopes and the rest undergo radio-active decay. Of these only Xenon^{135}[131] and Xenon^{133} have been used in biological work as the rest have unsuitable half-lives or modes of decay. Xenon^{133} is made by neutron bombardment of Uranium^{235} in an atomic pile. A thermal neutron is captured by U^{235} and the resultant nucleus U^{236} undergoes fission. The fission fragments fly apart with great velocity and are in highly excited states. These nuclei have an excess of neutrons, which are ejected. The fragments continue to reduce the neutron/proton ratio by a series of Beta decay processes to reach a stable state. The chain producing Xenon^{133} is:

$$_{51}Sb^{133} \xrightarrow[10\ min.]{\beta^-} {}_{52}Te^{133} \xrightarrow[1\ hour]{\beta^-} {}_{53}I^{133} \xrightarrow[22\ hours]{\beta^-} {}_{54}Xe^{133} \xrightarrow[5{\cdot}3\ days]{\beta^-} {}_{55}Cs^{133}$$

The main problem in the manufacture of Xenon^{133} is the subsequent purification of the isotope[132]. At present, the Radio-chemical Centre, Amersham, is the only laboratory supplying purified Xenon^{133}.

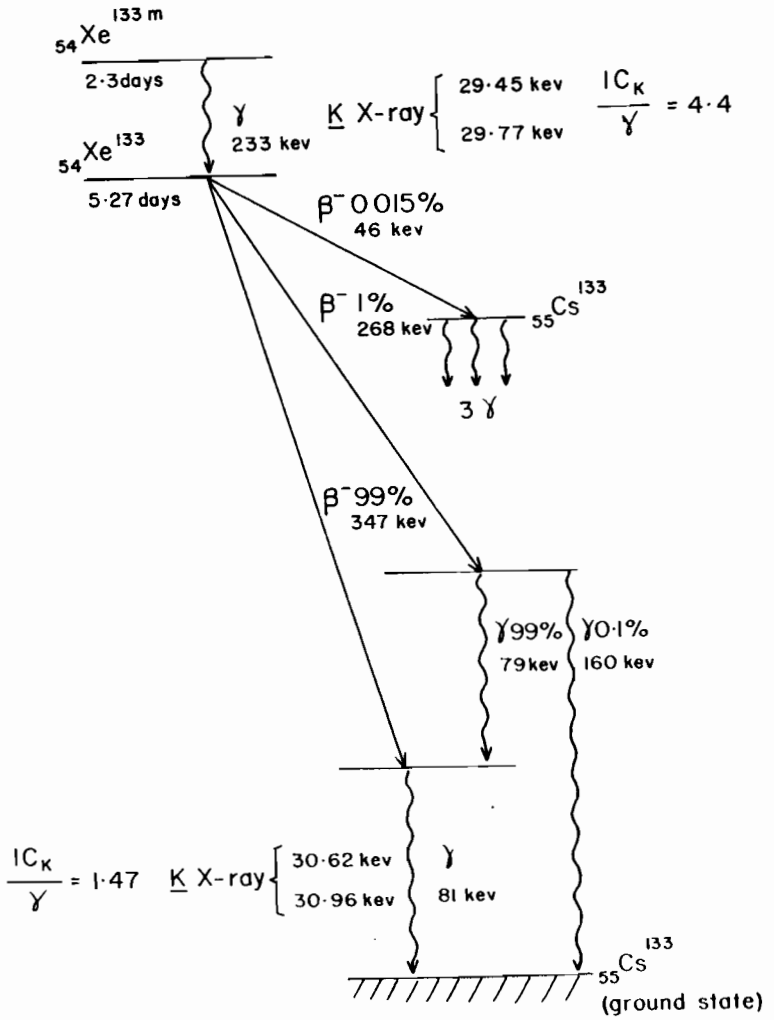

Figure IX - Decay scheme of Xenon^{133} to its ground state Caesium^{133}.

Xenon^{133} decays to stable Caesium with a half-life of 5.27 days. The full decay scheme is given on Figure IX. This shows that the nucleus decays by emitting negative Beta particles of maximum energy 0.347 Mev. This is absorbed by less than 1 mm. of tissue and is, therefore, of no use for external counting. The nucleus formed by Beta emission may reach a stable state either by emitting a gamma ray of energy 0.081 Mev. or by a process of internal conversion, which is accompanied by the emission of K X-rays of energy approximately 0.030 Mev.

The 0.081 and 0.030 Mev. emission is sufficiently high for external counting. It is also low enough that adequate protection from radiation and shielding of apparatus can be accomplished by 1/16th inch of lead. However, the low energy has some disadvantages. In collision with tissue nuclei the gamma energy may be lost (Photo-electric effect, Figure X). Alternatively the collision may result in the Compton Effect. In this process part of the gamma energy is transferred to an electron, knocking it out of the nucleus, while the gamma ray is deflected and its energy reduced. Compton Effect is potentially troublesome when attempting spatial localization, as gamma rays reaching the detector may have arisen outside the counter field and been scattered into it. However, it can be seen from Figure X that effect is more characteristic of intermediate energy (0.5 to 5 Mev.) gamma radiation , and that at the low energy of Xenon^{133} radiation, the probability of scatter is a function of the Atomic number of the target.

The Xenon^{133} used in these studies was prepared by the Radiochemical Centre, Amersham. It was sent Air Freight in a 6 ml ampoule

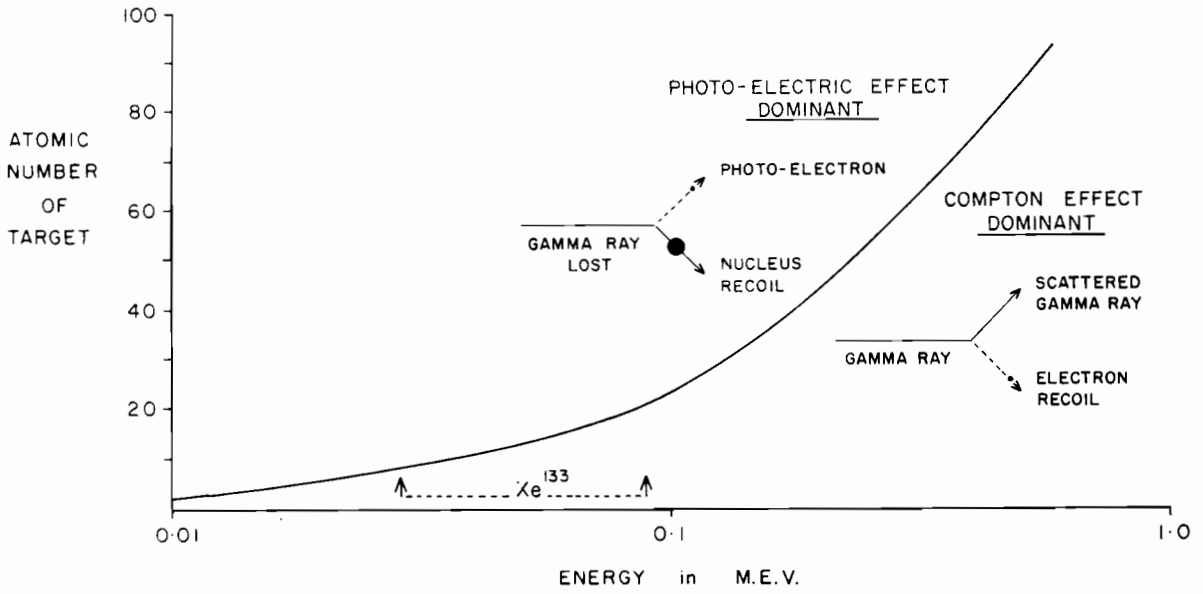

Figure X - Relationship between gamma energy and its fate after collision with targets of various atomic numbers.

under low pressure, enclosed in a lead container. For convenience in handling and dispensing, the Xenon^{133} was transferred to a 30 ml lead shielded tonometer diluted with pure CO_2. The CO_2 is of considerable importance in preparing solutions of Xenon. When a bubble of CO_2 and Xe^{133} is drawn into a saline syringe the CO_2 rapidly goes into solution and the volume of the bubble decreases. As a result the partial pressure of Xenon in the bubble rises and increases the rate at which the Xenon enters solution. The presence of air in the tonometer makes preparation of potent Xenon solutions difficult as both oxygen and nitrogen are relatively insoluble.

RADIATION DOSE

Xenon^{133} is a safe isotope for physiological experiments, because the radiation dose to the subject is relatively small. The physical half-life is short (5.27 days). Also because the uptake of inhaled Xenon^{133} is small and injected Xenon^{133} is promptly excreted, the biological half-life is very short, and even in patients with lung disease is generally less than 5 minutes. The combined effect of the biological and physical half-lives is called the "Effective Half-Life" which is obtained by;

$$\frac{1}{T\ 1/2\ \text{Effective}} = \frac{1}{T\ 1/2\ \text{Phys.}} + \frac{1}{T\ 1/2\ \text{Biol.}}$$

Putting in the figures for Xe^{133} in minutes:

$$\frac{1}{T\ 1/2\ \text{Effective}} = \frac{1}{18972} + \frac{1}{5}$$

Therefore, for practical purposes the biological half-life is the effective half-life.

The approximate radiation dosage can be calculated for the Xenon^{133}

experiments. It is most conveniently expressed as the Radiation Absorbed dose or RAD. The RAD is defined as the quantity of radiation that gives rise to 100 ergs per gram of tissue. Nearly all the radiation damage is caused by the Beta particles and dose is calculated on this basis. The average energy of the Beta particle is regarded as half the peak energy ($\bar{E}$). If an amount A millicuries (when 1 millicurie = 3.7×10^7 dissociations per second) is distributed in a mass of tissue M grams, then the energy expended in the mass is $A \times \bar{E} \times 3.7 \times 10^7$. Since the energy in 1 MEV = 1.6×10^{-6} Ergs; this represents:

$$\text{Energy in Ergs/gm/sec} = \frac{3.7 \times 16 \times \bar{E} \times A}{M}$$

or in RADs (100 Ergs/gm):

$$\text{RADs per second} = 0.592 \frac{\bar{E}\ A}{M}$$

The average energy of the Beta particle from Xenon^{133} $\bar{E}$ = 0.173 Mev. The mass of the average adult lung (M) is approximately 1200 grams. The amount of Xenon^{133} inhaled from the spirometer or injected intravenously is generally about 0.5 millicuries. Utilizing these figures in the above formula:

$$\text{Dose} = \frac{0.592 \times 0.173 \times 0.5}{1200} \quad \text{RADs/sec.}$$

$$= 42.6 \times 10^{-6} \text{ RADs/sec.}$$

Assuming that with breath-holding and subsequent washout the Xenon^{133} is in the lung for one minute, the total dose in Millirads = $(42.6 \times 10^{-6}) \times 60 \times 10^3$ or 2.5 Millirads.

Most of the radiation dose is contributed by the period of rebreathing

during which the subject equilibrates with the closed circuit spirometer. At equilibrium the amount of $Xenon^{133}$ in the lungs (A) is about 2.0 millicuries. In normal subjects the rebreathing continues for approximately 5 minutes and for this time:

$$\text{Dose} = \frac{0.592 \times 0.173 \times 2.0 \times 300 \times 10^3}{1200}$$

$$= 51 \text{ millirads}$$

The radiation dose from the complete experiment is, therefore, below 60 millirads in a normal subject. In patients with lung disease, where intra-pulmonary mixing is impaired, the rebreathing period must be prolonged and the dose increases accordingly. However, even a 15 minute rebreathing period only gives a dose of 153 millirads. These dosages are small compared to those received in many routine diagnostic radiological studies and insignificant compared to most diagnostic radioisotope techniques.

COUNTING AND RECORDING

SCINTILLATION COUNTERS

Scintillation counters are used to detect the gamma and K x-ray emissions from Xenon^{133}. These have the advantage over other types of detector of high gamma sensitivity and high speed counting. Commercial scintillation counters were too large, when this technique was started, limiting the number of counters that could be placed over the chest. To overcome this difficulty the present counters were built in this laboratory from components which could be assembled in a cylinder 1 1/4" diameter and 12" long. They consist of a Thallium activated Sodium Iodide crystal 3/4" diameter and 1/2" deep (Harshaw Chemical Co.). A gamma ray striking the crystal produces a light flash, or scintillation, proportional in intensity to the gamma energy. In optical contact with the crystal is a Photo-Multiplier tube (K 1716 Du Mont Laboratories) which converts the light flash into electrical energy. The photo-multiplier output is between 1 and 3 millivolts depending on the gamma energy. It is a high impedance device and its output enters a Linear Amplifier (T 108 Engineered Electronics Inc.), primarily for impedance matching and also to provide a first stage gain. The output of the amplifier is a signal between 20 and 100 millivolts. The overall gain of the optical system, photo-multiplier and amplifier varies considerably between counters, but this is subsequently standardized.

The counters have two power supplies: a 1000 volt stabilized, ripple free supply to the photo-multiplier and a 12 volt supply to the amplifier. The detectors used to measure the activity of the inspired air and the injected $Xenon^{133}$ are basically the same, but as size is not critical, they are in wider tubes.

The sensitivity of scintillation detectors is primarily dependent on the volume of the crystal. The present crystal is relatively small and in retrospect a larger crystal would have been preferable. It would somewhat increase the size of the counter, but in the present technique size is not too critical.

MAGNETIC TAPE RECORDING SYSTEM

Generally the output from scintillation detectors is displayed directly on to a Scalar counter or rate meter. However, in the present $Xenon^{133}$ technique direct recording is practically impossible. In these studies continuous, simultaneous recording was necessary from up to thirteen scintillation detectors. This would require the same number of rate meters and channels on a pen recorder. Even if these were available such a system would be unsatisfactory. Count rates from 300 cpm to 50,000 cpm are being recorded and for accurate interpretation it is essential that the gain of the pen recorder is set to ensure the maximum pen deflection in each case. At a fixed full-scale deflection of 50,000 cpm, a count of 300 cpm would be imperceptible. On the other hand a lower full-scale deflection would put higher count rates off scale. As in many cases it is impossible to guess the count rate in advance, rapid and con-

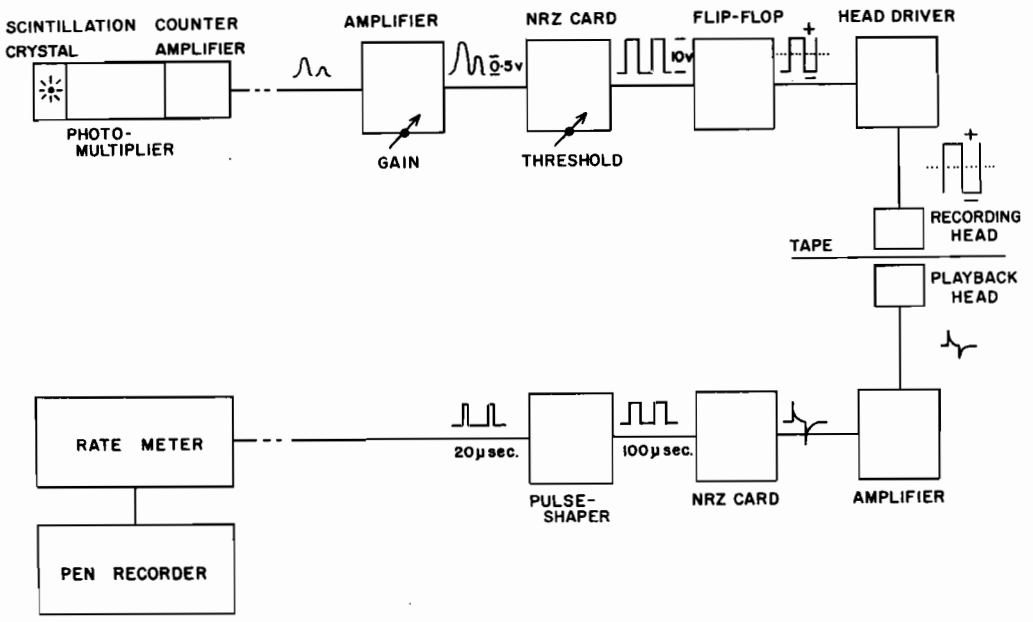

Figure XI - Schematic of signal path from the scintillation counter to the pen recorder.

tinual gain switching on multiple channels (duly recorded) would be impossible, without multiple technicians.

For these reasons all the raw count data is recorded on magnetic tape, with a running commentary of the experiment on a voice channel. During the experiment only selected channels are played out onto the pen recorder, to monitor zones of particular interest. The whole experiment is, therefore, permanently stored on tape and subsequently it is played back, piecemeal, through four rate meters onto a four channel pen recorder. Occasionally, it is necessary to replay parts of a record several times to produce the optimum recording from which the calculations will be made.

The output from a scintillation detector cannot be directly recorded on tape. The frequency content of the pulse waves is too high for either direct or frequency modulated recording. The method used is a Digital technique called Non-Return to Zero recording, which provides a high signal to noise ratio. Basically this technique converts a train of scintillation counter pulses into a train of maximum positive and maximum negative magnetic transitions on the tape. A block diagram of the recording is shown on Figure XI; the signal goes through the following stages:

1. PREAMPLIFIER

The output from each scintillation detector goes to a pre-amplifier. The signals from the detectors are of different voltages proportional to gamma energy, but the absolute voltage level varies from counter to counter, because of differences in the over-all gain in different counters. The

primary purpose of this pre-amplifier is to adjust the signals from each counter to a standard voltage output. Therefore, these amplifiers are periodically adjusted with a Xenon Source and an oscilloscope so that 30 Kev gamma energy pulses give a standard voltage output of 0.6 volts from each counter.

2. NON-RETURN TO ZERO CARDS

These circuits are Flip-Flop pulse height discriminators and the voltage required to trigger them can be varied. In normal operation they are set to flip at 0.5 volts, which is equivalent to a 25 Kev pulse. Energy levels below this are not recorded. In this way it is possible to discriminate against low energy scatter radiation and the appreciable amount of thermal noise generated in the photo-multiplier tube. In some experiments, where it was necessary to eliminate Compton scatter as far as possible, the threshold level has been raised to the equivalent of 60 Kev, this approximately halves the observed count rate because the K x-ray is not counted. Each pulse which triggers the flip-flop gives an output pulse of 10 volts with a minimum duration of 110 microseconds.

3. TRIGGER AND RESET FLIP-FLOP

This signal enters another flip-flop which has two stable states, fully positive or fully negative with no zero reference (hence NRZ recording).

4. HEAD DRIVER

This signal then goes to the head driver which provides power for and impedance matching with the Recording Heads.

5. RECORDING HEADS

There are two recording heads each capable of carrying fifteen separate channels of information. These impress the original pulses onto the tape as a series of magnetic transitions.

The playback side of the tape system is very similar. The signal from the playback head is essentially a differentiated square wave, because of the inductance of the head. This small signal is amplified by a 10 volt playback amplifier. The signal then goes to an NRZ playback card, which converts the pulses back to discrete, unidirectional pulses 100 micro-seconds long with an amplitude of 10 volts. This output has been further modified to shorten the pulses to 20 micro-seconds to match the input characteristics of the rate meter at high count rates. This is done in a further series of flip-flops external to the tape system.

6. F.M. DATA SYSTEM

Analog information is recorded on the tape by a frequency modulation technique. This consists of a recording oscillator with a centre frequency of 6.75 Kc. This has a $\pm$ 40% deviation in response to an input signal of $\pm$ 1.5 volts. The output of the recording oscillator are pulses which are fed into the tape recording heads. On playback the signal from the playback head is amplified and fed into an FM data discriminator. Here the signal is de-modulated giving a DC voltage linearly related to the frequency deviation. The frequency response of the system from input to output is flat from DC to 1000 cycles per second. Two FM record channels and one FM playback channel are

available at present. These are used to record spirometer volume, by means of a low-torque potentiometer.

RATE METERS

The information of the tape recorder is played back, four channels at a time, through two Dual Tullamore rate meters. These convert the randomly spaced pulses into an average count rate per minute.

As radio-active decay is a random process it is subject to statistical fluctuation which will affect the rate meter. The fluctuation follows a Poisson distribution, but at reasonably high count rates this can be approximated by a Gaussian or Normal distribution. In this approximation the Standard Deviation (SD) becomes equal to the square root of the mean counts per unit time (N).

N	$SD = \sqrt{N}$	% SD
10	3.16	31.6
100	10.0	10.0
1,000	31.6	3.16
10,000	100.0	1.0

From these figures it can be seen that although the Standard Deviation increases as the count rate increases, the percent deviation decreases. Thus by counting long enough (or by integrating the input pulses over a long enough interval) the error due to random decay can be reduced. Ideally then the integrating time constant should be long, particularly at low count rates, to give a smooth trace, with a small Probable Error. However, this inevitably means that the response of the rate meter is slow and rapid transients are lost. Therefore, a compromise must be reached between the Probable Error (PE), the

Time Constant (RC) and the full scale count rate (n). These factors are related by the following equation:

$$PE = \frac{0.67}{2n \cdot RC}$$

On the present rate meters Probable Error settings of 0.5%, 2%, 5% and 20% can be selected by shunting the appropriate capacitor across a high feed-back resistor. In the present studies counting over the lung a full scale deflection of 3×10^4 cpm is used, with a Probable Error setting of 2%, so that the rate meter time constant is 1.17 seconds. The only way to shorten this time constant is to operate at higher dosages, or manipulate the tape speed. The third alternative, working with a higher Probable Error is not satisfactory as the trace is very "noisy" and difficult to read. The Spirometer Scintillation Counter, which records higher count rates is operated at 10^5 cpm full scale, with a Probable Error of 0.5% as this provides a very smooth accurate trace and response time is not important.

The information from the rate meters is displayed on a standard Sanborn 150 four channel pen recorder, after DC amplification.

DEAD-TIME CORRECTION

Counting systems do not actually count nuclear events, but the intervals between such events. Following each event the counter has a brief refractory period, or dead-time, during which it will not respond to a further event. This is also true for elements of the tape system and rate meter, so the magnitude of this dead-time loss has to be estab-

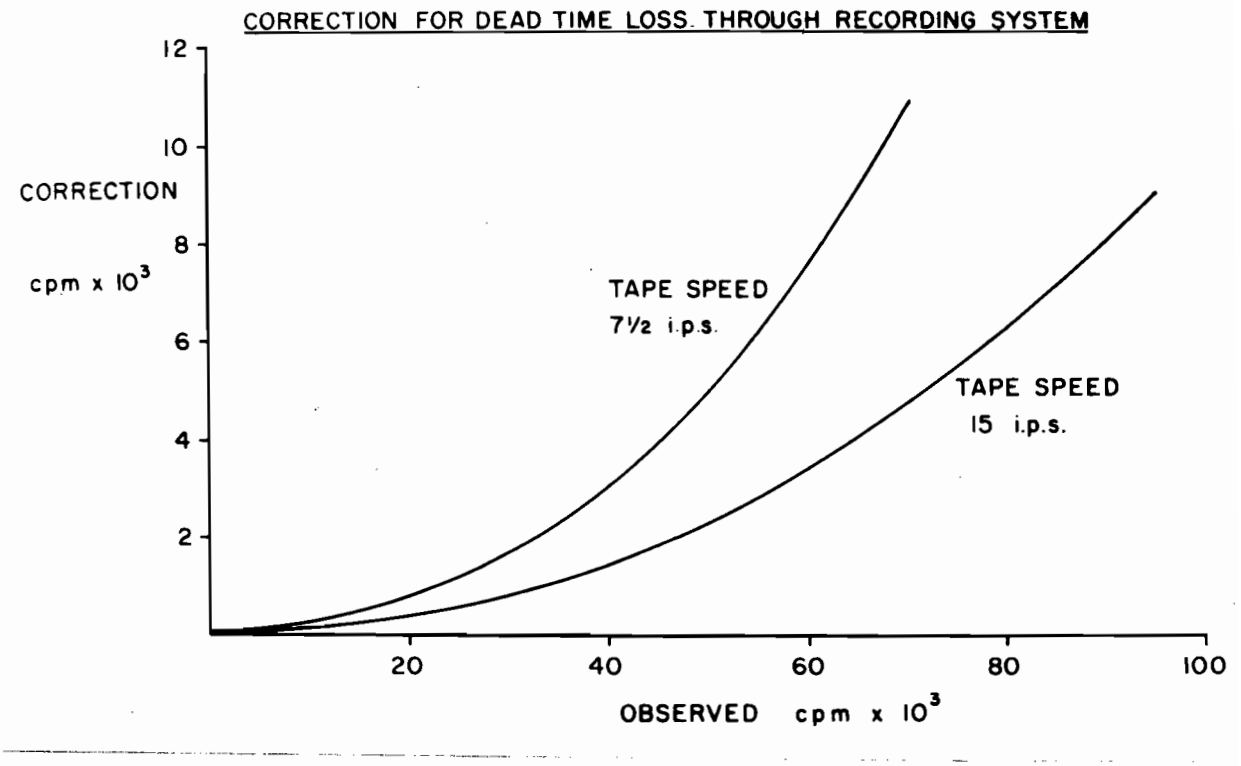

Figure XII - Graph of dead time loss through the recording system at two tape speeds.

lished for the whole system.

If the observed count rate is U cpm, then in a time t a total of Ut counts will be recorded. If the dead-time after each recorded count is T, then the total dead-time in t is UtT. The fraction of time that the counter is dead is UtT/t = UT, and the fraction of time the counter can record is 1 - UT. Therefore, the true count rate (U true), when the observed count rate is U will be:

$$1.\quad U \text{ true} = \frac{U}{1 - UT}$$

To determine the dead-time experimentally, a two-source method was used, in which each source was counted separately and then together. The count rate of the two sources together is lower than the sum of the separate sources because the relative dead-time loss is greater. From this difference a formula is available to predict the dead-time loss T. If U_1 and U_2 are the count rates of the two sources and U_{12} is the count rate when they are counted together, then:

$$2.\quad T = \frac{U_1 + U_2 - U_{12}}{2\,(U_1 \cdot U_2)}$$

Experimentally the dead-time loss of the present recording system is 100 microseconds at a tape speed of 7 1/2 ips and 51 microseconds at a speed of 15 ips. Utilizing these figures in Equation 1, a graph has been constructed showing the dead-time correction for each observed count rate (Figure XII). All observed count rates are corrected from this in all the subsequent calculations. The calibration counter which is recorded directly on a Scalar counter has a much lower

dead-time = 3.65 microseconds requiring correspondingly smaller correction to the observed count rate.

COLLIMATION

To confine the counting field of a scintillation counter to a selected volume of the subject's lung, some form of collimation is required. Improvement in spatial resolution is usually accompanied by a corresponding reduction in counter sensitivity. Therefore, the design of the collimators represents a compromise, which will be finally decided on the type of study being undertaken.

In these studies we were not interested in detecting small lesions of the lung, or in trying to describe the function of the normal lung in very fine detail. We wished to study the regional behaviour of the whole lung and in lung disease, to try to define the extent of more or less diffuse lesions. This approach appears realistic at the present stage of the development of isotope techniques as there are many practical and theoretical difficulties in attempting an analysis of the lung in finer detail. Therefore, the counters have been collimated to cover the upper, middle and lower zones of the left and right lung.

Collimators have been constructed out of thick lead pipe with an internal diameter of 1 5/8 inches. The length of the collimators (from the face of the crystal) is 4 inches. The spatial resolution of the collimated counters can be appreciated from the iso-count curves (Figure XIII) for a single counter and a pair of counters counted in parallel. These curves are made with a "point" source of potent $Xenon^{133}$ sealed in a

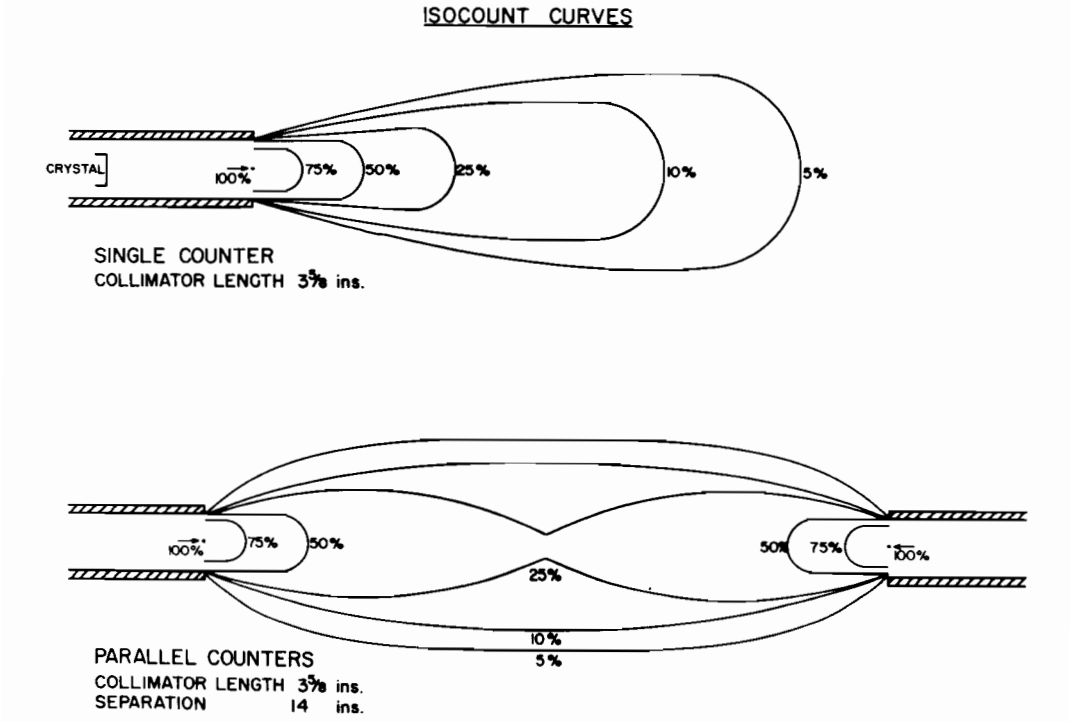

Figure XIII - Isocount curves from a point source for a single counter and a pair of counters counting in parallel.

small length of capillary tubing. The count rate is recorded with the source at various distances from the counter. The count rate at the centre of the face of the collimator is taken as 100% and all other counts expressed as a percentage of this. Curves are then drawn between points of equal count rate. These curves were done in air and the iso-count curve through tissue will be somewhat different. It is impractical to try to approximate these curves in the varying density of lung tissue. The general effect of a higher density medium will be to make the curves shorter and wider.

The iso-count curves for a single counter form a truncated cone, with the sensitivity falling off quite rapidly with distance (count rate is inversely proportional to the square of the distance for a point source). However, it is important to appreciate that the volume in the low sensitivity region is large so that the total number of counts received from these regions is relatively large; thus for a diffuse source the inverse square law is not valid. The uniformity of the counting field is dependent on the distance of the crystal from the chest. If the crystal is up close, count rates are high, but there is greater non-uniformity of the counting field.

The iso-count curves from two detectors counting in parallel, with their count rates summed, is also shown on Figure XIII. With this arrangement a much more satisfactory counting field is obtained. The diameter of the core is a function of the length and diameter of the collimator. The uniformity of the core depends on the distance between the

crystals.

These studies have been done using both single counters and parallel counters. Although the counter-field with parallel counters is obviously preferable, there are a number of practical difficulties to the routine use of twelve counters. It almost doubles the instrumentation and data reduction problems and does not add a commensurate amount of information, in normal subjects. The exceptions to this are circumstances where considerable differences in the function at the front or the back of the lung exist. In upright seated normals, we have not been able to detect significant differences between ventilation and perfusion measured from the front or the back. Therefore, routinely back counting alone is used. In the recumbent position, the perfusion at the back of the chest is significantly higher than the front. Therefore in the recumbent position, back and front parallel counting is essential to measure the mean function of the zone. All recumbent studies were done using parallel counting, with separate analysis of the front counters, the back counters and their summed outputs.

Only a limited number of studies have been done with parallel counting on patients with lung disease. The assumption that in these cases back counting is truely representative of the whole zone is open to question.

POSITIONING OF CHEST COUNTERS

The chest counters are positioned from standard co-ordinates on a 6 ft. P.A. chest x-ray taken in the upright or horizontal position

depending on the position in which the patient is studied. The upper zone counter is centered 1.5 inches below the highest projection of the lung, the lower zone counter 0.75 inches above the highest projection of the diaphragm and the mid-zone counter mid-way between. At each vertical level the counters are equidistant from the mid-line and in the centre of the lung projection at that level. These positions are marked on the x-ray on a viewing box with a grid. The 7th cervical spine is placed on the zero-reference of the grid and the vertical and lateral co-ordinates of the counter positions read off the grid. These co-ordinates are then used to position the counters over the patient.

The chest counters are mounted in a counter rack. They are held by aluminium holders shaped like snow-shovels. These are attached to an 18" x 18" steel frame by lathe tool posts running in slots in the frame. This arrangement provides both rigid support for the counters and an easy method of positioning them. The racks are rigidly mounted on the chair or bed on which the patient is to be studied:

(a) CHAIR - A Dexion frame chair has been constructed. This has a bucket seat which can be hydraulically raised and lowered. It also has adjustable arm and head rests. The back of the chair is made of 1/8" perspex and has a grid on it for positioning the counters. The counter rack is mounted rigidly behind this so that the ends of the collimators are in contact with the perspex. The counters are aligned on the grid from the chest x-ray co-ordinates. Once

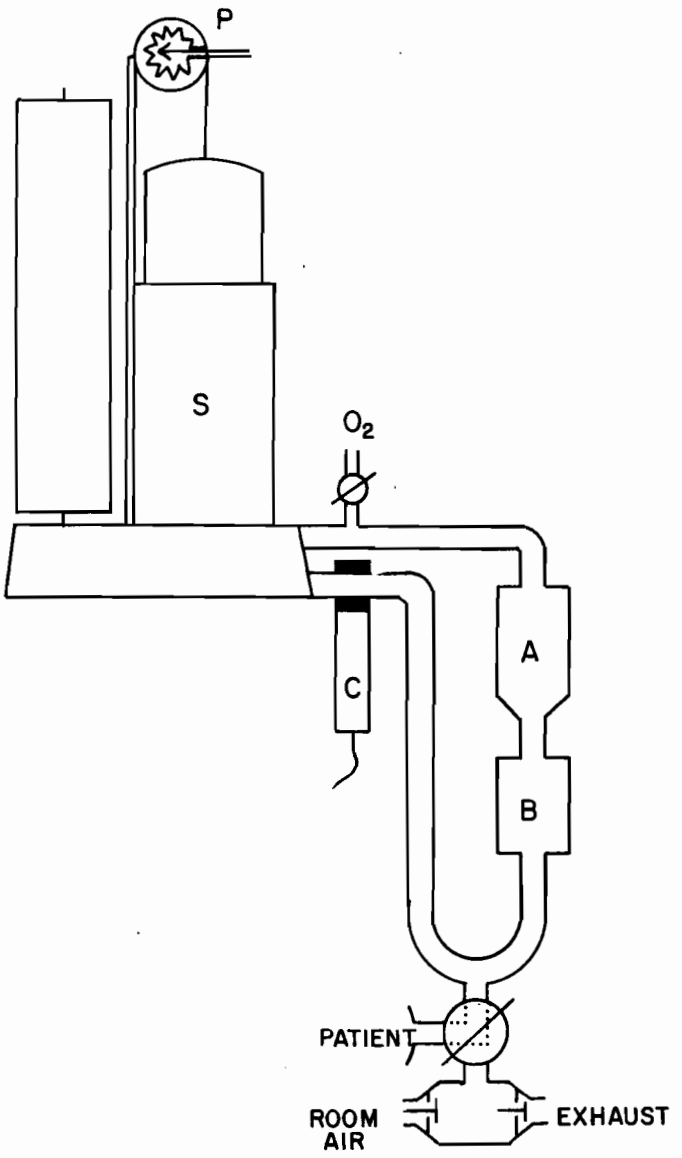

Figure XIV - Spirometer circuit. Volume recording potentiometer P. Spirometer S. Inspired air scintillation counter C. Carbon dioxide absorber A. Circulating pump B.

the patient is seated in the chair, the seat height is adjusted until his 7th cervical spine is aligned with the grid reference.

(b) BED - A Dexion frame bed has been constructed. This has a perspex window in the thoracic region also with a grid. All horizontal studies are done with parallel counting. The lower rack is permanently fixed. The upper rack is mounted on posts and is removable to allow the patients to get in and out. Both sets of counters are aligned on the grid co-ordinates and the patient is positioned using C 7 as the reference.

SPIROMETER CIRCUIT

The subject breathes Xenon from a closed circuit spirometer system (Figure XIV). This consists of a 9 litre Collins spirometer (S), a carbon dioxide absorber (A), and a pump (B). The pump circulates the gas in the system at 36 litres a minute to ensure complete mixing. Volume is calculated from the spirometer pen deflection. It is also recorded (via an FM channel) on tape from a potentiometer (P). The patient inspires from a mouth-piece and a small (15 ml) dead space tap which permits either breathing to and from the closed circuit or from room air to an exhaust line for disposal of radio-active gas.

The concentration of $Xenon^{133}$, in the closed circuit is continuously monitored by a scintillation counter (C), permanently mounted under a perspex section of the inspired line. As this is a fixed geometric relationship, the air counter can be calibrated to read the circuit $Xenon^{133}$ concentration. Prior to each study the spirometer is filled with 6.72

litres of air and sufficient Xenon^{133} to bring the initial concentration to approximately 0.5 millicuries per litre. During rebreathing on the closed circuit carbon dioxide is absorbed by the soda lime and sufficient oxygen is added continuously to maintain the spirometer volume as constant as possible.

PROCEDURE

Prior to the study the patient has a 6 ft. PA chest x-ray and a Functional Residual Capacity (Helium dilution method[83]). The chest counters are pre-positioned from the x-ray co-ordinates.

Two solutions of $Xenon^{133}$ are prepared for injection. A small bubble of $Xenon^{133}$ is drawn from the tonometer into a 10 ml syringe containing 5 ml of saline. The syringe is gently agitated (using tongs) until there is no further decrease in the bubble size. The remainder of the bubble is expelled and the syringe counted for 1 min. on the calibration counter. The first syringe should contain approximately 1 millicurie and the second about 0.5 millicurie. The syringes are fitted with 3-way Luer-lock stopcocks and a 20 ml syringe of saline is attached to the side arm.

The spirometer is filled with 6.72 litres of air. With the pump running and the activity being monitored by the spirometer counter, $Xenon^{133}$ is introduced until the concentration is about 0.5 mc/litre.

The subject is positioned in the chair or the bed, using C 7 as the reference. During the procedure this position has to be checked constantly as movement is a major source of error. It is important to make the subject as comfortable as possible in the chair by positioning the head and arm rests. The subject is also cautioned against movement during the respiratory manoeuvres.

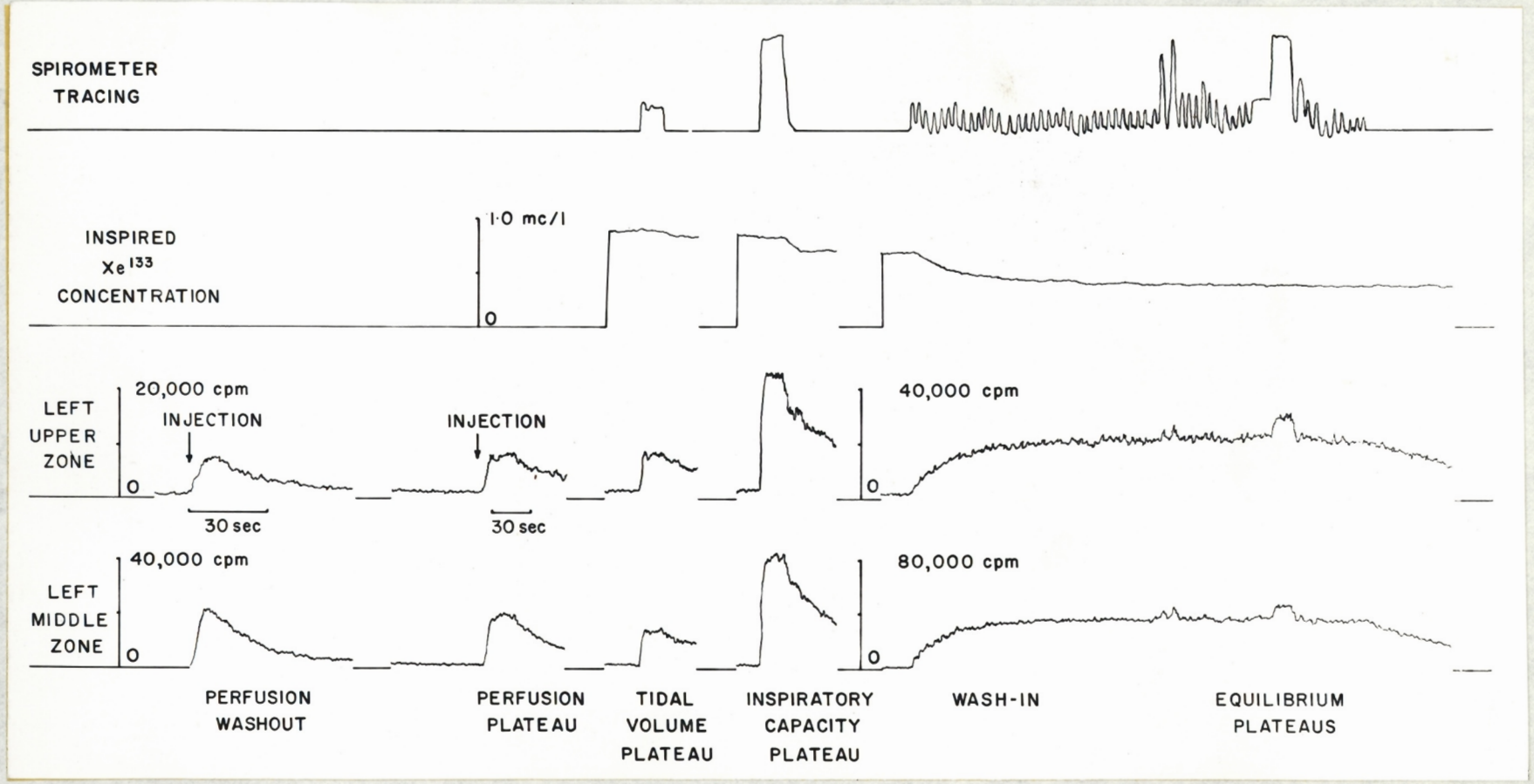

Figure XV - Typical experimental record.

The recording system is connected up so that the spirometer volume and three chest counter channels will be monitored on the Sanborn during the procedure. In patients the chest counters over the most diseased zones are monitored as these will equilibrate most slowly. Room background counts are recorded from the chest counters, with the patient in the chair, but all Xenon^{133} sources away from the counting field.

A heparinized 8" polythene catheter is introduced through a 14 gauge needle into an ante-cubital vein. The syringe containing the high dose of Xenon^{133} and a saline syringe is attached to the catheter as firmly as possible (to avoid leakage during the injection). The subject's nose is clamped and the mouth-piece inserted with the valve positioned so that he breathes from the room to the exhaust line. The tape is started and background again recorded. While the subject is breathing quietly the Xenon^{133}, then the saline syringe are injected as rapidly as possible starting at the end of expiration. Count rates rise to a peak over all lung zones and then fall as the Xenon^{133} is washed out of the lung during the subsequent respirations. A typical curve of an experiment is shown in Figure XV. The curve is recorded down to tissue background count. This curve is used to measure the ventilation of perfused alveoli (see Calculations).

After recording has stopped the syringes are replaced by the low activity Xenon^{133} syringe and another 20 ml saline flushing syringe. Recording is re-started when the chest counter background count is satisfactory. At the end of a normal expiration the Xenon^{133}, followed by the

saline are rapidly injected and the subject instructed to take an inspiratory capacity breath and to hold it. The count rates over the lung rise and plateau, when a satisfactory plateau is established, the subject is instructed to breathe normally. The empty syringe is counted to calculate the exact quantity injected, as some Xenon^{133} inevitably remains in the syringe. This perfusion plateau is used to derive the perfusion distribution (see Calculations).

The catheter is removed and when the chest background has fallen, recording is started again. The spirometer pump is turned on to mix the gas in the circuit. At the end of a normal expiration the spirometer tap is rotated so that the next inspiration is Xenon^{133} from the closed circuit spirometer. At the end of a tidal inspiration the subject is instructed to hold his breath. When a satisfactor count rate plateau is recorded, he is told to continue his inspiration to inspiratory capacity and again breath-hold. When a count rate plateau is established, he expires into the spirometer and is then switched out of the closed circuit to wash-out the remaining Xenon^{133}. These single breath plateaus are used to derive the tidal and inspiratory capacity distribution (see Calculations).

When the background count is satisfactory he is again switched into the closed circuit and continues quiet breathing. Oxygen is added as required to maintain the circuit volume. The count rate the concentration of Xenon in the lung is equilibrated with the spirometer concentration. When there appears to be no further rise in count rate, the subject is instructed to stop breathing at the end of a tidal inspiration;

after a plateau is recorded he continues to an inspiratory capacity breath-hold. When the subject resumes normal breathing the count rates should fall to the same value as before these manoeuvres. If they do not, true equilibrium has not been reached. In this case rebreathing is continued and the breathholding plateaus repeated. Once satisfactory equilibrium plateaus have been obtained the subject is switched out of the circuit and washes out his lungs to the exhaust line. The wash-in curve is used to derive the dynamic ventilation distribution (see Calculations). The plateaus at equilibrium are the calibration count rates used to derive Xenon^{133} concentrations (see Calculations).

CALCULATIONS

1. DATA

Following the experiment the information on the tape recorder is played out four channels at a time adjusting the Sanborn range to give the optimum deflection for all count rates (See Figure XV).

The following information is tabulated:

(1) Functional residual capacity.

(2) Scalar counts - (a) Syringe before injection +DT - BG*.

(b) Syringe after injection - BG.

(3) Spirometer Record - (a) Volume of initial tidal breath.

(b) Volume of initial IC breath.

(c) Volume of equilibrated tidal breath.

(d) Volume of equilibrated IC breath.

(e) Rate of breathing during equilibration.

(f) Average tidal volume during equilibration.

(4) Spirometer Counter - (a) Count rate prior to initial breaths +DT - BG.

(b) Count rate at equilibrium +DT - BG.

(5) Each Chest Counter - (a) Initial background.

(b) Background prior to perfusion plateau.

(c) Perfusion plateau +DT - BG (b).

---

* Dead time Correction
Background Correction

(d) Background prior to single breaths.

(e) Tidal plateau +DT - BG (d).

(f) IC plateau +DT - BG (d).

(g) Equilibrated TV plateau +DT - BG (a).

(h) Equilibrated IC plateau +DT - BG (a).

(i) Washout of injected Xenon: count rate read every 5-10 seconds and corrected for dead time.

(j) Wash-in slope: count rate read every 10 seconds, corrected for dead time and subtracted from the equilibrium count rate corrected for dead time.

All count rates are read to the nearest 100 counts per minute. In the case of parallel counting front and back counters were analysed separately and then summed.

To calculate the ventilation and perfusion indices the following information must be obtained from the corrected count rate data:

(1) Concentration inspired.

(2) Amount inspired.

(3) Amount injected.

(4) Concentration at equilibrium.

(5) Amount at equilibrium.

(6) Ratio of amount at equilibrium/amount inspired.

(7) Ratio of amount at equilibrium/amount injected.

(8) Ratio of inspired count rate/equilibrium count rate.

(9) Ratio of injected count rate/equilibrium count rate.

(10) Ventilation index by multiplying Ratio 6 x Ratio 8 x 100.

(11) Perfusion index by multiplying Ratio 7 x Ratio 9 x 100.

2. PRINCIPLES OF INDEX CALCULATION

Because of the complexity of body surface counting, the relationship between the concentration of Xenon in the lung (F) and the external count rate (U) will differ in different subjects and for different counter positions in the same subject. The count rate will depend on the volume of lung (V) seen by the counter and the iso-count curves (Figure XIII) show that this is not a simple "linear" volume. Furthermore, the count rate is attenuated by a whole variety of factors (λ) among which are: the distance of the counter from the chest wall, the shape thickness and density of the chest wall, the nature of the tissue within the thorax, the efficiency of the counter, etc. Clearly all these factors are unlikely to be the same in different people or different areas of the same person. The relationship between count rate (U) and concentration (F) can be expressed:

$$U = \lambda VF$$

In a given counter, over a fixed area of the chest, at a constant lung volume a change in concentration (F) will give a proportional change in count rate because the factors λ and V are the same in both situations:

$$\frac{U_1}{U_2} = \frac{\lambda VF_1}{\lambda VF_2} = \frac{F_1}{F_2}$$

If one of the concentrations is known, the other can be calculated from the ratio of the count rates. This is the principle underlying the equilibration procedure described by Ball [75]. After rebreathing from the closed circuit, at equilibrium the concentration of Xenon in the lung

will equal the concentration in the circuit, which is continuously measured by the spirometer counter. Thus for a counter over a fixed point on the chest and at a specified lung volume, the relationship between the known lung concentration at equilibrium, (F_1) and the observed external count rate (U_1) can be established. This can be regarded as finding the calibration factor λV for the counter. Now with the same counter position and lung volume an unknown concentration of Xenon^{133} (F_2) can be calculated from its external count rate U_2.

$$F_2 = U_2 \frac{F_1}{U_1}$$

This calibration is established at two levels of lung inflation - end tidal volume at at inspiratory capacity. This enables the regional concentration of Xenon after a tidal breath or inspiratory capacity breath to be calculated using the appropriate equilibrium volume calibration. Solving for concentration expresses the amount of Xenon per unit volume. The amount of Xenon depends on the regional ventilation and the volume is the regional FRC + TV. It should be emphasized that if the concentration after a single breath is low, this only indicates that the ventilation per unit volume is low, which may be due to poor ventilation or to a large regional volume. In a similar manner the regional concentration after an injection of Xenon can be calculated to express the regional blood flow per unit volume.

While differences in regional concentration in one individual give all the requisite information, it is difficult to compare different individuals

because the absolute concentrations will vary due to differences in dose and lung volumes. To facilitate comparison Ball[75] introduced the distribution index. This index expresses the observed regional concentration as a percentage of the concentration that would have existed if the amount of Xenon administered had been uniformily distributed throughout the lung. This "ideal" concentration is calculated from the concentration of Xenon inspired (F_I), the volume inspired (V_I), minus the instrument dead space (V_D) and the subjects lung volume at end inspiration ($FRC + V_I$). The "ideal" concentration is:

$$\frac{F_I \cdot (V_I - V_D)}{FRC + V_I} \qquad \text{millicuries/litre}$$

Therefore, if the observed regional concentration after a single breath is F, the ventilation distribution index is:

$$\frac{F}{F_I \cdot (V_I - V_D)/FRC + V_I} \times 100$$

In the case of the perfusion index the amount of Xenon inspired ($F_I (V_I - V_D)$) is replaced by A the amount of Xenon injected and the index becomes:

$$\frac{F}{A/FRC + V_I} \times 100$$

The indices are still measurements of the relative ventilation or perfusion per unit volume. If the distribution were entirely uniform with respect to lung volume and no dead space was present, all the indices should be 100.

3. INDICES AND LUNG VOLUME

While the indices express the ventilation or perfusion per unit volume, it is necessary to precisely define what volume this refers to.

(a) VENTILATION INDEX

The concentration of Xenon in a zone (Cz) is determined by the concentration (C_I) and volume (T) inspired, divided by the initial lung volume (F) plus the volume inspired (T):

$$Cz = C_I \cdot \frac{T}{F+T}$$

The ventilation index, therefore, expresses the ventilation per unit final lung volume. The ventilation per unit of functional residual capacit can be obtained by re-arranging the equation:

$$\frac{Cz}{C_I - Cz} = \frac{T}{F}$$

It makes no difference to the measured ventilation gradient expressing the results per unit T+F or per unit F. All the present results are expressed per unit T+F. However, it is probably more exact to express the results per unit of the functional residual capacity in the future.

It should also be recognized that the final concentration is dependant on the dead space of the zone V_{Dz}. It makes the volume of Xenon inspired smaller ($T - V_{Dz}$) and the volume in which it is diluted larger ($F+V_{Dz}$):

$$\frac{Cz}{C_I - Cz} = \frac{T - V_{Dz}}{F + V_{Dz}}$$

Therefore, unless the distribution of dead space is uniform, the distribution of inspired Xenon is not strictly the distribution of alveolar ventilation.

(b) PERFUSION INDEX

The perfusion index is measured at inspiratory capacity and is also expressed per unit of final lung volume (F+T). Where (A) is the amount of Xenon deposited, in the alveoli by perfusion:

$$Cz = \frac{A}{F+T}$$

However, in this case there is no simple way of manipulating the data to express the perfusion per unit FRC. Furthermore, because the distribution of the inspired gas is not uniform, the perfusion distribution will vary with the lung volume at which the measurement is made. The difference that lung volume makes can be approximated in the following way:

Assume a two-compartment lung with the FRC of the upper zone equal to the FRC of the lower zone. Further assume that there is three times as much perfusion in the lower zone. Then at FRC:

$$C \text{ upper} = \frac{A}{0.5F} \qquad C \text{ lower} = \frac{3A}{0.5F}$$

$$\text{or } \frac{C_L}{C_U} = \frac{3}{1}$$

That is, there is a three to one gradient of perfusion per unit FRC.

Now assume that an inspiratory capacity breath (T) = 1.0 litre is inhaled, and that the initial lung volume (F) = 2.4 litres. Then T/F = 0.417 or T = 0.417F. Assuming that there is an upper to lower ventilation, gradient is 1:1.4. Then:

$$T_U = 0.173F$$

$$T_L = 0.244F$$

Then at inspiratory capacity:

$$C_U = \frac{A}{0.5F+0.173F} \qquad C_L = \frac{3A}{0.5F+0.244F}$$

$$\frac{C_L}{C_U} = \frac{3 \times 0.673}{0.744} = 2.72$$

Therefore the perfusion gradient per unit final volume (F+T) is 9% lower than the gradient at FRC.

This point was missed during the experimental work because in a series of ten subjects no difference in perfusion distribution could be demonstrated measured at held inspiratory capacity and at held tidal volume. It was, therefore, concluded that perfusion distribution was independant of lung volume. However, although the over-all tidal volume expansion is smaller, the distribution of tidal volume is less uniform than the distribution of an inspiratory capacity breath (See Results). The effect of this can also be approximated:

Assume a tidal volume (T) = 0.5 litres

Now T/F = 0.28 or T = 0.28F

If the upper to lower ventilation gradient is 1:1.6

$$T_U = 0.108F$$

$$T_L = 0.172F$$

Then the concentrations at tidal volume are:

$$C_U = \frac{A}{0.5F+0.108F} \qquad C_L = \frac{3A}{0.5F+0.172F}$$

$$\frac{C_L}{C_U} = \frac{1.824}{0.672} = 2.71$$

Therefore, there is virtually the same underestimate of the gradient at tidal volume as at inspiratory capacity. It is arguable which is the true gradient - perfusion per unit FRC

or per unit final lung volume. But certainly some caution must be exercised in interpreting small changes in perfusion when there is a simultaneous alteration of ventilation distribution. Therefore, a measurement at FRC would be preferable.

4. WASH-IN CURVES

In a closed circuit system the rate at which a subject's lung equilibrates with a foreign insoluble gas is a function of the volume of the spirometer (V), the volume of the lung (F), the effective tidal exchange (T), and the respiratory frequency (f). If there is perfect mixing in the spirometer and the lung, the change in concentration will be an exponential and the concentration (Ut) at any time (t) can be predicted from the formula:

$$Ut = U\infty\ (1 - e^{kt})$$

where $U\infty$ is the concentration at equilibrium and k is a rate constant determined by V, F and T.

In the case of $Xenon^{133}$, if the ventilation per unit volume was perfectly uniform throughout the lung, the rate of rise of count rate in all zones would be equal and they would equal the rate of wash-in for the whole lung, which would obey the above formula. In practice the rates of wash-in in different regions of the lung are not equal, indicating that the ventilation per unit volume is not equal.

In order to compare the wash-in rates from different subjects with different lung volumes and ventilation rates, Bentivoglio [76] adopted

a technique which is in principle exactly the same as the Distribution Index, comparing the observed wash-in to a predicted "ideal" wash-in. Using a modification of the Helium mixing formula of Bates and Christie[84] a predicted time (t 90) for the lung to reach 90% of the equilibrium concentration can be predicted from the formula:

$$t\ 90 = \frac{-1}{\log Q\ f}$$

$$\text{where } Q = \frac{F}{F+T} \cdot \frac{V-T}{V}$$

where f is the respiratory frequency, F is the functional residual capacity, V the spirometer volume and T is the average tidal volume minus a calculated dead space [85]. The actual time to reach 90% equilibrium in each zone was then expressed as a per cent of the predicted time. However, the time to reach equilibrium is inversely proportional to ventilation per unit volume. Therefore, the reciprocal of the per cent predicted time is an alternative method of measuring relative ventilation per unit volume and another ventilation distribution index:

$$\text{Dynamic ventilation index} = \frac{\text{Predicted t 90}}{\text{Observed t 90}} \times 100$$

It has been called a dynamic index because it is measured during uninterrupted respiration as opposed to the static indices which are measured at breathholding.

The time to reach 90% equilibrium can be read from the count rate tracing. However, the curve is always re-plotted on graph paper as the logarithm of count rate at equilibrium minus the count rate at time t

against a linear plot of time. The 90% time is the time for the curve to fall through one logarithmic cycle. Such a plot should be a straight line, if the curve is a single exponential. If the line is not straight, some caution must be exercized in interpreting this measurement as the zone is not behaving homogeneously and cannot be adequately described by a single number.

(c) SOLUBILITY AND WASH-IN MEASUREMENT

The fact that Xenon has a finite solubility means that the wash-in cannot be a single exponential, because tissue uptake acts as an "exponential leak". Mathematically it is easier to describe the behaviour for an open circuit wash-in. With no "leak" the rate of change of concentration dC/dt depends upon the ventilation per unit volume k_1 and the concentration:

$$1. \quad \frac{dC}{dt} = k_1 C$$

The rate of leak also depends on the concentration and the rate of tissue uptake (k_2) which is determined by the solubility (α), the volume (V) and the perfusion (Q). The differential equation for wash-in is then:

$$2. \quad \frac{dC}{dt} = k_1 C - k_2 C$$

Solving this equation:

$$3. \quad Ct = Co\, e^{(k_1 - k_2)t}$$

To measure ventilation per unit volume the k_1 of different zones is required. But if there is a zonal variation in k_2 an error will be introduced. The uptake of Xenon by the blood can be approximated by

$$4. \quad k_2 = \frac{\dot{Q}}{V} \alpha$$

As there is a regional difference in $\dot{Q}/V$ ratios there will be a regional difference in k_2. Anticipating the results regional volume and perfusion data can be obtained from Table II.

A Bunsen coefficient of 0.1145 can be used. Then:

k_2 Upper zone = 0.133

k_2 Mid zone = 0.237

k_2 Lower zone = 0.426

Also from Table II the ventilation per unit volume k_2 can be calculated:

k_1 Upper zone = 1.58

k_1 Mid zone = 1.95 U:L gradient 1:1.58

k_1 Lower zone = 2.5

Combining $k_1 - k_2$:

$k_1 - k_2$ Upper zone = 1.45

$k_1 - k_2$ Mid zone = 1.71 U:L gradient 1:1.45

$k_1 - k_2$ Lower zone = 2.07

Therefore, the effect of tissue uptake is to reduce the ventilation gradient by about 8%. This is probably a considerable over-estimate of the error. As discussed in the Section on Solubility, the predicted rate of tissue uptake for the whole lung is 11% per minute, whereas experimentally there is a barely perceptible decline in count rate during prolonged breathholding.

5. WASHOUT OF INHALED XENON

Mathematically it is considerably easier to handle a washout curve. Assuming perfect mixing in a single chamber the washout will be a single exponential of the form: $Ut = Uo e^{-kt}$

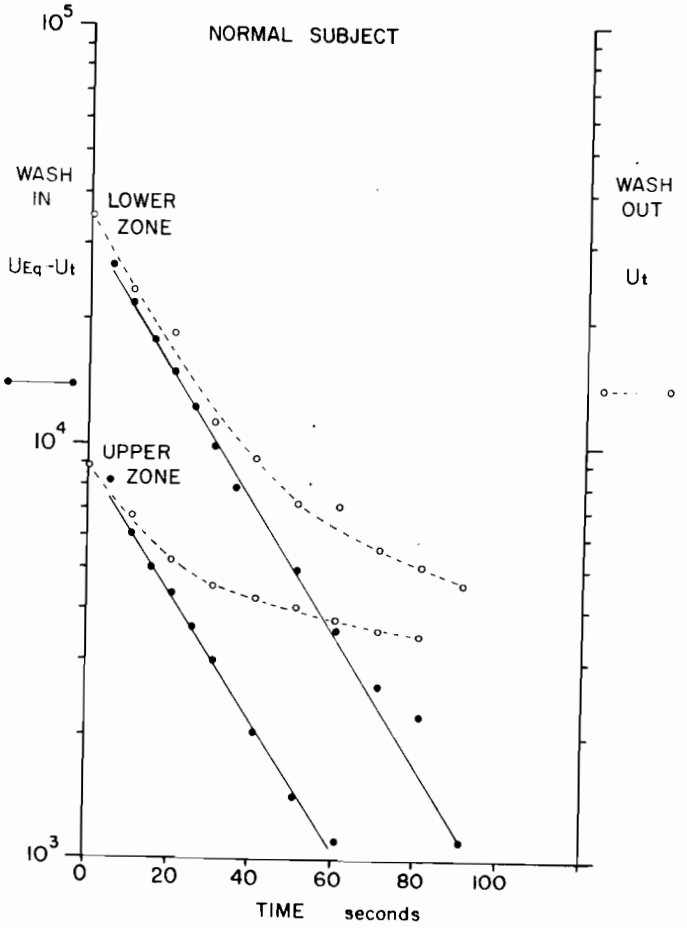

Figure XVI - Comparison of open circuit wash-in and washout showing the interference of tissue washout. On the ordinate the wash-in is plotted as log equilibrated count rate - count rate at time t, the washout is plotted as log. count rate at time t.

where U_0 is the initial count rate, U_t is the count rate at time t and k is the rate constant determined by the ventilation per unit volume. Unfortunately there are practical difficulties in attempting to measure regional distribution from the washout. Qualitative information can be obtained from watching the washout after the single breath manoeuvres, but the curve is distorted by the preceding breathholding manoeuvre. Furthermore, if the zone is not homogeneously ventilated most of the Xenon will be in the best ventilated alveoli and the subsequent washout will be dominated by these alveoli. These objections can be overcome by following the washout after the equilibration procedure[122]. However, during the equilibration procedure, particularly if this has been prolonged, a measurable quantity of Xenon has "leaked" out of lungs into the tissues. The washout of this tissue Xenon will, therefore, be superimposed on the washout of Xenon in the lungs. The effect of this is demonstrated in Figure XVI where the wash-in and washout curves are compared. As an open circuit equilibration takes longer than a closed circuit equilibration, an open circuit wash-in was done to make the wash-in and washout comparable. A bag box spirometer system was used to do these open circuit wash-in measurements. It can be seen from Figure XVI that the wash-in curves are reasonable approximations of single exponentials over most of their length. The washout curves, however, show large artefacts due to the superimposed tissue washouts, particularly in the upper zone where the initial count rate was low. For these reasons washout curves have not been routinely studied.

6. WASHOUT OF INJECTED XENON

The difficulty with all the previous methods of measuring ventilation distribution is that they are entirely unrelated to perfusion. The fact that inhaled Xenon enters a zone does not necessarily mean that the gas reaches a gas exchanging surface. This is particularly true in lung disease where the assumption of homogeneity in a zone cannot be made. To measure the ventilation of the gas exchanging surface the washout of injected Xenon was examined. This Xenon is delivered by the capillary blood through the gas exchange surface and its subsequent washout is solely determined by the ventilation of this surface. The washout will be delayed by private and common dead space as these will produce a reflux of Xenon back into the alveoli. However, this is the true gas exchange ventilation and corresponds to the Pi rather than the P_I modification of the 0_2:$C0_2$ Diagram in Figure V.

To measure this washout a saline solution of Xenon with high activity is injected intravenously while the subject is breathing quietly. The regional count rates rise to a peak and the subsequent washout is studied (see Figure XV). This is usually done at the start of the procedure when the tissue Xenon is lowest. The curve is re-plotted at 5 second intervals as the logarithm of count rate against time. If the region is homogeneous, the washout curve is a single exponential of the form:

$$Ut = U_o e^{-kt}$$

where U_o is the peak count rate, Ut the count rate at time t, and k the rate constant of gas exchange ventilation per unit volume. The regional

ventilation can either be compared by the regional rate constants or to compare different subjects, they can be expressed as indices in the same way as the wash-in curves. Knowing the total lung volume F, and the tidal volume T, and assuming perfect mixing, the time to washout 50% of the Xenon (t_{50}) in an open circuit can be predicted:

$$t_{50} = \frac{0.302}{\log Q\, f}$$

$$\text{where } Q = \frac{F}{F+T}$$

The ratio of the observed t_{50} to this predicted t_{50} multiplied by 100 yields an index of the ventilation of perfused alveoli.

The advantage of this technique carries an inherent disadvantage - the measurement depends on perfusion. When perfusion is high, quite satisfactory long curves can be plotted. When perfusion is low, the initial count rate in the region is small and only a short curve can be plotted before reaching background count rates. In these regions the curve can only be followed to 50% washout. There is also the danger of under-estimating the slope when the background count is a significant fraction of the peak count rate. Despite these difficulties quite satisfactory regional comparisons can be made in normal subjects, except occasionally in the upper zone, particularly when the subject is hyperventilating. In disease, however, the curves are frequently unsatisfac tory, both because of impaired perfusion and non-homogeneity within the zone producing a multiple exponential washout, which cannot be simply analysed.

MODEL EXPERIMENTS

To clarify some of the factors involved in external counting over the lung, some experiments were carried out using a lung model. This consisted of nine 1 inch deep rectangular perspex boxes. Each box had the AP and Lateral dimensions of the lung at the appropriate level, measured from PA and Lateral chest x-rays. These boxes were stacked to resemble the lung and the external counters placed in the standard position behind the "lung". As with human experiments the counters had to be calibrated first, by recording the count rate with a uniform known concentration of Xenon^{133} in the boxes. Subsequently the boxes could be filled with different Xenon concentrations and the accuracy of the counter estimates of the concentration checked. The model was used to explore the effect of movement and Compton scatter and to assess the error involved in volume assumptions.

(1) EFFECT OF MOVEMENT - Vertical movement of the lung model with the counters fixed radically alters the count rates. Lowering the model by 1/4" decreased the upper zone count by 8% and increased the lower zone count by 14% because the lung volume "seen" by the counter changes. The combined effect is to change the Upper:Lower concentration gradient by 24%. Lateral movement has much less effect: 1" changes the gradient by 16%. Horizontal movement away from the counters has little effect: 2" changes the gradient by less than 3%. This emphasizes how

important accurate counter placement and body positioning are.

(2) COMPTON - The error due to Compton Scatter of radiation from the opposite lung or adjacent zones was estimated using this model. A right and a left set of counters was erected in the standard counting position. The model containing Xenon was placed in front of the left set and a large block of fibre (density 0.3 gm/ml.) to act as a scattering medium was placed in front of the right set of counters. It was found that only 5% of the count rate on the left side was recorded on the right side. Similarly on replacing the upper "zone" (3 boxes) of the model by the fibre block, the upper counter count rate was 4% of the counts from the remaining boxes. Scatter, therefore, seems to be a minor problem, although it is a possible source of error in very severe cases of lung disease, where very uneven distribution may exist.

(3) VOLUME REPRESENTATION - Each external counter is summing the activity from an unknown volume of lung. In the present technique this volume is assumed to be homogeneous and can be represented by a single concentration. If the volume of the region were known, the regional amount of Xenon^{133} could be calculated and from this the regional gas or blood flow in litres/min. could be derived. There are many advantages to expressing the results in this way, even if the volume weighing is approximate. The simplest assumption is that if lines are

drawn mid-way between the counters, dividing the lung into upper, mid and lower zones, the appropriate counter will adequately represent the mean concentration of the whole underlying zone. This is certainly not exactly true, particularly in the upper zone, where a vertical concentration gradient exists and a volume gradient in the same direction (both decreasing toward the apex). The upper zone counter therefore "sees" more of the lower part of the upper zone, where the concentration is higher and will over-estimate the true mean concentration of the zone. The magnitude of the error that this would introduce was tested using this lung model. The upper, middle and lower three boxes correspond to the theoretical upper, mid and lower zones, with the counters in the standard position. Each box was then filled with Xenon to produce a linear concentration gradient down the model. The mean concentration calculated from the count rate was then compared to the actual mean concentration. The error is clearly proportional to the magnitude of the gradient. With a 1:4 gradient the maximum error was less than 5%.

This close agreement can only be applied to the human lung with caution. In this model the vertical gradient was linear and there was no front to back or lateral gradient of concentration. However, in normal subjects the vertical gradient

does appear to be reasonably linear and there is no significant front to back or lateral gradient. We have, therefore, accepted the observed mean concentration as reasonably representative of the true mean concentration of the zone, in normal subjects. Any error introduced by this approximation will always tend to under-estimate the unevenness of distribution. It must be noted that this simple approach cannot be used in the presence of lung disease, where the vertical gradient may not be linear and significant front to back or lateral gradients may exist.

VOLUME AND FLOW ASSUMPTIONS

One of the main purposes of volume weighing the Xenon data was to be able to compare it with the oxygen^{15} data and, therefore, as far as possible we have used the same assumptions. The Xenon upper, middle and lower zone counters correspond closely to the position of the 2nd, 5th and 7th oxygen^{15} counters (See Figure VIII). Also by dividing the lung into three zones by lines drawn mid-way between counters, each Xenon zone is approximately equal to three of the oxygen^{15} slices. Summing the approximate anatomical volume measurements made in the oxygen^{15} study for the upper, middle and lower three slices, the volumes of the Xenon zones are:

Upper zone - 25% of the lung volume.

Middle zone - 36% of the lung volume.

Lower zone - 39% of the lung volume.

Volume differences between the left and right lung were ignored and the

mean concentration of the left and right lung zones were used. Multiply- the zonal concentration of Xenon by the volume of the zone gives the amount of Xenon in the zone. The fraction of the total amount of Xenon in any zone is then proportional to the fraction of the total flow (either $\dot{V}A$ or $\dot{Q}c$) going to the zone.

The following values were used for total alveolar ventilation and cardiac output:

(1) SEATED RESTING - $\dot{V}A$ = 5 L/min.

$\dot{Q}c$ = 6 L/min.

These are the same values used in the oxygen[15] study.

(2) SEATED EXERCISE - $\dot{V}A$ = 26 L/min.

$\dot{Q}c$ = 12 L/min.

These values were taken from a study by McGregor[(78)] in this laboratory in which dye cardiac outputs were done on a group of normal subjects in the same position, at the same workload on the Elima ergometer. His figures for tidal ventilation were corrected for dead space from the Asmussen-Neilsen regression formula

(3) SUPINE RESTING - $\dot{V}A$ = 4.5 L/min.

$\dot{Q}c$ = 5.25 L/min.

These figures were also taken from the same study by McGregor, with the same $\dot{V}_T$ to $\dot{V}A$ correction.

EXPERIMENTAL CONDITIONS

The following studies have been carried out:

(1) SEATED, RESTING, BREATHING AIR - Twenty-five men and six women have had technically satisfactory studies under these conditions. All were apparently healthy and their ages ranged from 22 to 44 years. Measurements were started after 5-10 minutes rest in the chair. These were all studied using six back scintillation counters. In four subjects parallel counting over the front of the right lung was also employed. In ten of these subjects ventilation distribution was studied by single breath, wash-in and washout techniques. In the remainder ventilation distribution was only measured by single breath.

(2) SEATED, EXERCISING - Five normal young men were studied. They were seated in the chair and pedalled an Elima bicycle ergometer with a load of 300 kg/m/min. throughout the study. Measurements were started during the seventh minute of exercise. Six back scintillation counters were used. Great care was taken to prevent movement of the chest during these studies. In practice this was not a great problem as the subjects were well supported by the bucket seat of the chair and by taking a firm grip on the arm-rests.

(3) SEATED, RESTING, BREATHING 100% OXYGEN - Four subjects had duplicate studies, breathing either air or 100% oxygen. The oxygen was breathed for 10 minutes before and during the whole experiment.

This required filling the closed circuit spirometer with oxygen instead of air.

(4) SUPINE, RESTING - Seven normal subjects were studied, five men and two women. Measurements were started 5-10 minutes after lying down. In all these studies parallel counting was used with six scintillation counters behind the chest and six in front. The counters were positioned from a chest x-ray taken in the horizontal position. The Helium functional residual capacity was also estimated in the horizontal position.

(5) POSTURAL SYNCOPE - In one subject postural syncope was induced by prolonged passive tilting in a 75^{o} head-up position. Because of the technical difficulties only serial injections of $Xenon^{133}$ were carried out to study the change in perfusion distribution. The subject was an experienced fainter, but otherwise normal and was able to recognize and signal the onset of fainting. Injections were made immediately after assuming the upright position, after 15 minutes upright and after 35 minutes when the subject was fainting. Breathholding was insured during the last injection by clamping the mouthpiece.

PART II

RESULTS AND DISCUSSION

UPRIGHT – 31 NORMAL SUBJECTS

	UPPER	MID	LOWER	TOTAL
VOLUME	25%	36%	39%	
$\dot{V}$ INDEX	58±10	71±10	92±16	
$\dot{V}$ L/min	0.955	1.685	2.360	5
$\dot{Q}$ INDEX	41±12	73±19	133±23	
$\dot{Q}$ L/min.	0.696	1.782	3.522	6
$\dot{V}/\dot{Q}$ Ratio	1.37	0.95	0.67	

TABLE II

COMPARISON OF VENTILATION

INDICES – 10 SUBJECTS

		UPPER ZONE		MID ZONE		LOWER ZONE	
		RIGHT	LEFT	RIGHT	LEFT	RIGHT	LEFT
SINGLE BREATH	Tidal	59±9	60±10	69±9	78±12	90±14	105±18
	Inspiratory Capacity	70±5	77±9	84±5	94±9	100±8	113±10
WASHIN OF INHALED XENON		60±19	61±15	83±21	86±18	103±17	103±18
WASHOUT OF INJECTED XENON		57±32	49±28	80±32	83±31	105±32	109±40

TABLE III

RESULTS

(1) SEATED, RESTING

The results in 31 normal subjects, seated at rest breathing air are shown in Table II. The mean and standard deviation of the indices presented, with the volume weight regional flows. Data from the left and right lung have been combined as there was no significant difference between them. The differences between zones both for the ventilation and perfusion indices were highly significant ($P > 0.001$). The ventilation indices are at tidal volume and show a gradient of ventilation per unit volume from the upper to the lower zone of 1:1.6. The gradient of perfusion per unit volume is much steeper, 1:3.2. Because there is also a volume gradient (1:1.6), the differences in absolute regional flow are larger: for ventilation 1:2.5, for perfusion 1:5. Because of this inequality of distribution, the calculated Ventilation/Perfusion ratio is twice as high in the upper zone as in the lower zone.

A comparison of the methods of measuring ventilation distribution in ten normal subjects is presented in Table III. The ventilation gradient measured by a tidal single breath is 1:1.6, measured at inspiratory capacity it is 1:1.4. This difference is statistically significant ($P > 0.01$) indicating that the distribution becomes more uniform at larger inspired volumes. However, judged by the size of the standard deviation, the inspiratory capacity index is the more repeatable measurement. The

SUPINE 7 NORMAL SUBJECTS

	UPPER	MID	LOWER	TOTAL
VOLUME	25	36	39	
$\dot{V}$ INDEX	77±10	85±13	74±11	
$\dot{V}$ LPM	1.20	1.70	1.60	4.5
$\dot{Q}$ INDEX	105±15	102±19	85±18	
$\dot{Q}$ LPM	1.72	2.38	2.16	6.25
$\dot{V}/\dot{Q}$ Ratio	0.70	0.71	0.74	

TABLE IV

EXERCISE 5 NORMAL SUBJECTS

	UPPER	MID	LOWER	TOTAL
VOLUME	25	36	39	
$\dot{V}$ INDEX	86±14	88±12	91±7	
$\dot{V}$ L/min	6.318	9.282	10.400	26
$\dot{Q}$ INDEX	90±9	94±15	110±13	
$\dot{Q}$ L/min	2.724	4.092	5.184	12

TABLE V

Dynamic index derived from the wash-in measurement shows a gradient of 1:1.7 and is not statistically different from the static tidal index. The standard deviation of the Dynamic measurements is generally higher than for the Static measurements, particularly in the upper part of the lung. The indices derived from the washout of injected Xenon show a gradient of 1:2.0, which is not significantly different from the single breath and wash-in gradient. This suggests that in normal subjects, the distribution of ventilation and the distribution of alveolar ventilation are the same. However, it should be noted that the standard deviation of these measurements is large and fine comparison is not possible.

(2) SUPINE, RESTING

The results from seven normal subjects resting in the supine position are shown in Table IV. Compared to the upright resting data, the ventilation indices show significant ($P > 0.01$) increases in the upper and mid zone and reduction in the lower zone. As a result the gradient of ventilation per unit volume is abolished, although a volume weighted flow gradient remains. The gradient of perfusion indices has been reversed due to a large highly significant ($P > 0.001$) rise in the upper zone and decrease in the lower zone perfusion. When these figures are volume weighted, the Ventilation/Perfusion ratios of all zones appear to become equal. However, these figures were derived from the summed outputs of anterior and posterior parallel counters. There was no significant difference in the anterior and posterior ventilation indices. There was a significantly higher ($P > 0.01$) perfusion gradient in the middle and lower zones but no apparent difference

in the upper zone. The significance of these antero-posterior gradients is hard to assess, because it depends, not only on the magnitude of the true gradient, but also the extent to which the anterior and posterior counter fields overlap. As the A.P. diameter is larger in the mid and lower zone there is probably a larger gradient and more chance of detecting it because the counters are further apart. Therefore, despite apparent caudal uniformity of $\dot{V}_A/\dot{Q}$ ratios, there is an antero-posterior $\dot{V}_A/\dot{Q}$ gradient which cannot be accurately quantitated.

(3) SEATED, EXERCISING

The results from five normal subjects exercising on a bicycle ergometer with a 300 Kg/M/min. load are presented in Table V. Compared to the resting data, the upper and mid zone ventilation indices are significantly higher ($P > 0.01$). There is a very large highly significant ($P > 0.001$) rise in the upper zone perfusion. These changes make the distribution per unit volume much more uniform. Expressed as flow the most striking difference is the much larger increase in ventilation than in perfusion so that the $\dot{V}_A/\dot{Q}$ ratio of all zones is much higher.

(4) SEATED, BREATHING OXYGEN

The comparison of four subjects breathing air and oxygen in duplicate studies is shown in Table VI. The results show no difference in the distribution of either ventilation or perfusion. For unexplained reasons the absolute values of the perfusion indices are all lower than normal although the gradient is normal.

COMPARISON OF AIR & 100% OXYGEN
4 NORMAL SUBJECTS

		UPPER	MID	LOWER
VENTILATION INDEX	Breathing Air	80 ± 7	94 ± 11	107 ± 7
	Breathing 100% O_2	83 ± 8	96 ± 7	106 ± 8
PERFUSION INDEX	Breathing Air	33 ± 12	59 ± 8	96 ± 14
	Breathing 100% O_2	35 ± 12	59 ± 9	95 ± 12

TABLE VI

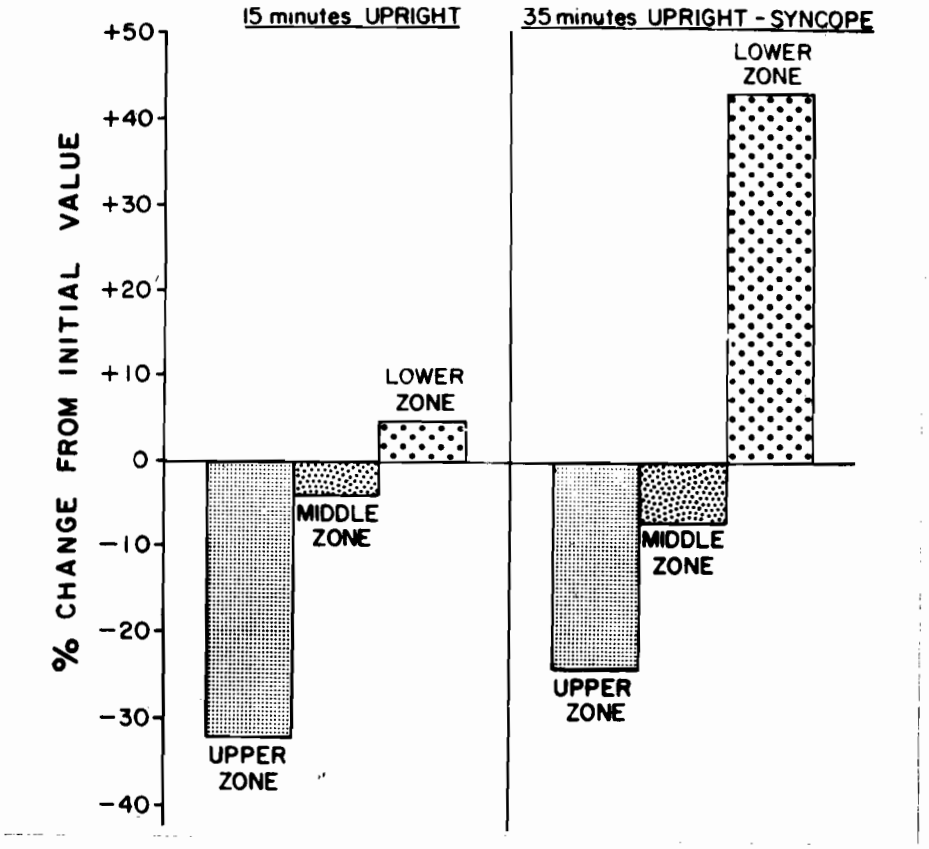

Figure XVII - Perfusion changes during prolonged standing.

(5) POSTURAL SYNCOPE

The results of serial perfusion studies in one subject during prolonged passive standing are shown in Figure XVII. Results are expressed as percentage change from the count rate observed immediately after tilting into the upright position. The results show a progressive reduction in the upper zone and increase in the lower zone perfusion.

The main results of these studies are summarized graphically in Figure XVIII.

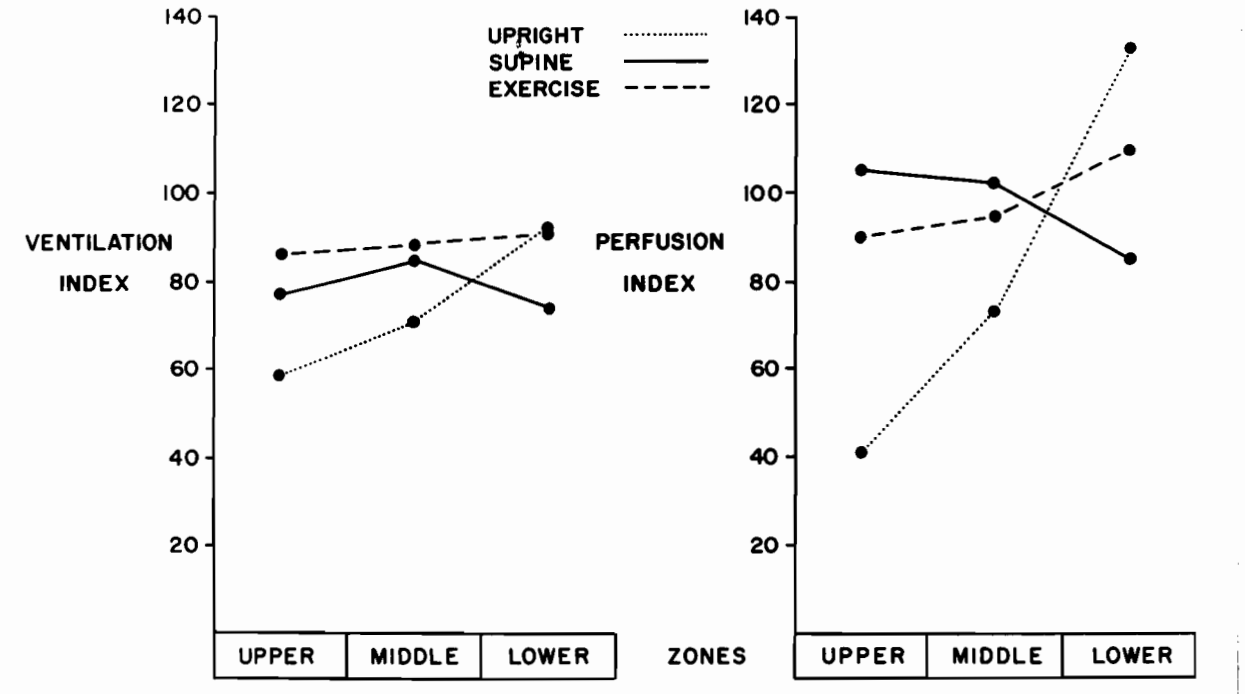

Figure XVIII - Summary of changes in Ventilation and Perfusion distribution indices.

COMPARISON OF Xe^{133} & $C^{15}O_2$ RESULTS

		UPPER	MID	LOWER
VENTILATION L/MIN	Xe^{133}	0·95	1·68	2·36
	$C^{15}O_2$	0·99	1·78	2·31
PERFUSION L/MIN	Xe^{133}	0·70	1·78	3·52
	$C^{15}O_2$	0·58	1·98	3·44

TABLE VII

DISCUSSION

The most important conclusion from this data is that the distribution of ventilation and perfusion in the lung are not matched. Furthermore, there is no fixed relationship as the distribution is constantly changing during normal activity. The discussion will be primarily concerned with:

1. The mechanical factors that determine the normal distribution of ventilation and perfusion.
2. The consequences on gas exchange of the Ventilation/Perfusion distribution patterns in normal subjects.

Before discussing these topics it is necessary to compare the present data with other studies of regional distribution and consider the possible sources of error in the method.

There is an extraordinarily close agreement between the present data and the results obtained with radio-active CO_2 by West and Dollery[63]. Their results from the upper, middle and lower three counter fields have been summed to compare with the Xenon counter fields in Table VII. The greatest discrepancy is that the upper zone perfusion measured by $Xenon^{133}$ is 120 ml/min. higher than when measured with $C^{15}O_2$. Expressed as an upper to lower perfusion gradient per unit volume it is 1:3.2 for $Xenon^{133}$, and 1:3.9 for $C^{15}O_2$. The ventilation gradient is very similar (1:1.6 compared to 1:1.5) but there is a flow difference of 100 ml/min. in the middle zone.

This measure of agreement is very satisfactory because the two

methods of measurement are quite dissimilar. This is particularly true for the perfusion measurement, where the Xenon technique depends on gas excretion and $C^{15}O_2$ depends on gas uptake. The ventilation methods are superficially similar, but in fact most of the oxygen^{15} ventilation figures represent intelligent estimates and not entirely based on experiment. It is also quite surprising that the volume assumptions made with the relatively crude Xenon counter fields yield figures that are comparable to the sharply defined $C^{15}O_2$ counter fields.

Only partial studies on change of posture and exercise were made with $C^{15}O_2$ and the data cannot be compared quantitatively. However, there is general agreement that in the supine position the caudal gradient is abolished. On exercise the $C^{15}O_2$ data showed a smaller reduction in the perfusion gradient than Xenon^{133}. This difference may be explained by the fact that the $C^{15}O_2$ measurements were made after the exercise period and the exercise load was not the same.

The most important discrepancy between the two methods is that $C^{15}O_2$ gives a bigger gradient of perfusion than Xenon^{133}. The errors in the $C^{15}O_2$ technique have been examined (63, 64, 65) and discussed in the description of this technique. Nearly all these errors will tend to underestimate the upper zone perfusion and so exaggerate the perfusion gradient. The potential errors with the Xenon^{133} technique have been fully discussed by Ball(75) and examining these it is possible that Xenon over-estimates the upper zone perfusion and under-estimates the true perfusion gradient:

1. As the activity in the upper zone is smaller than in the rest of the lung, proportionately more of the count rate over this zone may be Compton scatter from other zones.
2. Uptake of Xenon by the blood is proportional to the flow per unit volume and is, therefore, unequally distributed. This will tend to under-estimate the lower zone perfusion.
3. Body movement between the initial manoeuvres and the equilibrium plateau is a serious potential source of error, although it is constantly checked. Vertical movement is the most serious, antero-posterior movement has little effect. The tendency is to slide down during the experiment, which would reduce the equilibrium count rate over the upper zone and lead to an over-estimate of upper zone perfusion.

Summarizing it appears probable that $C^{15}O_2$ over-estimates and Xenon^{133} under-estimates the true perfusion gradient.

It is difficult to compare these regional studies with the lobar-spirometry data of Martin[12] and Mattson[13], because of the differences between lobes and regions. However, there is qualitative agreement. Calculations from their data (Table I) show that the $\dot{V}_A/\dot{Q}$ ratio of upper lobe 2.5 times (Martin) or 2.7 times (Mattson) higher than the lower lobe. The Xenon data makes the $\dot{V}_A/\dot{Q}$ ratio of the upper zone twice as high as the lower zone.

VENTILATION DISTRIBUTION

Nearly all the inert gas methods of studying distribution have demonstrated the presence of some uneven ventilation in the normal lung. The present results show that this unevenness has a definite topographical distribution which can be altered to some extent by the depth of breathing, posture and exercise. It is of interest that the changes in ventilation distribution are always in the same direction as the changes in perfusion, but the magnitude of the change is smaller. In the upright position there is a caudal gradient of ventilation, measured by the tidal index of 1:1.6. There is no significant difference between this static method of measuring distribution and the Dynamic Wash-In method (gradient 1:1.7). Distribution measured after an inspiratory capacity breath is more uniform (1:1.4) due to a significant rise in the upper zone index. There is a higher inspiratory capacity index in the left lower zone than the right which is highly significant ($P > 0.001$). This difference is not demonstrable during tidal breathing. In the supine position the caudal gradient disappears, the highest ventilation being now to the mid zone. On exercise the caudal gradient is markedly reduced and the distribution becomes practically uniform (1:1.06). There is apparently no change in ventilation distribution breathing 100% oxygen.

Fowler[79] reviewing the causes of uneven ventilation concluded that it was due to variations in the per cent volume change and/or preferential distribution of dead space within the lung. While preferential dis-

tribution of dead space may occur, the original concept seems unten able. It was used in a "first in, last out" hypothesis to explain the shape of the single breath N_2 washout. Alveoli filling fast, but emptying slowly implies a sudden reversal of time constants which is difficult to visualize physiologically. Certainly it would be very difficult for preferential distribution of dead space to explain the present geographical distribution. Assuming a common dead space of 80 ml, 75% of this would have to go to the upper zones, 25% to the mid zones and none to the lower zones to account for the distribution. For this to occur it would be necessary to postulate radically different regional time constants, which with present techniques cannot be demonstrated[80].

Regional differences in the per cent volume change or "regional volume expansion ratio" provide a more satisfactory explanation for the uneven distribution. It is important to recognize that this is a ratio with a volume increment dV over an end-expiratory volume V and that unequal distribution can be caused by differences in regional dV or V.

VARIATION IN dV

Three factors will determine the distribution of the volume increment (dV):

1. Differences in airway resistance.
2. Differences in the distensibility of the terminal air units or their compliance (compliance in the ensuing discussion refers to compliance per gram of tissue, which is hypothetical, but less misleading than other terms).

3. Differences in the local intra-thoracic pressure.

The last of these can be regarded as the driving force or voltage and the first two as impedances. These impedances behave in fundamentally different ways as the airway resistance is proportional to flow rate, whereas compliance is independent of flow. The way in which these impedances interact to determine distribution has been brilliantly analyzed by Otis et al.[80] using a simple electrical analog. The analogous electrical and physiological terms are:

R = Resistance (ohms) = Airway resistance (cm/L/sec.).

C = Capacitance = Compliance (L/cm).

E = Voltage (volts) = Intra-pleural pressure (cm).

I = Current (amps) = Flow (L/sec.).

Q = Charge (coul) = Volume (L).

A single bronchus and terminal air unit can then be represented by a series RC network. The relationship between the input voltage and the charge on the capacitor can be written:

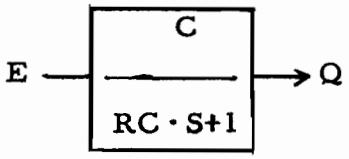

DYNAMIC

That is, the charge in response to a given voltage will be determined by the transfer function within the box. The term RC is the denominator in the time constant of the system and will determine the rate of change of charge. However, when a steady state is reached S = 0 and RC S = 0 and the only factor determining the charge following a step input of voltage

will be the capacitance.

STEADY STATE

Exactly the same situation applies to the lung. The product of the airway resistance and compliance is the time constant of the unit (cm/L) sec. x L/cm = time. This will determine the rate of change of volume in the terminal air unit. Inspiring and breathholding is analogous to a step input of voltage. During breathholding flow ceases RC•S goes to zero and for a given change of intra-pleural pressure the volume change will be solely determined by the compliance and independent of airway resistance. It follows that for two of these systems in parallel that the steady state distribution of tidal air between them can only differ if either they have different compliances or they are subject to different intra-pleural pressure changes.

This analysis is of considerable importance in interpreting the Xenon ventilation distribution results. The TV and IC single breath indices are measured during breathholding, that is under no-flow conditions, when airway resistance becomes zero. Therefore, the observed difference in distribution can only be due to differences in compliance or local intra-pleural pressure.

(a) COMPLIANCE differences do not appear to be the cause. As the Static and Dynamic methods of measuring ventilation distribution give almost exactly the same results in normals the regional time constants must be equal. If the compliances within the lung were unequal this must mean opposite differences in the airway resistance to keep the RC product equal.

To get more tidal air into the lower zone it must, therefore, have a higher compliance and lower airway resistance. However, as there is over three times as much blood per unit volume in the lower zone as in the upper, it is logical to suspect that the lower zone would be relatively stiffer. For the lung as a whole, this appears to be true as inflation of a G-suit, which increases the central blood volume decreases the lung compliance[81].

(b) INTRA-PLEURAL PRESSURE differences appear to be the most logical cause of differences in the distribution of tidal air (dV). Daly and Bondurant[82] have recently made direct measurements of the regional intra-pleural pressure in normal subjects in the upright position. Using a specially designed needle system, pressures were recorded from small (less than 2 ml) pneumothoraces induced at various levels down the chest. Their results were expressed as pulmonary elastance $\Delta P / \Delta V$ where ΔP is the local intra-pleural pressure change and ΔV the over-all lung volume change. The values for elastance down the chest were:

3rd Intercostal Space	3.73 ± 1.13 SD
5th Intercostal Space	3.82 ± 0.58
8th Intercostal Space	6.13 ± 1.02
Oesophagus	5.28 ± 0.74

After deliberate induction of 200 ml pneumothorax the local

differences in ΔP disappeared and equalled the oesophageal ΔP. Unfortunately no satisfactory studies have been done in the supine position.

These results have to be interpreted with some caution because there are a number of forces acting on the bubble:

(1) True intra-pleural pressure applied to the surface of the bubble.

(2) Forces depending on the volume, shape and surface tension of the fluid forming the bubble.

(3) Forces applied to the bubble by the surrounding lung and chest wall.

If the bubble is small during respiration the main force should be the true intra-pleural pressure and the artefacts in 2 and 3 should only vary to a small extent. However, there is a source of error implicit in their further observation that the absolute, end-expiratory pressure varies down the lung. Their mean figures are:

3rd Intercostal Space	3.33 cm H_2O
5th Intercostal Space	4.17
8th Intercostal Space	1.80

As the absolute pressure is lower in the upper part of the thorax, the bubble will be bigger and the forces acting upon it different from a smaller bubble lower down the thorax. The only other evidence to support variations in ΔP is indirect. Krueger [83] measured the regional intra-pleural

pressure in dogs with a fluid filled Balloon, which is less susceptible to the artefacts mentioned above. This paper is only concerned with the level of the absolute intra-pleural pressure. However, it contains an illustration which shows an apparent increase in ΔP down the lung. Therefore, there appears to be strong evidence that there is some variation in ΔP down the lung. However, further proof is required and to use it to explain regional distribution further studies are required to show that it changes with posture.

VARIATIONS IN V

Variations in the denominator of the volume expansion ratio(V) the end expiratory volume may well account for the observed distribution. Daly's data quoted above shows a considerable increase in the end-expiratory intra-pleural pressure down the lung. Krueger's work[83] with a more acceptable method, in dogs, also shows that when the dog is upright the absolute pressure increased by 0.21 cm H_2O per centimeter descent down the lung. This gradient disappeared when the dog was supine. He explains this increase on a hydrostatic basis and related the gradient to the density of lung tissue in the dog (0.221 gm/cm^3). Extrapolating from the density of human lung tissue, he predicted a similar gradient in man of 0.275 cm H_2O per cm descent in upright man. Milic-Emili[84] showed a similar gradient of oesophageal pressure in man. Accepting these figures the end-expiratory intra-pleural pressure under the upper zone Xenon counter would be approximately 5 cm H_2O more negative than under

the lower Xenon counter. Assuming that the compliance of the lung was uniform this difference in pressure would produce a larger end-expiratory alveolar volume in the upper zone. Then equal increments of tidal volume (dV) to the upper and lower zones would produce a lower volume expansion ratio in the upper zone. If this is so the observed "uneven ventilation" is due to uneven distribution of alveolar volume per unit of thoracic volume and not due to uneven distribution of tidal ventilation.

In the horizontal position, assuming men behave like Krueger's dogs, the caudal pressure gradient would be abolished. With uniform end-expiratory pressures, the end-expiratory volumes would be the same and equal increments of volume would produce an equal volume expansion ratio, accounting for the observed supine distribution. There is good support for this in the lobar spirometric work of Martin[11] who measured the ventilation and the nitrogen washout simultaneously from the upper lobe compared to the middle and lower lobe. He found no significant difference in the proportion of tidal ventilation to the two regions in the upright or the supine position. However, in the upright position the nitrogen clearance was slower from the upper lobe, while in the supine position the differences between lobes decreased. The only explanation for this appears to be a change in the relative volume of the lobes with the change in position.

PERFUSION DISTRIBUTION

The present data demonstrates the remarkable lability of the distribution of perfusion during normal activity. In the upright position the distribution is very uneven. The gradient of blood flow per unit of volume between the upper and lower zones is 1:3.2. In terms of flow the lower zone is receiving over 50% of the total blood flow, whereas the upper zone is receiving less than 12%. In the supine position there is a considerable redistribution of flow. The caudal gradient is abolished and the gradient is reversed, so that the upper zone receives more perfusion per unit volume than the lower (1:0.8). The results also indicate that in this position a front to back gradient exists. Studying these changes on the Tilt table, it was apparent that they occur very rapidly. Exercise also produces a relative increase in the upper and mid zone flow leading to a more uniform distribution. Breathing 100% oxygen appears to have no effect on the distribution.

This variability in distribution is to be expected because the pulmonary circulation is a low pressure pumping system operating in a gravitational field. However, there is still considerable uncertainty about the factors governing flow through the pulmonary vascular bed and the special conditions existing in this circulation need to be examined.

1. GENERAL PRINCIPLES OF FLOW

Flow through rigid tubes obeys Poiseuille's Law:

$$F = \Delta P \cdot \frac{\pi}{8} \cdot \frac{1}{n'} \cdot \frac{r^4}{L} \quad \text{or} \quad R = \frac{\Delta P}{F} = \frac{8}{\pi} \cdot n \times \frac{L}{r^4}$$

Where F = Flow ΔP = Driving Pressure

Where R = Resistance

$\frac{\pi}{8}$ = Integration constant

n = Coefficient of viscosity

r = Radius

L = Length

If the pulmonary circulation were a rigid system Δ P would be the pressure difference between the pulmonary artery and the left atrium. In a rigid system flow would be uninfluenced by gravity because the principles of a syphon would operate, and flow is solely determined by the P between the ends of the tube and uninfluenced by an intermediate pressure. While there is some evidence that, in dogs, the pulmonary circulation behaves like a rigid system[85] this seems quite improbable in man.

Analysis of flow through a distensible system is considerably more difficult because the driving pressure and the resistance become interdependent [86]. The radius of a distensible tube will vary with the trans-mural pressure across the tube. Small changes in radius will produce large changes in resistance ($R \propto 1/r^4$). The trans-mural pressure (P_{TM}) is the intra-vascular pressure (P_{IV}) minus the pressure in the surrounding tissues (P_T).

$$\text{i.e. } P_{TM} = P_{IV} - P_T$$

The total distending force in a vessel is therefore $2\pi r P_{TM}$. This force is opposed by the circumferential tension developed in the wall of the vessel (T_c). At equilibrium $P_{TM} = \frac{T_c}{r}$

The circumferential tension is developed b the elastic tension, which is a function of the radius (by the Laplace relationship) and by active tension resulting from vasomotor activity.

In the systemic circulation, where the driving pressure is high, the main resistance vessels are the arterioles and the flow is primarily controlled by variations in the vasomotor circumferential tension. However, in the low pressure pulmonary circulation it also appears that hydrostatic forces and the tissue pressure surrounding the capillaries play important roles in the normal distribution of flow.

2. PULMONARY INTRA-VASCULAR PRESSURE

The normal pulmonary artery pressure in the supine position varies from a systolic of 20 mm Hg. to a diastolic of 9 mm Hg. with a mean of 15 mm Hg. These figures are not true "absolute pressures" as they are referenced to an arbitrary hydrostatic pressure level outside the thorax (5 cm. below the sternal angle, 10 cm. above the table) and not the tip of the catheter. Data on pressure in the upright position is scanty, mainly because of difficulties with a pressure reference level, but the pressures appear to be somewhat lower [87]. As the heart and main pulmonary vessels lie within the pleural space changes in the intra-pleural pressure are transmitted to the intra-vascular pressure. During quiet breathing the pulmonary artery pressures vary approximately $\pm$ 3 mm Hg. and during deep breathing $\pm$ 9 mm Hg.

In this low pressure circulation hydrostatic forces have a considerable influence on the intra-vascular pressure in the branches of the

pulmonary artery and will vary with the orientation of the body in the gravitational field. The apex of the lung is about 12 cm. from the root of the pulmonary artery, in the upright position at 1-G, assuming a density of 1.05 gm/cm^3 for blood, a hydrostatic pressure of 12.6 mm Hg. will be developed. Subtracting this from the mean pulmonary artery pressure only leaves 2.4 mm Hg. intra-vascular pressure at the apex. In contrast the intra-vascular pressure will be considerably higher than mean pulmonary artery pressure. In the supine position this caudal pressure gradient will largely disappear, but be replaced by a smaller front to back gradient.

Similar considerations apply to the venous side of the system. The mean left atrial pressure is about 5 mm Hg. with the local pressure depending on the effect of gravity.

An important limitation of pulmonary artery pressure measurements is that a normal cardiac catheter only measures the "static" pressure or the potential energy of the system [88, 89]. The pressure available from kinetic energy is not measured but appears to be an important factor in distribution. Its importance can be seen from Bernoulli's theorem which states that the sum of the forces due to pressure, position and velocity are a constant, or:

$$P + \rho gh + \frac{V^2}{2} = \text{Constant}$$

Where P = applied pressure

ρ = density

g = gravitational force

h = hydrostatic height

V = velocity

The applied pressure (P) and the positional pressure (ρgh) are the Static Pressure (Ps) of the system, or its potential energy, while the velocity term $V^2/2$ is the kinetic energy. By reducing flow to zero, the kinetic energy is converted into Potential energy producing a dynamic pressure. Therefore, the total pressure (P_T) in a flowing system is:

$$P_T = Ps + \frac{V^2}{2}$$

As flow velocity is not reduced to zero at the openings of either side hole or end hole catheters pointed in the direction of flow, the dynamic pressure is not recorded. Indeed in an end hole catheter the velocity may even produce a negative pressure by the Venturi action over the tip.

The kinetic energy is a small fraction of the total energy in the systemic circulation at rest because the static pressure is so high. However, in the pulmonary circulation, while the flow velocity is approximately the same, the static pressure is much lower. From curves of flow velocity (in the aorta) published by Fry [90] this contribution can be calculated. In these curves the peak systolic velocity is 105 cm/sec., the mean velocity during systole is about 58 cm/sec. and the mean velocity calculated over the whole cycle about 29 cm/sec. From these figures the kinetic energy per ml of blood would be 5512/dyne/cm^2 during peak systole, during the time mean for systole 2326 dyne/cm^2, and the time mean for the whole cycle 1433 dyne/cm^2. These could exert an equivalent pressure of about 4 mm Hg. at peak systole, 1.8 mm Hg. throughout systole and 1 mm Hg. throughout the cycle. Therefore, in the pulmonary artery static pressure measurement under-estimates the total pressure by about 20% in peak systole and the mean pressure by 7% at rest. This error becomes enor-

mous as the flow velocity goes up, for example, when the cardiac output increases from 5 LPM to 25 LPM, the flow velocity increases approximately by five. As kinetic energy is proportional to the square of the velocity, the kinetic energy will increase by 5^2 or twenty-five times, equivalent to 100 mm Hg.

3. PULMONARY TISSUE PRESSURE

The perivascular pressure around the heart and main pulmonary vessels is the intra-pleural pressure. When the vessels enter the lung they are subject to more complex forces. Howell [91] and Permutt[92] have suggested that the larger vessels are distended as the lung inflates by the radial traction of the adjacent alveoli in the same manner as the bronchi. However, the capillaries which run in the walls of the alveoli will be compressed by the alveolar pressure as the lung expands. As Staub [93] has pointed out, quick frozen lung sections do not show hemispherical shape, they are polygonal. Models based on hemispherical alveoli, therefore, have to be treated with some caution. Lloyd [94] has demonstrated the perivascular pressure on these vessels is slightly less than alveolar pressure. When the lung is fluid filled, to eliminate surface tension forces, the perivascular pressure equals the alveolar pressure. The effect of lung inflation is therefore complex - it lowers pulmonary artery pressure, lowers the resistance in the large vessels but compresses the small ones.

4. VASCULAR WATERFALL

Whereas conventionally pulmonary vascular resistance is calculated from the pressure drop between pulmonary artery to pulmonary

vein, Permut and his colleagues [95, 96] have shown that flow can be independent of the venous pressure. They have used the analogy that over a waterfall flow is independent of height of the fall and shown that a similar situation exists in collapsible tubes. If pressure around a collapsible tube (P_C) is higher than the outflow pressure (P_O) but lower than the inflow pressure (P_I), at some point in the tube the pressure inside the tube will equal the pressure outside (P_C). Then the flow Q will depend on the difference between (P_I) and (P_C) and the resistance (R) upstream of the equal pressure point.

$$Q = \frac{P_I - P_C}{R}$$

Changes in the outflow pressure P_O (as long as P_C is greater than P_O) will have no influence on flow as they are met by changes in the flow resistance of the collapsible tube downstream of the equal pressure point.

In the pulmonary circulation P_I is the pulmonary vascular pressure, P_C is the perivascular or alveolar pressure and P_O the pulmonary venous pressure. At the apex of the lung the pulmonary venous pressure (left auricular pressure minus the hydrostatic column) is lower than alveolar pressure. Therefore, flow is determined by the inflow pressure and the alveolar pressure. During much of the cardiac cycle the pulmonary artery pressure will be below the alveolar pressure so flow will be intermittent. Further down the lung pulmonary artery pressure will be higher than alveolar pressure and flow will depend on the difference (P_I-P_C) and the resistance up to the equal pressure point. As the alveolar pressure is still higher than pulmonary venous pressure, venous pressure has no

influence on the flow. Only in the lower part of the lung where pulmonary venous pressure exceeds alveolar pressure will the flow be determined by the arterio-venous pressure difference and the over-all resistance.

5. VASOMOTOR TONE

The distribution of perfusion may be influenced by regional differences in vascular resistance. It is possible that local gas tensions influence the vasomotor tone in the pulmonary vascular bed. Hypoxia produces a marked rise in pulmonary vascular resistance [97] and severe local hypoxia leads to a local reduction in perfusion [98]. The resistance change appears to occur in both pre- and post-capillary vessels. High oxygen tensions have no apparent effect on pulmonary vascular resistance, suggesting that, despite the low oxygen tension in mixed venous blood, there is little "tonic" action in the resistance vessels under normal circumstances. The present results also support this as there is no change in perfusion distribution breathing 100% oxygen, which would remove any tonic action of hypoxia on the resistance vessels of the lower zone. However, it must be stressed that these are large zones and any effect would presumably be small.

These conclusions are at variance with the results of Larson and Severinghaus [42] who showed an increased AaD_{C0_2} while breathing 100% oxygen. They interpreted this as evidence of relaxation of basal vessels, reducing the flow to the upper part of the lung creating a larger alveolar dead space. This discrepancy has not been fully resolved. Some increase in AaD_{C0_2} may be expected from the Haldane effect on $C0_2$ transfer, with

no change in distribution. At a high oxygen tension for the same CO_2 content the pCO_2 will be higher than at a low oxygen tension. Therefore, on 100% oxygen the mixed venous blood and the low $\dot{V}_A/\dot{Q}$ alveoli will have a higher pCO_2. However, this elevation will be progressively smaller at higher $\dot{V}_A/\dot{Q}$ ratios, because even on air the pO_2 in them is high. The effect of this is a wider distribution of pCO_2 values for a given $\dot{V}_A/\dot{Q}$ distribution, the magnitude of which depends on the proportion of alveoli with low $\dot{V}_A/\dot{Q}$ ratios. The wider the distribution of pCO_2, the larger the AaD_{CO_2} will be. This partially explains the increase in AaD_{CO_2} breathing oxygen. But, if it is entirely due to the Haldane effect the arterial pCO_2 should rise, with little or no change in the alveolar pCO_2 because most of the arterial blood comes from the low $\dot{V}_A/\dot{Q}$ alveoli. In Larson's data the reverse occurs - $P_{A_{CO_2}}$ falls and there is no change in Pa_{CO_2}. His results were:

	Pa_{CO_2}	$P_{A_{CO_2}}$	AaD_{CO_2}
Air	37.3	35.9	1.4 - 2.0
Oxygen	37.2	33.8	3.4 - 2.5

This can only be explained by an increase in high $\dot{V}_A/\dot{Q}$ alveoli. However, an increase in AaD_{CO_2} of 2 mm implies a very considerable redistribution of perfusion; it is greater than the change they found between sitting and supine, and such a redistribution would certainly have been apparent using $Xenon^{133}$. Therefore, one must conclude that if a redistribution occurs it is a small one and that the magnitude of the AaD_{CO_2} is due to the Haldane effect. It should also be noted that if a redistribution does occur,

it is not necessarily due to change in vasomotor tone. Breathing 100% oxygen has been frequently reported [97] to lower the cardiac output. If the pulmonary vascular resistance is unaltered [99] this must reduce the pulmonary artery pressure and the redistribution can be accounted for on the Waterfall hypothesis.

It has been suggested that reduction of the oxygen tension may account for the redistribution of perfusion during exercise. The oxygen tension of mixed venous blood does fall, but because the over-all $\dot{V}_A/\dot{Q}$ of the lung rises, the alveolar oxygen tensions are all normal or higher than at rest. However, a fall in the mixed venous oxygen tension may alter the tone of the pre-capillary vessels.

SUMMARY OF PERFUSION RESULTS

The Waterfall hypothesis appears to satisfactorily explain all the perfusion distribution patterns that have been observed. In the seated position there is a perfusion gradient that agrees well with the measured pulmonary artery pressure and the hydrostatic pressure within the lung. The gradient should ideally have been more linear, but the present technique probably does slightly over-estimate the upper zone perfusion. The redistribution that occurs in the supine position results from the reduction in the hydrostatic gradient. The slight reversal of perfusion is due to the fact that in the supine position the buttocks tip the long axis of the lung apex down. In this position there is also a front to back hydrostatic gradient producing a front to back perfusion gradient, particularly in the lower zone where the antero-posterior diameter is large. The more uniform

distribution on exercise is due to the increased total pressure in the pulmonary artery, with the caution that measured PA pressure is always smaller than the total pressure, particularly at high flows. When the pulmonary artery pressure is reduced, as in postural syncope, the hydrostatic effect is greater and there is a progressive reduction in apical perfusion. Oxygen inhalation produces no major redistribution in perfusion. A small increase in gradient may occur, but this may be due to a reduction of pulmonary artery pressure or to regional changes in pulmonary vascular resistance.

CONSEQUENCES OF V/Q VARIANCE

UPRIGHT POSITION

With fixed mixed venous and inspired gas tensions the alveolar and capillary gas tensions will be determined solely by the Ventilation/Perfusion ratio and are independent of the metabolic rate [30]. It is, therefore, possible to use the Ventilation/Perfusion ratio data derived by Xenon^{133} to calculate the regional gas tensions. In this way lung models representing the different distribution patterns occurring with postural change and exercise can be constructed. These models are only approximations of the true situation, as each Xenon counter is summing the activity in about 50 x 10^6 alveoli. This clearly sets restrictions on the amount of interpretation that is possible from the models.

REGIONAL GAS TENSIONS

The gas tensions cannot be directly computed from the Ventilation/Perfusion equation since there are too many unknowns. They must be solved graphically by the method described by Rahn and Fenn[31] by construction of a Ventilation Perfusion curve on the O_2:CO_2 Diagram. A curve has been constructed (Figure XIX) within the following fixed values:

$P\bar{V}_{O_2}$	40 mm Hg.
$P\bar{V}_{CO_2}$	45 mm Hg.
$P_{I_{O_2}}$	149 mm Hg.
$P_{I_{CO_2}}$	0
pB-47	713

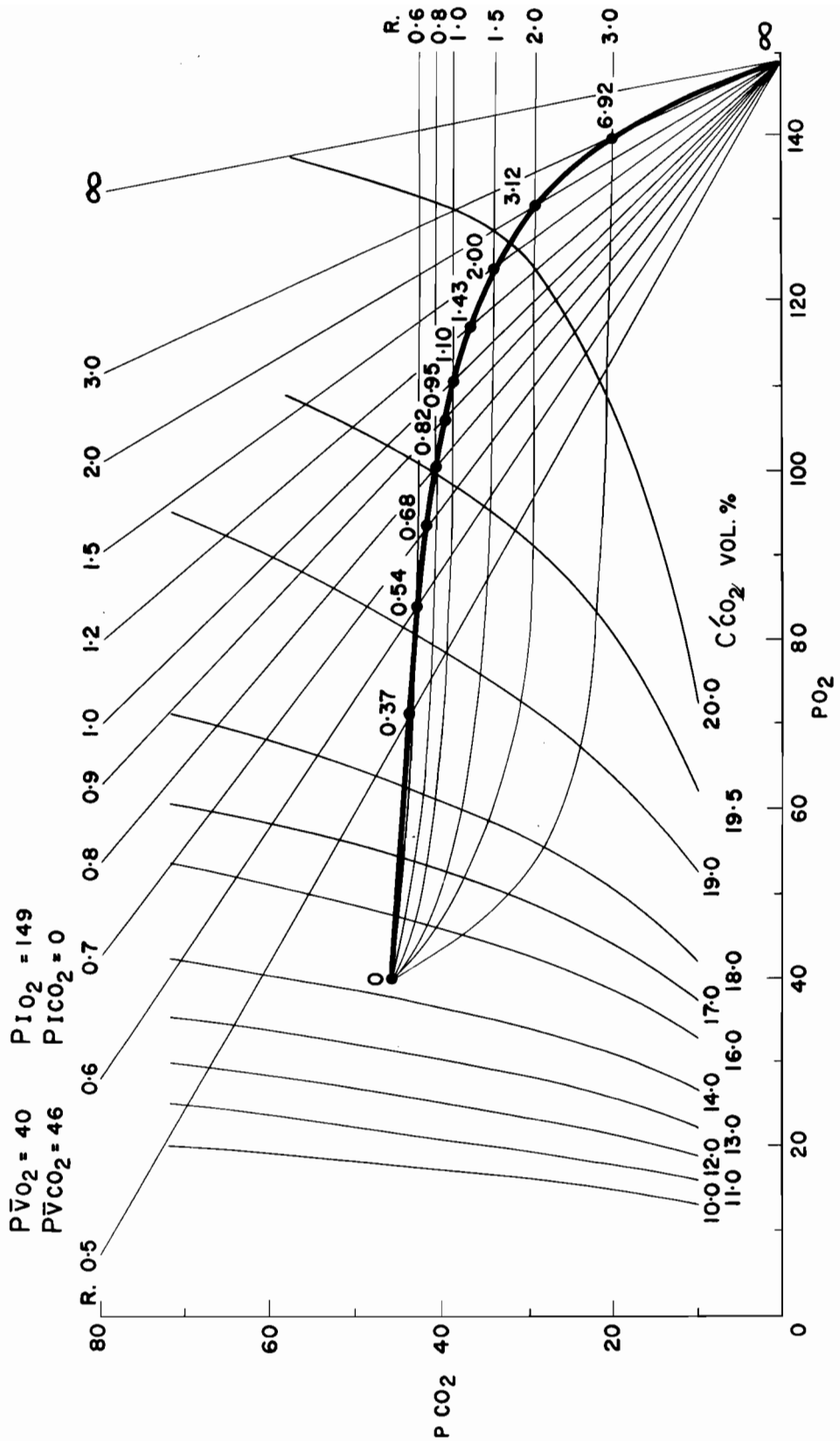

Figure XIX - 0_2:$C0_2$ diagram constructed to calculate gas tensions from the present data.

Oxygen content isopleths and R lines are superimposed. At each R intercept with the $\dot{V}_A/\dot{Q}$ curve, the arterio-venous oxygen content difference is determined and the P_{AC0_2} read off. The Ventilation/Perfusion ratio for this point can then be calculated from:

$$\frac{\dot{V}_A}{\dot{Q}} = \frac{0.863 \times R \times Ca_{0_2} - C\bar{v}_{0_2}}{P_{AC0_2}}$$

By interpolation the Ventilation/Perfusion ratios determined with Xenon can then be located on the curve. The data from seated, resting subjects (Table II) give the following gas tensions:

	Upper	Middle	Lower
$\dot{V}_A/\dot{Q}$ Ratio	1.37	0.95	0.67
$p0_2$ mm Hg.	115.5	106.0	92.0
$pC0_2$ mm Hg.	37.5	40.0	42.2
pN_2 mm Hg.	560.0	567.0	578.8

This data is presented in Figure XX.

The large regional differences in the tensions of all three gases must underestimate the real situation because of the large regions studied. West [63] using smaller fields calculated that there would be a 40 mm Hg. difference in $p0_2$ between the apex and base, and a 14 mm Hg. difference in $pC0_2$.

Assuming that there is no diffusion defect these tensions would also exist in the end-capillary blood. Using the appropriate dissociation curve it is then possible to calculate the regional blood gas contents. A small correction must also be added for dissolved oxygen ($p0_2\alpha/pB$). The calculated contents are:

GAS EXCHANGE UPRIGHT

$\dot{V}/\dot{Q}$	P_{O_2} mmHg.	P_{CO_2} mmHg.	Cc'_{O_2} Vol.%	Cc'_{CO_2} Vol.%	$\dot{V}_{O_2}$ ml/min	$\dot{V}_{CO_2}$ ml/min	R
1.37	115.5	37.5	20.06	47.26	38	43	1.02
0.95	106	40	19.83	48.47	93	82	0.88
0.67	92	42	19.59	50.04	175	120	0.69
Mixed Alveolar Gas	101.2	40.5			306	245	0.8
Mixed Arterial Blood	98	41	19.7	49.2			

Figure XX - Summary of gas tensions, contents and exchange calculated for the seated, resting subjects.

	Upper	Middle	Lower
$C\acute{c}_{O_2}$ Vol.%	20.06	19.83	19.59
$C\acute{c}_{CO_2}$ Vol.%	47.26	48.47	50.04

REGIONAL GAS EXCHANGE

From this data the regional gas exchange can be calculated by:

$$\dot{V}_{CO_2} = V_A F_{A_{CO_2}} (.863)$$

$$\dot{V}_{O_2} = Q (C_{c_{O_2}} - C_{V_{O_2}})$$

	Upper	Middle	Lower	Total
$\dot{V}_{O_2}$ ml/min.	38	93	175	306
$\dot{V}_{CO_2}$ ml/min.	43	82	120	245

These differences in regional gas exchange are very striking, the lower zones being responsible for 57% of the total oxygen uptake and 47% of the total carbon dioxide output. This is not simply due to volume difference of the zones, because even when expressed "per unit volume" a gradient still exists. The oxygen uptake gradient per unit volume is of the same order as the perfusion gradient and the $\dot{V}_{CO_2}$ gradient is similar to the ventilation gradient. However, this is coincidental. Fahri [100] has calculated the theoretical efficiency of gas exchange with $\dot{V}_A/\dot{Q}$ variation and similar calculations on the present data (Table II) help to explain the regional differences in gas exchange. The amount of ventilation required to transfer 1 ml. of oxygen increases considerably as the $\dot{V}_A/\dot{Q}$ increases, but there is little difference for carbon dioxide. The amount of perfusion required to transfer 1 ml. of oxygen decreases slightly as the $\dot{V}_A/\dot{Q}$ in-

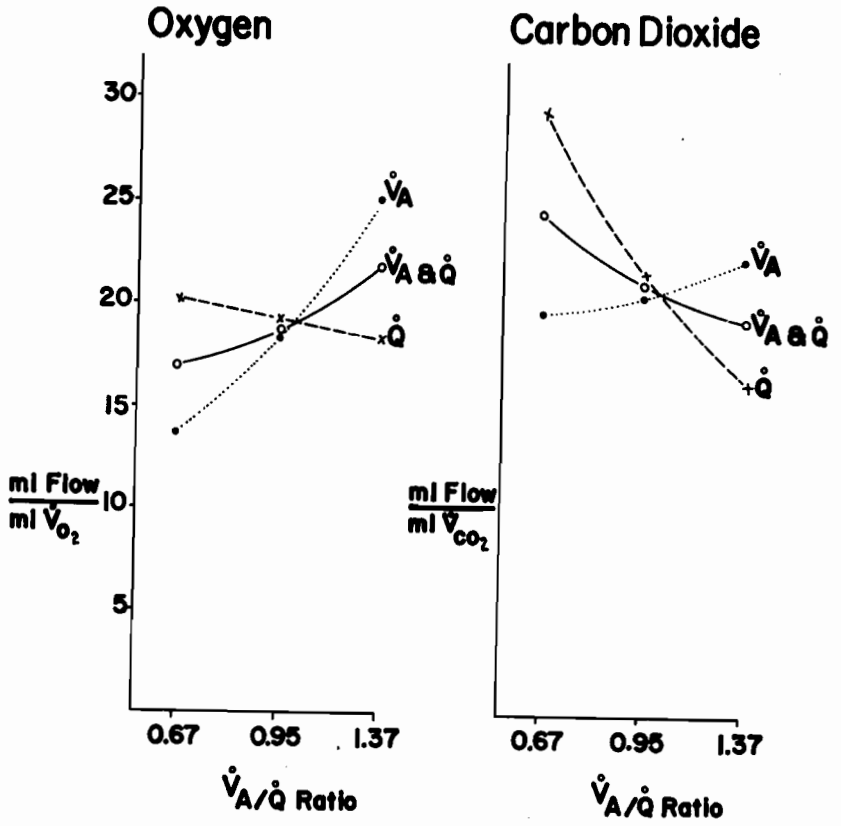

Figure XXI - The quantity of flow (ventilation, perfusion and ventilation + perfusion) required to transfer 1 ml. of oxygen or carbon dioxide as a function of the $\dot{V}_A/\dot{Q}$ ratio of the upper, middle and lower zones.

creases, but for $C0_2$ there is a large decrease in flow required. Summing the Ventilation and Perfusion requirements to transfer oxygen, the least total flow occurs at a low $\dot{V}_A/\dot{Q}$ ratio, but to transfer $C0_2$ the least total flow is at a high $\dot{V}_A/\dot{Q}$ ratio. Therefore, the lower zone has optimal conditions for oxygen uptake, a large perfusion and a low $\dot{V}_A/\dot{Q}$ ratio. To increase $\dot{V}_{0_2}$ the ideal situation is an increase of perfusion in excess of ventilation, keeping the $\dot{V}_A/\dot{Q}$ low. The optimal conditions for $C0_2$ output are quite different. The optimum $\dot{V}_A/\dot{Q}$ exists in the upper zone and as a result the regional differences in $\dot{V}_{C0_2}$ are less than in $\dot{V}_{0_2}$. Furthermore, to increase $\dot{V}_{C0_2}$ the ideal situation is to increase ventilation in excess of perfusion to maintain a high $\dot{V}_A/\dot{Q}$ ratio. This in fact occurs during exercise and the crucial importance of this will be discussed subsequently.

MIXED ALVEOLAR AND ARTERIAL TENSIONS

The mixed alveolar gas tensions can be calculated by Ventilation weighting the regional tensions. The mixed arterial tensions are calculated by Perfusion weighting of the regional blood gas contents and then converting back to tensions.

	pO_2	pCO_2	pN_2
Mixed Alveolar	101.2	40.5	571
Mixed Arterial	98	41	574
aAD	3.2	0.5	3

IDEAL ALVEOLAR AIR

Before discussing the significance of the arterial alveolar differ-

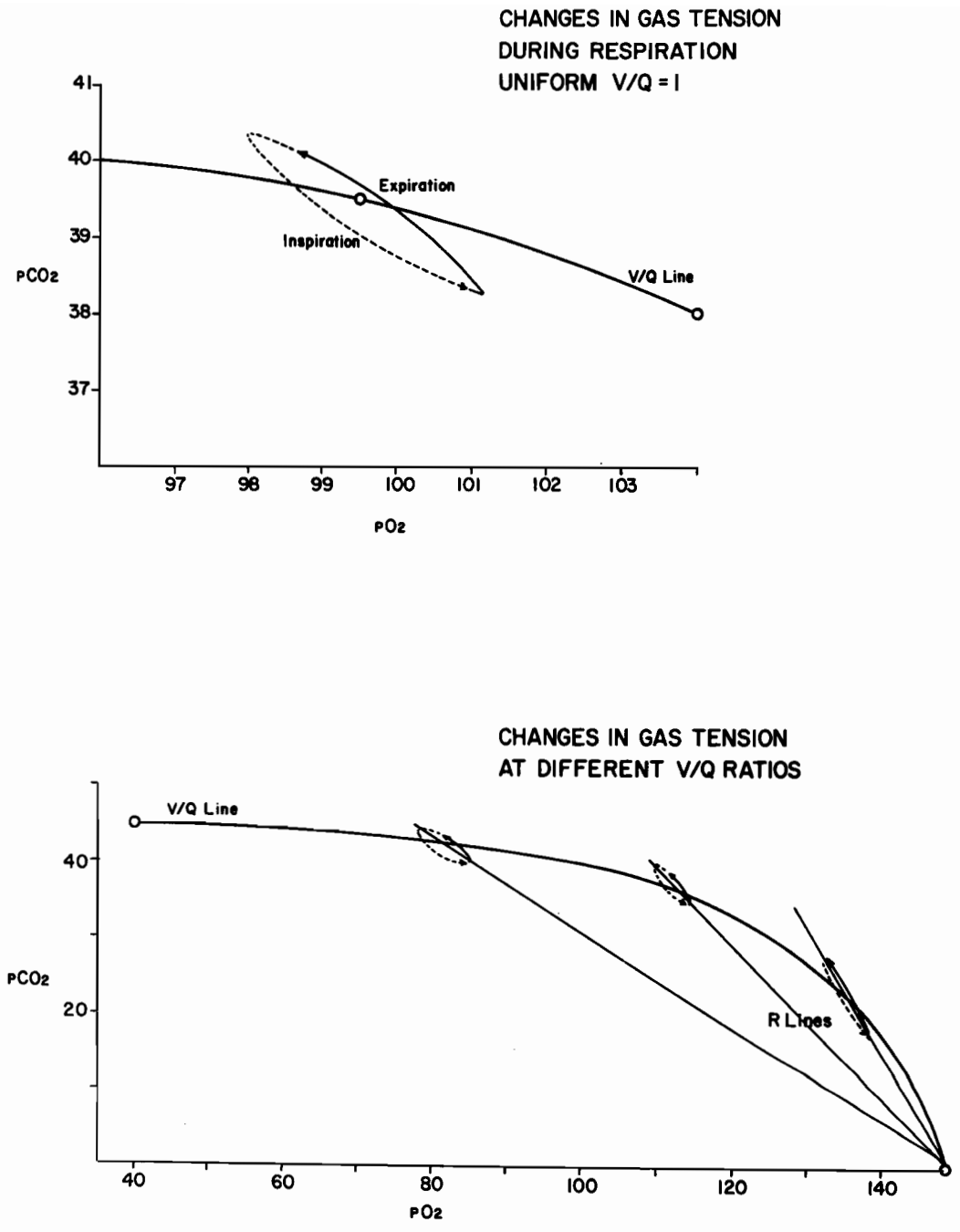

Figure XXII - Calculated variation of the alveolar gas composition during respiration. Above, loop of an alveolus with a $\dot{V}/\dot{Q}$ ratio of one, from Dubois [101]. Below, approximate loops calculated for alveoli with various $\dot{V}/\dot{Q}$ ratios. The main axis of the loop is parallel to the appropriate R. line.

ences derived from this model, it is necessary to examine some of the practical problems encountered in the measurement of alveolar gas tensions in man and the concept of Ideal Alveolar air. The concentration of expired gas is continually changing and at first sight this appears to be a simple reflection of the variations in regional gas tension that have been demonstrated in this study. However, if the expiratory time constants are equal, which they appear to be [80], the proportional emptying of each alveolus and hence the mean expired gas tension would remain constant. Dubois[101] has shown that even with a uniform V_A/Q ratio the alveolar gas tensions will change with time, because expiration is a discontinuous process. He has aptly described expiration as breathholding with a decreasing lung volume, because gas exchange is a continuous process and so the pO_2 will fall and the pCO_2 rise in the alveolus during expiration. Therefore, the gas tension calculated from the O_2 CO_2 Diagram represents a mean, and that in time the true gas tension describes an ellipse around this mean. The shape of this ellipse is dependent on the Ventilation/Perfusion ratio and in Figure XXII representative loops have been drawn for three lungs having different uniform $\dot{V}_A/\dot{Q}$ ratios. These loops are only approximate, because the method involves a number of assumptions. However, in general it can be seen that the major axis of the ellipse is nearly parallel to the appropriate R line. Furthermore, the lower the $\dot{V}_A/\dot{Q}$ ratio the wider the minor axis of the loop. In other words, a lung with a high $\dot{V}_A/\dot{Q}$ ratio should show large changes in expired pCO_2 and small changes in pO_2.

The reverse will occur with a low $\dot{V}_A/\dot{Q}$.

It appears practically impossible to construct these loops for a non-homogeneous lung, particularly for CO_2. The CO_2 loop is constructed using an equivalent lung volume, that is a volume of gas containing CO_2 and a volume of "tissue" containing CO_2, which in Dubois' calculations is approximately 50% of the gas volume. Attempting to distribute this tissue volume regionally is difficult. However, reasoning that the major component of this tissue is blood and distributing it accordingly, it appears the pCO_2 loop is no bigger and probably smaller than those in Figure XXII.

If equal points in time on these loops are joined and the values ventilation weighted, it is clear that during expiration the pCO_2 will rise and the pO_2 fall. As the time course of the alveolar gas tensions describes an ellipse around the mean, no single sample can accurately measure the mean pO_2 and pCO_2. Some point in mid expiration would be preferable and from the practical point of view the point of the mean expired R is probably the most satisfactory.

For different reasons Riley and Cournand based their concept of the Ideal Alveolar air on the mean R value of expired gas[32]. However, uneven the distribution it can be represented by a theoretical ideal situation with alveolar gas tensions that are consistent with the observed gas exchange. This ideal point lies at the intersect of the blood and gas R lines equal to the expired gas R. This is a powerful theoretical concept because it has provided a fixed point against which to measure. In practice this point is calculated using the alveolar air equation, measuring the

expired R.Q and using the arterial pCO_2 instead of the alveolar pCO_2, because of the difficulties of measuring the true alveolar pCO_2. If there is no aAD_{CO_2} this manoeuvre is successful. If an aAD_{CO_2} exists use of the arterial value will over-estimate the mean alveolar pO_2. For example, in the model in Figure II, the true mean P_{AO_2} = 107, the theorectical ideal P_{AO_2} is 101; the P_{AO_2} calculated from the Pa_{CO_2} is 102 and calculated from P_{ACO_2} it is 108. Therefore, when a figure for aAD_{O_2} is quoted, it is the difference between the arterial and ideal alveolar oxygen tension, not the true, larger gradient between artery and mean alveolar oxygen.

The "Ideal Alveolar Air" has been graphically calculated for the present model. The values are:

P_{AO_2}	=	Pa_{O_2}	100.8 mm Hg.
P_{ACO_2}	=	Pa_{CO_2}	41
P_{AN_2}	=	Pa_{N_2}	571
$C\acute{c}_{O_2}$			19.79 Vol. %
$C\acute{c}_{CO_2}$			49.3
$\dot{V}_{O_2}$			312 ml/min.
$\dot{V}_{CO_2}$			249
R			0.8

Calculating P_{AO_2} from the alveolar air equation gives practically the same value because the aAD_{CO_2} is small.

ALVEOLAR ARTERIAL OXYGEN DIFFERENCES

The aAD_{O_2} derived from the Xenon model is 3.2 mm Hg. To compare it with the measured aAD_{O_2} it is necessary to add something for the anatomical shunt component. Fahri [36] has estimated that approximately 2% of the cardiac output is normally shunted, which would contribute about 4 mm Hg. to the aAD_{O_2}. Therefore, the total aAD_{O_2} is 7.2 mm Hg. for this model.

Most of the figures quoted in the literature (37, 102, 103) are higher than this - 8-10 mm Hg. However, recently Bishop [104] in a large series measured the following values:

	Under 40 years	Over 40 years
Sitting	5.9 ± 5.2	16.7 ± 4.8
Supine	6.4 ± 5.6	15.6 ± 6.9

These figures emphasize the variability of the normal aAD_{O_2} but it is not clear why these values are so different from the usual values quoted.

ALVEOLAR ARTERIAL CO_2 DIFFERENCES

Direct measurement of the $aADC_{O_2}$ is possible, however, there is some confusion about the "normal value" because the exact conditions of the measurement are crucial. Some of the causes of the discrepancies will be discussed later. In a series by Larson and Severinghaus [42] under conditions similar to the Xenon experiments, a gradient of 1.4 ± 2.0 mm Hg. was found. Therefore, the calculated gradient from the Xenon model of 0.5 mm Hg. appears too small. This implies that Xenon is underestimating the $\dot{V}_A/\dot{Q}$ variance. An $aADC_{O_2}$ reflects the presence of high

$\dot{V}_A/\dot{Q}$ alveoli and as discussed under the section of Errors, it is probable that Xenon over-estimates the perfusion at the apex of the lung. Probably for the same reason the calculated mean alveolar pCO_2 is slightly higher than the measured value.

ALVEOLAR ARTERIAL NITROGEN DIFFERENCES

The calculated aAD_{N_2} is also slightly lower than that reported by Klocke and Rahn [105] by 4-6 mm Hg. in normal subjects. If the Xenon is over-estimating upper zone perfusion, it also proportionately under-estimates the lower zone perfusion. Therefore, the aAD_{N_2}, which reflects low $\dot{V}_A/\dot{Q}$ alveoli, will be under-estimated.

PENALTIES OF NORMAL V_A/Q VARIANCE

The maximum surface area of contact between alveolar air and pulmonary capillary blood can only be achieved when all alveoli have the same Ventilation/Perfusion ratio. If there was ideal distribution (see Ideal Alveolar Air), the oxygen uptake would be 312 ml/min. and the carbon dioxide output 249 ml/min. The gas exchange calculated from the Xenon model where the distribution is uneven, gives an oxygen uptake of 306 ml/min. and a carbon dioxide output of 245 ml/min. Therefore, despite the considerable inequality of the $\dot{V}_A/\dot{Q}$ ratios, the penalty is only 6 ml/min. of oxygen and 5 ml/min. of carbon dioxide. This is insignificant, particularly when one considers the extra cardiac work that would be required to achieve ideal distribution of the blood flow.

The remarkable ability of the lung to function efficiently in the presence of an inefficient distribution is largely the result of the shape of

the Dissociation curves of oxygen and carbon dioxide. The oxygen dissociation curve becomes flat and the carbon dioxide curve steep in the normal range of gas tensions. If these curves were linear, the "normal" $\dot{V}_A/\dot{Q}$ variance would have disastrous consequences.

UNSTEADY STATE

These results were obtained from seated, resting subjects in a reasonably steady state, although no procedure involving venipuncture, radio-activity and such alarming equipment is a sure steady state particularly in naive individuals. During clinical studies two patients fainted while perfusion distribution was being studied. Both showed a gross exaggeration of the normal perfusion gradient. To further investigate this, postural syncope was deliverately induced in one normal subject. The subject was an experienced fainter, who could signal the onset of syncope and cooperate to a certain extent during the event. However, a technically correct experiment could not be performed. Only perfusion distribution was measured and the results simply expressed as percentage change from the initial count rate on first assuming the upright position. The results (Figure XVII) from the second injection after 15 minutes upright appear reliable, but the results during syncope do not "add up", probably due to convulsive movements by the subject; however, their general direction is probably reasonable.

The effects on gas exchange can be approximately predicted from the 15 minute data. It is necessary to assume that there was a normal ventilation distribution. It is also necessary to assume that there was no

change in total cardiac output or ventilation.

	Upper Zone	Middle Zone	Lower Zone
Normal $\dot{Q}$ L/min.	0.696	1.78	3.52
% Change	-32	-4	+5
Resultant $\dot{Q}$ L/min.	0.452	1.71	3.77
Normal $\dot{V}$ L/min.	0.95	1.68	2.36
$\dot{V}_A/\dot{Q}$	2.1	0.98	0.62

Making the further assumption that the mixed venous gas tensions had not changed, the regional gas tension can be calculated. The calculated mean alveolar pCO_2 would be 40 mm Hg. and the arterial pCO_2, 42 mm Hg. This aAD_{CO_2} of 2 mm Hg. is four times as high as the aAD_{CO_2} computed in the seated position.

It is impractical to make similar calculations for the data during the faint, cardiac output, ventilation and mixed venous tensions are altered and the Xenon data is not entirely reliable. However, the results indicate further decrease in perfusion to the top of the lung producing a wider $\dot{V}_A/\dot{Q}$ variance and increase in alveolar-arterial gas tension differences. Bjurstedt [106] has studied the effect of postural syncope on gas exchange. He showed a progressive increase in the aAD_{CO_2}, but the first indication of impending syncope was a considerable increase in ventilation. This lowered both the arterial and alveolar pCO_2 but maintained the oxygen saturation normal throughout. Therefore, the failing gas exchange due to the $\dot{V}_A/\dot{Q}$ disturbance appears to be partially compensated for by hyperventilation.

GAS EXCHANGE SUPINE

$\dot{V}/\dot{Q}$	0.7	0.71	1.6	Mixed Alveolar	Mixed Arterial
P_{O_2} mmHg	95	95.5	97	96	97
P_{CO_2} mmHg	41.9	41.7	40.5	41.5	41.5
Cc'_{O_2} Vol %	19.35	19.36	19.42		19.41
Cc'_{CO_2} Vol %	49	49	49		49
$\dot{V}_{O_2}$ ml/min	80	110	106	295	
$\dot{V}_{CO_2}$ ml/min	61	86	80	227	
R	0.76	0.78	0.75	0.77	

Figure XXIII - Summary of gas tensions, contents and exchange calculated for the supine resting subjects.

In the standing position it is difficult to achieve a steady state, because most subjects will faint in time. In the seated position there is little postural stress on the circulation and fainting has an emotional origin. However, it is clearly necessary to have subjects as tranquil as possible while making Xenon perfusion measurements to avoid misleading results.

SUPINE POSITION

In the supine position there is a major re-distribution of perfusion and a smaller charge of ventilation leading to a more uniform distribution of $\dot{V}_A/\dot{Q}$ ratios. As a result there must be considerable changes in the regional gas tensions and gas exchange. However, some caution must be exercised in computing from this data because the apparent uniformity of perfusion is misleading. In this position there is a front to back hydrostatic gradient and a front to back perfusion gradient exists. In the absence of a similar ventilation gradient, the $\dot{V}_A/\dot{Q}$ ratio at the back will be higher than at the front. However, by lumping the data from back and front counters, an approximate mean of the regional gas tensions can be calculated. These are illustrated in Figure XXIII.

Because of the uniformity of $\dot{V}_A/\dot{Q}$ ratios the regional gas tensions and gas exchange become more uniform. The most striking difference is that in the supine position 27% of the oxygen uptake occurs in the upper zone in contrast to 8% in the upright position. These changes are in good general agreement with the measurements by regional spirometry (12, 13)

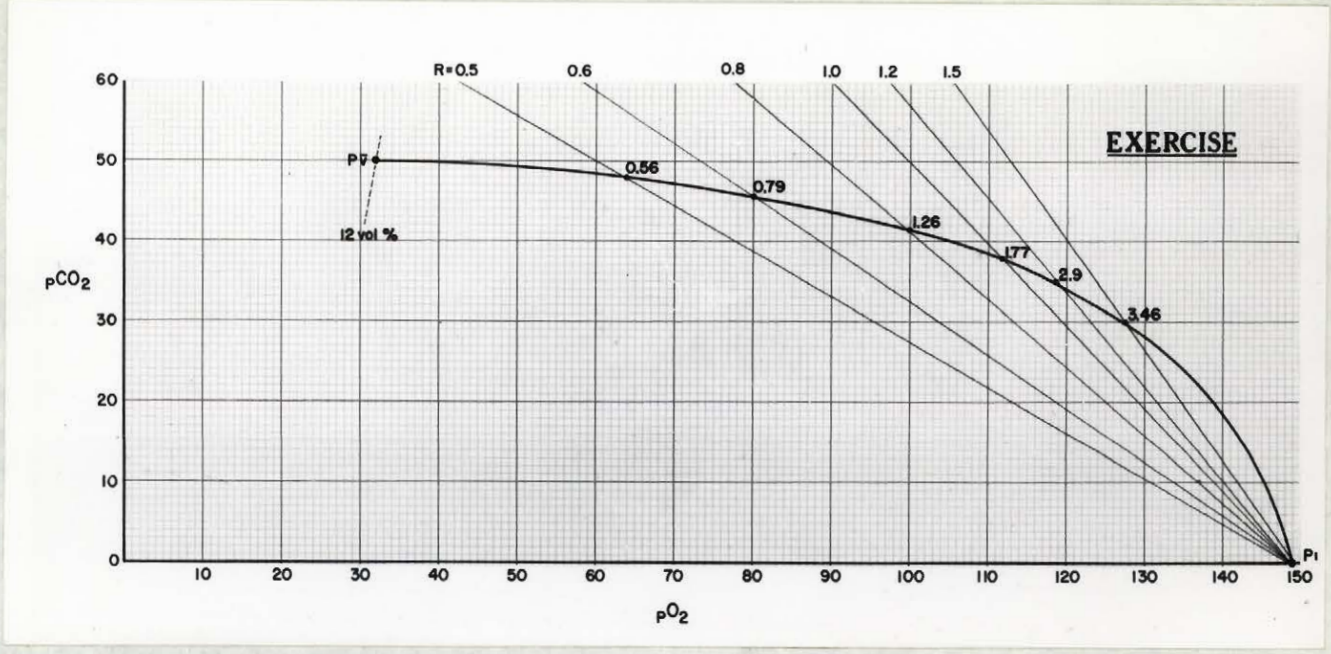

Figure XXIV - $\dot{V}_A/\dot{Q}$ line constructed from mixed venous tensions ($P_{V_{O_2}} = 32$, $P_{V_{CO_2}} = 50$) occurring during exercise. The change in mixed venous tensions changes the gas tensions of all $\dot{V}_A/\dot{Q}$ ratios (compare with Fig. XIX).

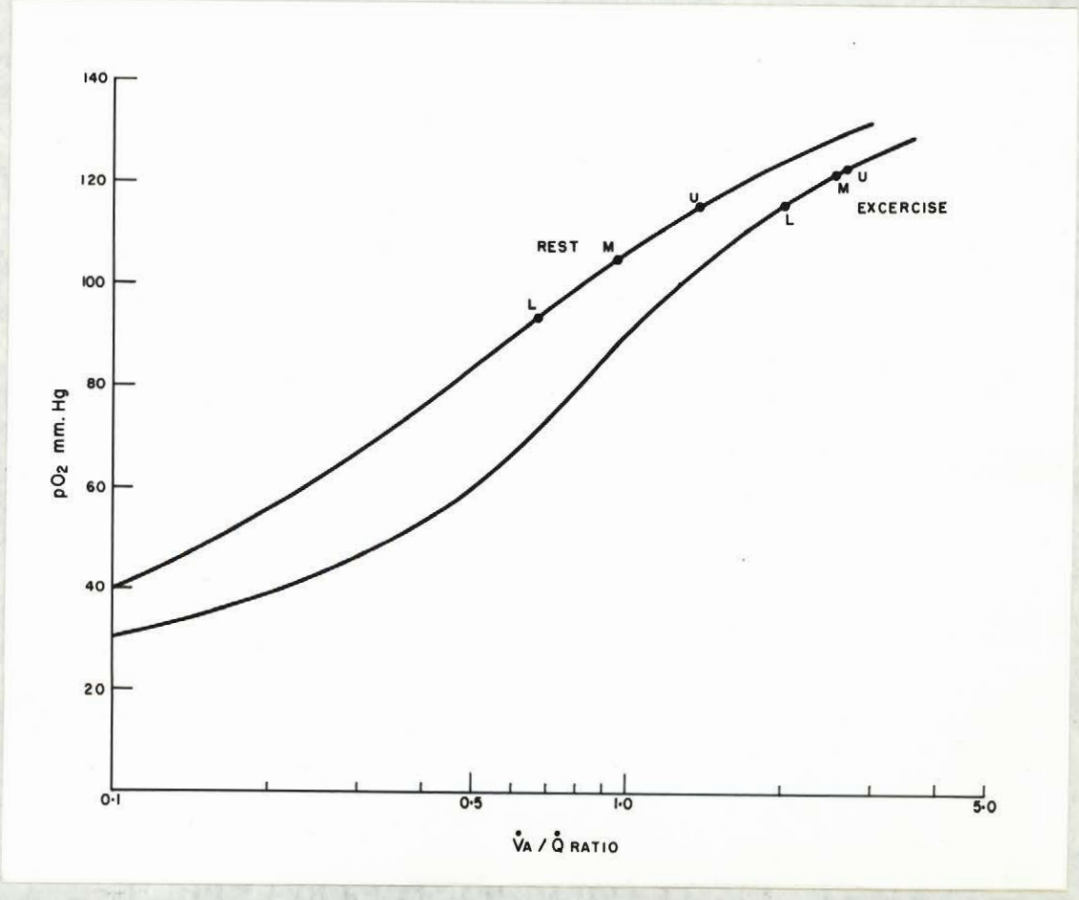

Figure XXV - The relationship between the $\dot{V}_A/\dot{Q}$ ratio and $p0_2$ with rest and exercise mixed venous gas tensions. The increase in the $\dot{V}_A/\dot{Q}$ ratio of all zones on exercise maintains a high $p0_2$.

but cannot be exactly compared because of the difference between lobes and zones. The alveolar arterial differences for all gases decrease in the supine position, which agrees with the measurements of alveolar arterial difference reported in the literature (42, 43, 104).

EXERCISE

These results show that during moderate exercise the distribution of ventilation and perfusion becomes practically uniform. However, in the discussion on "Ideal Alveolar Air" it was shown that uniformity per se had little effect on gas exchange. The important change during exercise is that the increase in ventilation is much greater than the increase in perfusion so that the over-all $\dot{V}_A/\dot{Q}$ ratio of the lung rises. The significance of this can be clearly seen using the 0_2:$C0_2$ Diagram. During exercise, the mixed venous oxygen tension falls, and the carbon dioxide tension rises. Therefore, the $\dot{V}_A/\dot{Q}$ line has to be redrawn (Figure XXIV) from the new mixed venous tensions (assumed to be $P0_2$ = 32, $PC0_2$ = 50). This alters the gas tensions at all $\dot{V}_A/\dot{Q}$ ratios, so that for a given ratio the oxygen tension falls on exercise. Thus if the mean $\dot{V}_A/\dot{Q}$ ratio had remained at 0.85, the mean alveolar oxygen tension would have dropped to about 82 mm Hg. Because the $\dot{V}_A/\dot{Q}$ rises to a mean of 2.2, the mean alveolar oxygen tension is about 120 mm Hg. and because of the uniformity, all zones have closely similar tensions (Figure XXV).

This makes a considerable difference to the oxygen uptake. By achieving a high $\dot{V}_A/\dot{Q}$ ratio, the a-V oxygen difference is about 8 vols.%

and at a cardiac output of 12 L/min. this gives an oxygen uptake of 960 ml/min. If the $\dot{V}_A/\dot{Q}$ had remained at 0.85, the oxygen uptake would have been about 100 ml/min. lower than this.

The effect on carbon dioxide transport is even more important. At a $\dot{V}_A/\dot{Q}$ of 2.2, the respiratory exchange ratio is approximately 1, so that the CO_2 output would also be about 960 ml/min. If the $\dot{V}_A/\dot{Q}$ had remained at 0.85, the respiratory exchange ratio would have been about 0.7, so that only 600 ml/min. of CO_2 would be eliminated. Therefore, the relative "hyperventilation" of exercise increases oxygen uptake by about 10% and increases carbon dioxide output by about 37%.

There is an important general principle in this conclusion. In lung disease, if the mixed venous oxygen tension falls, a much higher ventilation is required to provide adequate gas exchange, particularly to eliminate carbon dioxide. In fact most patients with gas exchange failure do "hyperventilate" when they are mechanically capable of doing so.

VENTILATION PERFUSION RATIO AND DIFFUSING CAPACITY

The term Diffusing Capacity (D_L) is misleading because the measurement has very little to do with diffusion. What is in fact measured is the ability to transfer a gas from the inspired air into the circulation. It is, therefore, critically dependent on the distribution of ventilation and perfusion. Indeed the diffusing capacity can be regarded as one method of assessing $\dot{V}_A/\dot{Q}$ variance. It is doubtful if the diffusing capacity is ever abnormal in the absence of an abnormal $\dot{V}_A/\dot{Q}$ distribution, even in the classical diffusion defects - the alveolar capillary block syndromes[107-108].

The $\dot{V}_A/\dot{Q}$ distribution effects D_L in a variety of ways:

1. The $\dot{V}_A/\dot{Q}$ of an alveolar determines the $P_{A_{O_2}}$ and therefore determines the driving pressure for diffusion. In upright subjects the diffusion gradient is highest at the apex, but because of the difference in blood flow, the oxygen uptake is much greater at the base. Therefore, the D_{O_2}, which is oxygen uptake divided by the pressure gradient, will be higher at the base of the lung. While the $P_{A_{O_2}}$ depends on the V_A/Q ratio, the P_{CO} is only determined by the ventilation distribution. This makes the D_{CO} particularly sensitive to ventilation distribution.

2. Roughton and Forster[109] divided the resistance to diffusion into a membrane component (D_M) and a pulmonary capillary volume (V_C) gas reaction rate (θ) component:

$$\frac{1}{D_L} = \frac{1}{D_M} + \frac{1}{V_C\theta}$$

The membrane component varies with the surface area of the alveolar capillary membrane. This depends on the $\dot{V}_A/\dot{Q}$ distribution, because neither an unventilated nor an unperfused part of the lung can contribute to the surface area available for gas diffusion. Presumably the optimum surface area is achieved at the optimum Ventilation/Perfusion ratio for any gas.

It is more difficult to characterize the effect of $\dot{V}_A/\dot{Q}$ on what is called pulmonary capillary blood volume (V_C). Staub [93] has written: "Are increases in V_C accomplished by perfusing more of the total capillary bed or by stuffing more erythrocytes through capillaries already being perfused"? Correlating the Xenon results with diffusing capacity measurements, it is probable that much of the increase comes from stuffing more erythrocytes through, although the distribution may be important.

3. The transit time of erythrocytes through the capillaries determines the completeness of their equilibration with the alveolar gas. Transit time depends on the ratio of pulmonary capillary volume to flow $V_C/\dot{Q}_C$. With an uneven distribution of $\dot{Q}_C$, transit time will vary unless there is an appropriate variation in V_C. There are, therefore, two alternatives. V_C and $\dot{Q}_C$ have the same distribution and transit times are uniform, or V_C is uniform and there is a regional variation of transit times. The first alternative, matching volume and flow appears logical, but this means that in normal upright man, V_C is over three times as big per unit volume in the lower zone than in the upper zone. As D_M is also smaller in the upper zone due to unperfused alveoli, the diffusing capacity in the upper

zone will be considerably lower than in the lower zone.

In normal resting subjects, the $\dot{V}_A/\dot{Q}$ variance has a small effect on the diffusing capacity. From the Xenon model an oxygen uptake of 306 ml/min. was calculated (Figure XX), assuming a mean alveolar- mean capillary $p0_2$ gradient of 15 mm Hg., the calculated D_{0_2} is 20.6 ml/min/mm Hg. Assuming the same cardiac output and a uniform distribution of $\dot{V}_A/\dot{Q}$ ratios, the oxygen consumption only increases to 312 ml/min. Assuming the same $p0_2$ gradient, the "ideal" D_{0_2} would only increase to 20.8 ml/min/mm Hg.

In the supine position, Bates [110] found a mean increase of 3 ml/min/mm Hg. in the D_{C0}. This increase appears too large to be accounted for by the uniformity of V_A/Q ratios in the supine position, particularly as this uniformity is somewhat spurious because of the front to back gradient. The increase is probably the result of the increase in cardiac output and total pulmonary blood volume (V_C) occurring in the supine position.

The diffusing capacity normally increases considerably during exercise. Riley [111] measuring D_{0_2} showed a rapid increase between oxygen consumptions of 0.6 to 1.2 L/min., the subsequent rise was much smaller and there was little rise after 2.2 L/min. From this, Cohn [112] calculated a Maximum Diffusing Capacity formula based on age and body surface area. Similar studies of exercise D_{C0} do not show this plateau and it does not appear that a true maximum diffusing capacity has been demonstrated. The Xenon data shows that the ventilation and perfusion distribution becomes

practically uniform during relatively mild exercise, when the oxygen consumption is approximately 1.1 L/min.[84]. This corresponds to the period of sharp rise in D_{O_2} demonstrated by Riley at the same level of oxygen consumption. On exercise there is an over-all rise in $\dot{V}_A/\dot{Q}$ ratios raising the mean alveolar oxygen tension, at the same time the mixed venous oxygen tension falls so that the diffusion gradient increases. The increase in upper zone perfusion and the perfusion of more alveoli in other zones increases the surface area available for gas transfer, so that D_M rises. The total amount of blood in the pulmonary capillary bed (V_C) also increases. These increases in V_C and D_M have been shown to occur in exercise [113, 114]. The increase in V_C is greater and more consistent than the increase in D_M. As the distribution is practically uniform at 300 KgM/min., there should be little increase in D_M at higher levels of exercise. V_C on the other hand could theoretically increase to the maximum pulmonary capillary volume. Weibel [115] has calculated that the maximum anatomical pulmonary capillary volume is about 170 ml. Staub [93] calculating from acetelyne measurement of the lung tissue volume has estimated an upper limit of 350 ml. Transit time would decrease because the increase in flow is greater than the increase in V_C, but Staub[108] has shown that for oxygen there is great "reserve" in alveolar capillary equilibration because of variations in 0 with pO_2.

The relationship between $\dot{V}_A/\dot{Q}$ and D_L is further complicated by the different methods of measuring D_L. While all the methods yield essentially the same results in normal subjects in the presence of abnormal

Ventilation/Perfusion distribution, they measure different things.

STEADY STATE METHODS

The problem in the D_{CO} measurement is determining the P_{ACO}. This cannot be measured and must be calculated from the Bohr equation using some value for dead space. The Bates' technique [116] uses an anatomical dead space, ignoring $\dot{V}_A/\dot{Q}$ variance. The Filley technique [117] uses a physiological dead space, which partially compensates for the presence of the $\dot{V}_A/\dot{Q}$ variance. By excluding that part of the lung with a high $\dot{V}_A/\dot{Q}$ ratio this technique will always over-estimate the true diffusing capacity, when there is an abnormal V_A/Q distribution.

The magnitude of the error depends on the pattern of $\dot{V}_A/\dot{Q}$ distribution. Ball [118] has recently demonstrated this using a computer model containing two alveoli. Only when the $\dot{V}_A/\dot{Q}$ ratios of the two units are equal will the two techniques measure the true diffusing capacity. When the Ventilation/Diffusion ratios are equal, but perfusion is unequally distributed, the true diffusing capacity is inevitably over-estimated using the physiological dead space. With a 4 to 1 inequality of perfusion, it over-estimates to true D_L by 50%, whereas using an anatomical dead space the error is only ~1%. When the Diffusion/Perfusion ratios are equal, inequality of ventilation causes both methods to under-estimate the true D_L, but the error is considerably smaller. The use of an anatomical dead space is, therefore, preferable in measuring steady state D_{CO}.

SINGLE BREATH METHOD

The same difficulty in computing the alveolar carbon monoxide

exists with the single breath method. The assumption is made that the disappearance of CO from the lung is an exponential function:

$$F_{ACO} = F_{ACOo} e^{-\frac{D713}{V_A} \frac{t}{60}}$$

Experimentally the disappearance is not a single exponential even in normal subjects[119]. This is not surprising because of the regional variations in D_M and V_C which have already been discussed. With greater V_A/Q variance the differences in diffusion per unit volume will increase and it becomes increasingly arbitrary to pick a single value to characterize the slope of the "exponential".

There is a further difficulty with this method in determining the lung volume (V_A) due to the peculiar mechanics of single breath ventilation distribution. This is a static distribution and as discussed in the section on Ventilation Distribution, this will be different from the dynamic (steady state) distribution in the presence of regional airway resistance. Therefore, the single breath and steady state D_{CO}, are potentially studying two different populations of alveoli. As the normal distribution is a dynamic distribution, the steady state D_{CO} appears the most realistic method of measurement.

CLINICAL APPLICATION

It is quite clear that the measurement of Ventilation and Perfusion distribution with Xenon^{133} has great clinical potential, both in clarifying the natural history of disease and in matching therapy to the physiological impairment. A number of papers have already been presented on clinical studies (75, 76, 77, 121, 122, 123). These have demonstrated often startling anatomical changes in distribution. However, there has been only limited success in correlating the changes in distribution with the functional disturbance. Once the natural order of the normal lung is destroyed by disease, some of the assumptions made to measure the normal distribution become invalid and care must be taken in interpreting the results.

There are a number of technical problems in studying patients but the fundamental difficulty is measuring ventilation and relating it to perfusion. In normal subjects the methods of measuring ventilation give similar results (Table III). Furthermore, the dynamic measurements are easy to make because the curves are close approximations to single exponentials because the zones behave homogeneously. In disease the ventilation measurements often give very different results and the dynamic curves are usually not exponentials. The reasons why the methods might give different results have already been discussed, each method is measuring a different aspect of ventilation. In disease changes in the single breath distribution reflect primarily changes in regional compliance. Abnormal wash-in curves reflect

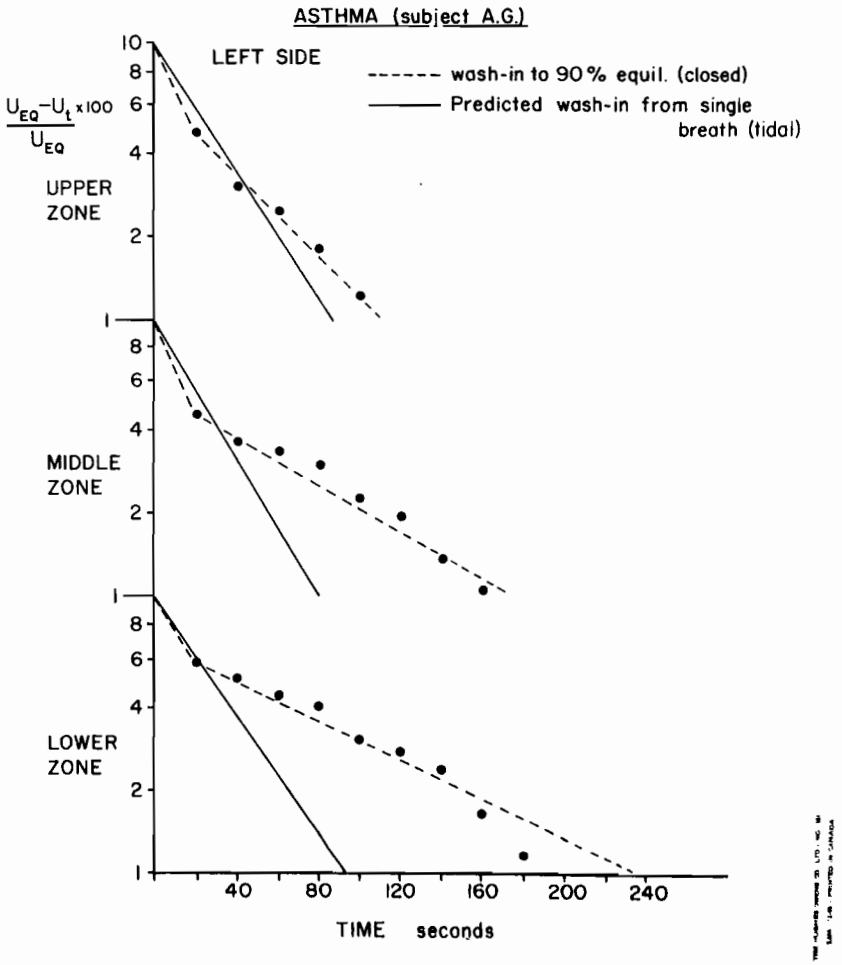

Figure XXVI - Wash-in curve predicted from a single breath index compared to the actual wash-in data. Dotted line shows the erroneous plot to the 90% of Equilibrium value.

regional changes in the product of resistance and compliance. Abnormalities of the washout of injected Xenon reflect changes in the ventilation to the perfused units of the region. The dynamic measurements are generally the most interesting but unfortunately the method of analysis is most unsatisfactory. The curves are treated as single exponential functions which they usually are not so that the results have little mathematical validity. This problem can be illustrated from the basic data in Bentivoglio's paper on distribution in Asthma [76]. Three zones from one patient are plotted in Figure XXVI. From the single breath index, assuming a homogeneous zone, a theoretical wash-in curve can be predicted (by reversing the equation for converting a wash-in curve into a dynamic index). The actual wash-in curves are grossly different from the predicted curves because the airway resistance was abnormal which is reflected in the dynamic but not in the static measurement. The difficulty arises when one attempt to quantitate this difference. The curves are not even approximately single exponentials, but a line is drawn through the straightest part of the curve and the zones compared at the point where they reach 90% of their equilibrium count-rate. There is no mathematical or physiological justification for the choice of 90% equilibrium time, but the comparison of the methods will entirely depend on what percentage is chosen. At 90% there is a very large difference between them, but if the curves were compared at 50% of equilibrium they would show virtually no difference. This only means that some of the zone is washing in rapidly and some washing in slowly and by picking 90% equilibrium the measurement is biased by the slow wash-in

components. Exactly the same dilemma is present in the measurement of the washout of injected Xenon, except that for technical reasons, comparison is made at the 50% equilibrium time which biases the measurement to the fast wash-in component.

This is essentially the same problem as the analysis of the nitrogen washout curves, compounded by the statistical fluctuations of radio-active decay and the relatively poor resolution of the detector. It is, therefore, hazardous to attempt to strip exponentials off the curve, it is clearly impossible on the curves in Figure XXVI. It is, therefore, necessary to seek an alternative approach that has mathematical validity. Gomez [28] has described a method of obtaining a statistical distribution of washout rates but the procedure is formidable. A more practical approach has been suggested by Zeirler [124, 125] re-stating in vigorous terms the principles of the Stewart [126] and Hamilton [127] methods of analyzing indicator dilution curves. This approach appears to have considerable merit and the following sections are Zeirler's arguments applied as a possible method of analyzing Xenon^{133} "indicator dilution" curves.

1. WASHOUT OF INJECTED XENON

When a quantity q of Xenon arrives in a zone, its concentration c(t) changes as it is washed out by a ventilation $\dot{v}$. The amount leaving during dt is the concentration c(t) multiplied by the volume $\dot{v}\,dt$. As the amount leaving must eventually equal the amount that arrived:

$$(1) \quad q = \int_0^\infty c(t)\, v\, dt = \dot{v} \int_0^\infty c(t)\, dt$$

$$(2) \quad \dot{v} = \frac{q}{\int_0^\infty c(t)\, dt}$$

Introducing a function h(t):

$$(3) \qquad h(t) = \frac{\dot{v}\, c(t)}{q}$$

As v c(t) is the rate of washout at time t and is the total amount, h(t) is the fraction of Xenon leaving the system per unit time at time t. The function h(t) is, therefore, the distribution of washout times. It may be redefined from Equation 1 as:

$$(4) \qquad h(t) = \frac{c\,(t)}{\int_0^\infty c(t)\, dt}$$

Thus the distribution of washout times can be obtained directly from the concentration/time curve.

Each element of volume (dV) in the zone has a different washout time. The fraction of Xenon which washes out of dV between t and t + dt is h(t) dt. The rate at which they washout of dV is v h(t) dt. The volume of Xenon in dV is the rate of washout multiplied by the total washout time:

$$(5) \qquad dV = t\, \dot{v}\, h(t)\, dt$$

The total volume of the system is the sum of all the volumes:

$$(6) \qquad V = \dot{v} \int_0^\infty t\, h(t)\, dt$$

Since h(t) is the frequency function of washout times $\int_0^\infty t\, h(t)\, dt$ is the mean washout time $\bar{t}$.

$$(7) \qquad V = \dot{v}\, \bar{t} \quad \text{or} \quad \frac{\dot{v}}{V} = \frac{1}{\bar{t}}$$

The mean washout time can be obtained from the concentration/time curve and is analogous to finding one coordinate of the centroid of an area. From Equations 4 and 5:

$$(8) \qquad dV = \frac{\dot{v}\, t\ c(t)\, dt}{\int_0^\infty c(t)\, dt}$$

Integrating the volumes:

$$(9) \quad V = \dot{v} \frac{\int_0^\infty t\ c(t)\ dt}{\int_0^\infty c(t)\ dt}$$

From Equation 7:

$$(10) \quad \bar{t} = \frac{\int_0^\infty t\ c(t)\ dt}{\int_0^\infty c(t)\ dt}$$

or expressed in words, the mean wash-in time is the moment of the area of the concentration time curve divided by the area.

The mean washout time is a unique description of a washout, which requires no assumptions about the shape of the curve and is, therefore, clearly preferable to the present technique. Finding the moment of the area is tedious manually but a relatively simple computer problem.

2. WASH-IN

It is easier to develop this argument for a system with a constant inspired concentration, i.e. an open circuit. If Xenon is introduced at a constant rate I (gms/min) with a ventilation $\dot{v}$ (litres/min) the concentration I is $I/\dot{v}$ inspired. The concentration in the lung c(t) will increase with time to C equil. when it equals the inspired concentration $I/\dot{v}$. The amount of indicator in the zone at any time M(t) is the input up to time t, minus the output:

$$\begin{aligned} M(t) &= It - \int_0^t \dot{v}\, c(t)\, dt. \\ &= \dot{v} \int_0^t \frac{I}{\dot{v}} - c(t)\ dt. \\ &= \dot{v} \int_0^t \left[C \text{ equil.} - c(t)\right] dt. \end{aligned}$$

The concentration in the system at time t is:

$$\frac{M(t)}{V} = \frac{\dot{v}}{V} \int_0^t \left[C \text{ equil.} - c(t)\right] dt.$$

The limit of concentration is C equil. therefore:

$$V = \frac{\dot{v}}{C \text{ equil.}} \int_0^{\infty} [C \text{ equil.} - c(t)] \, dt.$$

It can also be shown that as volume equals ventilation times the mean wash-in time:

$$\bar{t} = \frac{\int_0^{\infty} [C \text{ equil.} - c(t)] dt}{C \text{ equil.}} = \frac{V}{\dot{v}}$$

That is the mean wash-in time is the area between the curve c(t) and the line C equil. extended back to zero, divided by the equilibrated concentration.

Again the mean wash-in time is a unique description of the wash-in which requires no assumptions about the shape of the curve. The distribution of wash-in times around the mean is obtained from the differential of the concentration time curves.

That was a way of putting it - not very satisfactory;

A periphrastic study in a worn out poetical fashion,

Leaving one still with the intolerable wrestle

With words and meaning.

T. S. Eliot
Burnt Norton.

ACKNOWLEDGEMENTS

A project of this nature is inevitably a cooperative venture involving many people whose assistance I would like to acknowledge. The experimental work was carried out with Dr. L. G. Bentivoglio and Dr. F. Beerel. The model experiments were carried out with the help of Mr. A. Zidulka. Many people contributed to my interpretation of the results. Dr. W.C. Ball was of great assistance in the development of the method section. I am greatly indebted to Dr. P. T. Macklem for help in understanding the mechanical aspects of ventilation distribution. Dr. M. McGregor assisted in understanding the distribution of perfusion. Miss H. McLeish, as well as acting as technician, contributed greatly to the section of gas exchange. W/C R. A. Stubbs gave valuable assistance in the mathematical treatment of the wash-in curves. Discussions with Dr. M.R. Becklake were very valuable. Throughout the project Mr. L.D. Pengelly gave invaluable electronic and theoretical support. I would like to acknowledge help from Mr. L.S. Bartlett with apparatus and Mr. J. Nowaczek who carried out the routine function tests.

Finally I must acknowledge the support of Dr. D.V. Bates who directed this project. His insight into the problems of pulmonary physiology, his enthusiasm and his assistance were invaluable at all stages of the work.

The work was made possible by the Surgeon General, Canadian Forces Medical Service, who gave me the opportunity to study at the Cardio-Respiratory Service in the Royal Victoria Hospital, Montreal.

BIBLIOGRAPHY

1. Orth, J. Atiologisches und Anatomisches uber Lungenschwindsucht Hirschwald, Berlin. p.20.

2. Siebeck, R. Uber den gasaustauch zwischen den aussenluft und den alveolen III Die Lungenventilation beim emphysem. Deutsches Arch f. klin Med. 102:309-405, 1911.

3. Krogh, A. and J. Lindhard. The volume of the dead space in breathing and the mixing of gases in the lungs of man. J. Physiol. 51:59, 1917.

4. Haldane, J. S. Respiration. Yale University Press, p.137, 1922.

5. Laurell, B. A. Om abnorma statiska circulationsfenomen och darmed samman hangande sjukliga symptom. Den arteriella orthostatiska anamin on forsummad sjukdansbild. Upsala Lakareforen Fork. 33:1-27.

6. Fraser, R. G. and D. V. Bates. Body section roentgenography in the evaluation and differentiation of chronic hypertrophic emphysema and asthma. Am. J. Roentgenol. 82:39, 1959.

7. Bjorkmann, S. Bronchospirometrie. Acta. Med. Scand. Suppl. 56:1, 1934.

8. Dock, W. Apical localization of phthisis; its significance in treatment by prolonged rest in bed. Am. Rev. Tuberc. 53:297, 1946.

9. Rothlin, E. and E. Undsitz. Beitrag zur lokalisationsregel der Tuberkulose. Schweiz. Ztschr. allg. Path. 15:690, 1952.

10. Martin, C., F. Cline and H. Marshall. Lobar alveolar gas concentrations; effect of body position. J. Clin. Invest. 32:617, 1953.

11. Martin, C. and C.J. Young. Lobar ventilation in man. Am. Rev. Tuberc. 73:330, 1956.

12. Martin, C. and A. Young. Ventilation perfusion variations within the lung. J. Appl. Physiol. 11:371, 1957.

13. Mattson, S. B. and E. Carlens. Lobar ventilation and oxygen uptake. J. Thoracic Surg. 30:676, 1955.

BIBLIOGRAPHY (Cont'd)

14. Krogh, A. and J. Lindhard. The volume of the dead space in breathing. J. Physiol. 47:30, 1913-1914.

15. Lilly, J.C. The mixing of gases within the respiratory system, with a new type of nitrogen meter. J. Physiol. 196:342, 1950.

16. Fowler, K.T. and P. Hugh Jones. Mass spectrometry applied to clinical practice and research. Brit. Med. J. 1:1205, 1957.

17. Sonne, C. Inequality of ventilation of different parts of the lungs as a source of error in respiratory physiology experiments. Scandinav. Arch. f. Physiol. 75:127, 1936.

18. Brath, G. Lung volume and ventilation efficiency. Changes in collapse treated and no collapse treated pulmonary tuberculosis and in pulmonectomy and lobectomy. Acta Med. Scand. Supp. 154:1, 1944.

19. Darling, R.C., A. Cournand and D. Richards. Studies on intra-pulmonary mixture of gases V. Forms of inadequate ventilation in normal and emphysematous lungs, analyzed by means of breathing pure oxygen. J. Clin. Invest. 23:55, 1944.

20. Fowler, W., E. Cornish and S. Ketty. Lung function studies VIII. Analysis of alveolar ventilation by pulmonary N_2 clearance curves. J. Clin. Invest. 31:40, 1952.

21. Robertson, J. W. Siri, and H. Jones. Lung ventilation patterns determined by analysis of nitrogen elimination rates; use of the mass spectrometer as a continuous gas analysis. J. Clin. Invest. 29:577, 1950.

22. Becklake, M.R. A study by an open circuit method of the intrapulmonary mixture of inspired air. Thorax. 6:433, 1951.

23. Blair, E. and J.B. Hickam. Effect of changes of body position on lung volume and intrapulmonary mixing in normal subjects. J. Clin. Invest. 34:383, 1955.

24. Bates, D.V. and R.V. Christie. Intrapulmonary mixing of Helium in health and disease. Clin. Sci. 9:17, 1950.

25. Buxton, R. and J.L. D'Silva. Use of the Helium dilution method to assess the mixing of gases in the lungs. Tubercle. 37:264, 1956.

26. Bouhuys, A. and G. Lundin. Distribution of inspired gas in the lungs. Physiol. Rev. 39:731, 1959.

BIBLIOGRAPHY (Cont'd)

27. Nye, R. E. Theoretical limits to measurement of uneven ventilation. J. Appl. Phys. 16:1115. 1961.

28. Gomez, D. M. A mathematical treatment of the distribution of tidal volume throughout the lung. Proc. Natl. Acad. Sci. 49:312, 1963.

29. Rossing, R. G. and S. M. Cain. Analysis of Nitrogen washout curves utilizing a digital computer. Fed. Proc. 23:1579, 1964.

30. Rahn, H. A concept of mean alveolar air and the ventilation-blood flow relationship during pulmonary gas exchange. Am. J. Physiol. 158:21, 1949.

31. Rahn, H. and W. O. Fenn. A graphical analysis of the respiratory gas exchange. Am. Physiol. Soc. Monograph, Washington, 1955.

32. Riley, R. L. and A. Cournand. Ideal alveolar air and the analysis of ventilation-perfusion relationships in the lungs. J. Appl. Physiol. 1:825, 1949.

33. Riley, R. L. and A. Cournand. Analysis of factors affecting partial pressures of 0_2 and $C0_2$ in gas and blood of the lungs. Theory. J. Appl. Physiol. 4:77, 1951.

34. Fahri, L. E. and W. O. Fenn. The oxygen-carbon dioxide diagram for alveolar air. WADC Tech. Rep. 55-357, p. 290, 1955.

35. Dill, D. B., H. T. Edwards and W. V. Consolazio. Blood as a physico-chemical system XI Man at rest. J. Biol. Chem. 118:635, 1937.

36. Fahri, L. E. and H. Rahn. A theoretical analysis of alveolar-arterial 0_2 difference, with special reference to the distribution effect. J. Appl. Physiol. 7:699, 1955.

37. Riley, R. L., A. Cournand, and K. W. Donald. Analysis of factors affecting partial pressure of 0_2 and $C0_2$ in gas and blood of lungs. Methods. J. Appl. Physiol. 4:102, 1951.

38. Rahn, H. and L. E. Fahri. Ventilation-perfusion relationship. Pulmonary Structure and Function. Ed. De Reuck AVS, M. O'Connor, Churchill, p. 139, 1962.

39. Canfield, R. E. and H. Rahn. Arterial-alveolar N_2 gas pressure differences due to ventilation perfusion variations. J. Appl. Physiol. 10:165, 1957.

BIBLIOGRAPHY (Cont'd)

40. Rahn, H. Biological role of Nitrogen gas. Harvey Lectures. 33:173, 1959-1960.

41. Ross, B. B. and L. E. Fahri. Dead space ventilation as a determinant in the ventilation perfusion concept. J. Appl. Physiol. 15:363, 1960.

42. Larson, C. P. and J. W. Severinghaus. Postural variations in dead space and CO_2 gradients breathing air and O_2. J. Appl. Physiol. 17:417, 1962.

43. Riley, R. L., S. Permutt, S. Said, M. Godfrey, T. O. Cheng, J. B. L. Howell, R. H. Shepard. Effect of posture on pulmonary dead space in man. J. Appl. Physiol. 14:339, 1959.

44. Bjurstedt, H., C. M. Hesser, G. Liljestrand, G. Matell. Effects of posture on alveolar-arterial CO_2 and O_2 differences and on alveolar dead space. Acta Physiol. Scand. 54:65, 1962.

45. Lilienthal, J. L., R. L. Riley, D. D. Proemmel, R. E. Franke. An experimental analysis in man of the oxygen pressure gradient from alveolar air to arterial blood during rest and exercise at sea level and at altitude. Am. J. Physiol. 147:199, 1946.

46. Briscoe, W. A. A method for dealing with data concerning uneven ventilation of the lung and its effects on blood gas transfer. J. Appl. Physiol. 14:29, 1959.

47. Briscoe, W. A., E. M. Cree, J. Filler, H. E. J. Houssay, and A. Cournand. Lung volume, alveolar ventilation and perfusion interrelationships in chronic pulmonary emphysema. J. Appl. Physiol. 15:785, 1960.

48. Gurtner, H. P., N. A. Briscoe, and A. Cournand. Studies of the ventilation perfusion relationships in the lungs of subjects with chronic pulmonary emphysema, following a single intravenous injection of radio-active Krypton (Kr^{85}). I - Presentation and validation of a theoretical model. J. Clin. Invest. 39:1080, 1960.

49. Chidsey, C. A., H. W. Fritts, A. Hardewig., D. W. Richards and A. Cournand. Fate of radio-active Krypton (Kr^{85}) introduced intravenously in man. J. Appl. Physiol. 14:63, 1959.

BIBLIOGRAPHY (Cont'd)

50. Briscoe, W. A. and A. Cournand. The degree of variation of blood perfusion and of ventilation within the emphysematous lung, and some related considerations. Pulmonary Structure and Function. Ed. De Reuck, AVS, M. O'Connor. Churchill, p. 304, 1962.

51. Roelsen, E. Fractional analysis of alveolar air after inspiration of hydrogen as a method for the determination of the distribution of inspired air in the lungs. Acta Med. Scand. 95:452

52. West, J.B., K. T. Fowler, P. Hugh-Jones, and T. V. O'Donnell. Measurement of the ventilation perfusion ratio inequality in the lung by the analysis of a single expirate. Clin. Sci. 16:529, 1957.

53. West, J. B., K. T. Fowler, P. Hugh-Jones, T. V. O'Donnell. The measurement of the inequality of ventilation and of perfusion in the lung by the analysis of single expirates. Clin. Sci. 16:549, 1957.

54. Strang, L. B. Alveolar gas and anatomical dead space measurements in normal newborn infants. Clin. Sci. 21:107, 1961.

55. Rahn, H. P. Sadoul, L.E. Farhi and J. Shapiro. Distribution of ventilation and perfusion in the lobes of the dog lung in the supine and erect position. J. Appl. Physiol. 8:417, 1956.

56. West, J. B.and P. Hugh-Jones. Effect of bronchial and arterial constriction on alveolar gas concentrations in a lobe of the dog's lung. J. Appl. Physiol. 14:743, 1959.

57. Hugh-Jones, P. and J. B. West. Detection of bronchial and arterial obstruction by continuous gas analysis from individual lobes and segments of the lung. Thorax 15:154, 1960.

58. Inada, K., S. Kishimoto, A. Sato and T. Watanabe. Broncho-spirometry with the Carlens double lumen catheter. J. Thorac. Surg. 27:173, 1954.

59. Rothstein, E., F. B. Landis, and B. G. Narodick. Broncho-spirometry in the lateral decubitus position. J. Thorac. Surg. 19:821, 1950.

60. Dyson, N.A., P. Hugh-Jones, G. R. Newberry and J. B. West. Preparation and use of Oxygen 15 with particular reference to its value in the study of pulmonary function. Second United Nations Conference on Peaceful uses of Atomic Energy, Geneva. Vol. 26, 1959.

BIBLIOGRAPHY (Cont'd)

61. Dyson, N. A., P. Hugh-Jones, G. R. Newberry, J.D. Sinclair, and J. B. West. Studies of regional lung function using radio-active oxygen. Brit. Med. J. 1:231, 1960.

62. Dollery, C.T., P. Heimburg, and P. Hugh-Jones. The relationship between blood flow and clearance rate of radio-active carbon dioxide and oxygen in normal and oedematous lungs. J. Physiol. 162:93, 1962.

63. West, J. B. and C. T. Dollery. Distribution of blood flow and ventilation perfusion ratio in the lung, measured with radio-active $C0_2$. J. Appl. Physiol. 15:405, 1960.

64. West, J.B., A. B. Holland, C.T. Dollery and C.M.E. Matthews. Interpretation of radio-active gas clearance rates in the lung. J. Appl. Physiol. 17:14, 1962.

65. West, J.B. and C.T. Dollery. Uptake of oxygen-15 labelled $C0_2$ compared with carbon-11 labelled $C0_2$ in the lung. J. Appl. Physiol. 17:9, 1962.

66. West, J.B. Regional differences in gas exchange in the lung of erect man. J. Appl. Physiol. 17:893, 1963.

67. West, J.B. Distribution of gas and blood in the normal lungs. Brit. Med. Bull. 19:1:53, 1963.

68. Knipping, H.W., W. Bolt, H. Venrath, H. Valentin, H. Ludes and P. Endler. Eine neur methode zur Prufung der Herz-und Lungens-function. Die regionale Funktionsanalyze in der Lungen - und Herzklinik mit Hilfe des radioaktiven Edelgases Xenon^{133}. Dtsch. med. Wschr. 80:1146, 1955.

69. Knipping, H. W., W. Bolt, H. Valentin, H. Venrath, P. Endler. Technik und Moglichkeiten der regionalen Ventilationsanalyse mittels des radioaktiven Edelgases Xenon ^{133}. Z. Tuberc. 111:259, 1957.

70. Knipping, H. W., W. Bolt, H. Valentin, H. Venrath, P. Endler. Regionale Funktionsanalyse in der Kreislauf - und Lungen Klinik mit Hilfe der Isotopenthorakographic der selektiven Angiographic der Lungeneffase. Munch. med. Wschr. 99:46, 1957.

71. Venrath, H. Die Lungenfunktionsprufung mit Hilfe von Isotopen in Lungen and kleiner Kreislauf. Ed. W. Lochner and E. Witzlab. Berlin Springerverlag. p. 144, 1957.

BIBLIOGRAPH (Cont'd)

72. Bolt, W. and H. Rink. Studies zur regionalen analyse der Lungenventilation und Lungenzirkulation. Thoraxchirmgie 29:5, 1958.

73. Fucks, W. and H. W. Knipping. Bildliche Darstellung der Verteilung und der Benegung von radioaktiven substanzen in Raum (Rontgen chue Rontgenrohre) unter Berucksichtigung einiger Probleme der Herz und Lungenklinik. Atomkernenergie. 6:209, 1958.

74. Trippe, H. Diagnose regionaler Ventilations-storungen der Lunge mit Hilfe von Xenon^{133}. Cologne, Photostelle der Universitat zu Koln, 1959.

75. Ball, Jr. W. C., P. B. Stewart, L. G. S. Newsham, D. V. Bates. Regional pulmonary function studied with Xenon^{133}. J. Clin. Invest. 43:519, 1962.

76. Bentivoglio, L. G., F. Beerel, A. C. Bryan, P. B. Stewart, B. Rose and D. V. Bates. Regional pulmonary function studied with Xenon^{133} in patients with bronchial asthma. J. Clin. Invest. 42:1193, 1963.

77. Bryan, A. C., L. G. Bentivoglio, F. Beerel, W. C. Ball, H. MacLeish and D. V. Bates. Measurement of ventilation/perfusion ratios in the human lung using Xenon ^{133}. Fed. Proc. 21:439, 1962.

78. McGregor, M., Wm Adam, and P. Sekelj. Influence of posture on cardiac output and minute ventilation. Circ. Res. 9:1089, 1961.

79. Fowler, W. S. Intra-pulmonary distribution of inspired gas. Physiol. Rev. 32:1, 1952.

80. Otis, A. B., C. B. McKerrow, R. A. Bartlett, J. Mead, M. B. McIlroy, N. J. Selverstone and E. P. Radford. Mechanical factors in the distribution of pulmonary ventilation. J. Appl. Physiol. 8:427, 1956.

81. Ross, J. C., R. Frayser and J. B. Hickam. A study of the mechanism by which exercise increases the pulmonary diffusing capacity for carbon monoxide. J. Clin. Invest. 38:916, 1959.

82. Daly, W. J. and S. Bondurant. Direct measurement of respiratory pleural pressure changes in normal man. J. Appl. Physiol. 18:513, 1963.

83. Krueger, J. J., T. Bain and J. L. Patterson Jr. Elevation gradient of intrathoracic pressure. J. Appl. Physiol. 16:465, 1961.

BIBLIOGRAPHY (Cont'd)

84. Milic-Emili, J., J. Mead and J. M. Turner. Topography of oesophageal pressure as a function of posture in man. J. Appl. Physiol. 19:212, 1964.

85. Hamlin, R. L., W. P. Marsland, C. R. Smith and L. A. Sapirstein. Fractional distribution of right ventricular output in the lungs of dogs. Circ. Res. 10:763, 1960.

86. Ruch, T. C. and J. F. Fulton. Medical physiology and biophysics. 18th Edition. J. B. Saunders, 1960.

87. Lagerlof, H., H. Eliasch, L. Werko, and E. Berglund. Orthostatic changes of the pulmonary and peripheral circulation in man. Scand. J. Clin. Lab. Invest. 1:147, 1949.

88. Prandtl, L. and O. G. Tretjens. Applied Hydro and Aeromechanics. Engineering Soc. Monograph. Dover: New York.

89. Prec, O., L. N. Katz, L. Sennett, R. H. Roseman, A. P. Fishman and W. Hwang. Determination of kinetic energy of the heart in man. Am. J. Physiol. 159:483, 1949.

90. Fry, D. L., F. W. Noble and A. J. Mallos. An electric device for instantaneous and continuous computation of aortic blood velocity. Circ. Res. 5:75, 1957.

91. Howell, J. B., S. Permutt, D. F. Proctor and R. L. Riley. Effect of inflation of the lung on different parts of the pulmonary vascular bed. J. Appl. Physiol. 16:71, 1961.

92. Permutt, S., B. Bromberger-Barnea and H. N. Bane. Alveolar pressure, pulmonary venous pressure and the vascular waterfall. Med. Thorac. 19:239, 1962.

93. Staub, N. C. The interdependence of pulmonary structure and function. Anaesthesiology. 24:831, 1963.

94. Lloyd, T. C. Jr. and Geo. W. Wright. Pulmonary vascular resistance and vascular transmural gradient. J. Appl. Physiol. 15:241, 1960.

95. Permutt, S. and R. L. Riley. Haemodynamics of collapsible vessels with tone; the vascular waterfall. Fed. Proc. 750, 1963.

96. Permutt, S. and R. L. Riley. Haemodynamics of collapsible vessels with tone; the vascular waterfall. J. Appl. Physiol. 18:924, 1963.

BIBLIOGRAPHY (Cont'd)

97. Fishman, A. P. Respiratory gases in the regulation of the pulmonary circulation. Physiol. Rev. 41:214, 1961.

98. Rahn, H. and H. T. Bahnson. Effect of unilateral hypoxia on gas exchange and calculated pulmonary blood flow in each lung. J. Appl. Physiol. 6:105, 1953.

99. Handbook of Physiology: Circulation Vol. II. Dynamics of the Pulmonary Circulation. p. 1667, American Physiological Society, Washington, 1963.

100. Fahri, L. E. and H. Rahn. Total flow requirements for gas transport. WADD Tech Rep. 60-1:147, 1960.

101. Dubois, A. B., A. G. Britt and W. O. Fenn. Alveolar CO_2 during the respiratory cycle. J. Appl. Physiol. 4:535, 1952.

102. Asmussen, E. and M. Nielsen. Alveolo-arterial gas exchange at rest and during work at different O_2 tensions. Acta Physiol. Scand. 50:153, 1960.

103. Lenfant, C. Measurement of ventilation/perfusion distribution with alveolar arterial differences. J. Appl. Physiol. 18:1090, 1963.

104. Bishop, J. M. and J. M. Raine. Aa difference in O_2 tension and physiological dead space in normal man. J. Appl. Physiol. 18:284, 1963.

105. Klocke, F. J. and H. Rahn. The arterial-alveolar inert gas ("N_2") difference in normal and emphysematous subjects as indicated by the analysis of urine. J. Clin. Invest. 40:286, 1961.

106. Bjurstedt, H., C. M. Hesser, G. Liljestrand, and G. Mattel. Effects of posture on alveolar arterial CO_2 and O_2 differences and on alveolar dead space in man. Acta Physiol. Scand. 54:65, 1962.

107. Finley, T. N., E. W. Swenson and J. H. Comroe. The cause of arterial hypoxaemia at rest in patients with "alveolar-capillary block syndrome". J. Clin. Invest. 41:618, 1962.

108. Staub, N. C. Alveolar-arterial oxygen tension gradient due to diffusion. J. Appl. Physiol. 18:673, 1963.

BIBLIOGRAPHY (Cont'd)

109. Roughton, F.J.W. and R.E. Forster. Relative importance of diffusion and chemical reaction rates in determining rate of exchange of gases in the human lung with special reference to true diffusing capacity of pulmonary membrane and volume of blood in the lung capillaries. J. Appl. Physiol. 11:290, 1957.

110. Bates, D. V. and J. F. Pearce. Pulmonary diffusing capacity. J. Physiol. 132:232, 1956.

111. Riley, R. L., R.H. Shepard, J. E. Cohn, D.G. Carroll and B. W. Armstrong. Maximal diffusing capacity of the lungs. J. Appl. Physiol. 6:573, 1954.

112. Cohn, J. E., D. G. Carroll, B. W. Armstrong, R.H. Shepard, and R. L. Riley. Maximal diffusing capacity of the lungs in normal male subjects of different ages. J. Appl. Physiol. 6:588, 1954.

113. Johnson, R. L., W.S. Spicer, J.M. Bishop and R.E. Forster. Pulmonary capillary blood volume, flow and diffusing capacity during exercise. J. Appl. Physiol. 15:893, 1960.

114. Bates, D.V., C.J. Varvis, R.E. Donevan and R.V. Christie. Variations in the pulmonary capillary blood volume and membrane diffusion component in health and disease. J. Clin. Invest. 39:1401, 1960.

115. Weibel, E.R. and D.M. Gomez. Architecture of the human lung. Science. 137:577, 1962.

116. Bates, D.V., N. G. Boucot and A.E. Dormer. The pulmonary diffusing capacity in normal subjects. J. Physiol. 129:237, 1955.

117. Filley, G.F., D.J. MacIntosh and G.W. Wright. CO uptake and pulmonary diffusing capacity in normal subjects at rest and during exercise. J. Clin. Invest. 33:530, 1954.

118. Ball, Jr. W. C. Effect in a lung model of non-uniformity on estimates of CO diffusing capacity by Filley and Bates techniques. Fed. Proc. 23:1583, 1964.

119. Forster, R. E., W. S. Fowler, D.V. Bates and B. Van Lingen. The absorption of carbon monoxide by the lungs during breathholding. J. Clin. Invest. 33:1135, 1954.

BIBLIOGRAPHY (Cont'd)

120. Bentivoglio, L. G., F. Beerel, P. B. Stewart, A. C. Bryan, W. C. Ball and D. V. Bates. Studies of regional ventilation and perfusion in pulmonary emphysema using Xenon ^{133}. Am. Rev. Resp. Dis. 88:3, 1963.

121. Dollery, C. T. and P. Hugh-Jones. Distribution of gas and blood in the lung in disease. Brit. Med. Bull. 19:59, 1963.

122. Dollery, C. T., P. Hugh-Jones and C. M. E. Matthews. Use of radio-active Xenon for studies of regional lung function. Brit. Med. J. p. 1006, Oct. 20, 1962.

123. Dollery, C. T. and P. M. S. Gillam. The distribution of blood and gas within the lungs measured for scanning after administration of Xenon^{133}. Thorax 18:316, 1963.

124. Zierler, K. L. Theory of the use of arterio-venous concentration differences for measuring metabolism in steady and non-steady states. J. Clin. Invest. 40:2111, 1961.

125. Zierler, K. L. Circulation times and the theory of indicator dilution methods of determining blood flow and volume. Handbook of Physiology: Circulation Vol. 1, American Physiological Society, Washington, 1963.

126. Stewart, G. N. Researches on the circulation time in organs and on the influences which affect it. IV - Output of the heart. J. Physiol. 22:159, 1898.

127. Hamilton, W. F., J. W. Moore, J. M. Kinsman, and R. G. Spurling. Simultaneous determination of the pulmonary and systemic circulation times in man and of a figure related to cardiac output. Am. J. Physiol. 84:338, 1928.

128. Ed. Hodgman, C. D., R. C. Weast, R. S. Shankland, and S. M. Selby. Handbook of Chemistry and Physics. 44th Edition. Chemical Rubber Pub. Co., Ohio, 1963.

129. Bartlett, N. Xenon Hexafluoroplatinate (V). Proc. Chem. Soc. London, 218: June 1962.

130. Conn, Jr. H. L. Equilibrium distribution of radioxenon on tissue; xenon-haemoglobin association curve. J. Appl. Physiol. 18:513, 1963.

131. Pittinger, C. B., H. L. Conn, R. M. Featherstone, E. Stickley, L. Levy and S. C. Cullen. Observations on the kinetics of transfer of xenon and chloroform between blood and brain in the dog. Anaesthesiology 17:523, 1956.

132. Wilson, E. J., H. P. Dibbs, S. Richards, and J. D. Eakins. Preparation of Xenon^{133} radiography sources from spent fuel. Nucleonics 16:110, 1958.